

Photon-Photon Elastic Scattering in the Low Energy Regime

by

Ibrar Hussain



A dissertation submitted in partial fulfillment of the requirements
for the degree of Master of Philosophy in Physics

Supervised by

Dr. Rizwan Khalid

School of Natural Sciences (SNS)

National University of Sciences and Technology
Islamabad, Pakistan

© Ibrar Hussain

National University of Sciences & Technology**M.Phil THESIS WORK**

We hereby recommend that the dissertation prepared under our supervision by: Ibrar Hussain, Regn No. NUST201260314MCAMP78112F Titled: Photon-Photon Elastic Scattering in the Low Energy Regime be accepted in partial fulfillment of the requirements for the award of **M.Phil** degree.

Examination Committee Members1. Name: Prof. Asghar QadirSignature: 2. Name: Dr. Shahid IqbalSignature: 3. Name: Dr. Muhammad Jamil AslamSignature: 4. Name: Dr. Mansoor ur RehmanSignature: Supervisor's Name: Dr. Rizwan KhalidSignature: 


Head of Department

13-06-2016
Date

COUNTERSIGNEDDate: 13/06/16


Dean/Principal

Abstract

Photon-photon ($\gamma\gamma$) elastic scattering is a quantum mechanical process, which is predicted by Quantum Electrodynamics (QED) because of virtual particle-antiparticle pair production that polarizes the vacuum. In a source-free regions, classical electrodynamics is a linear theory which forbids any electromagnetic self interaction. An effective lagrangian taking into account vacuum polarization either in light of the Dirac's 'positron sea' or QED can of course be written which will allow a semiclassical description of this process.

In this thesis, we have done low energy QED calculations of photon-photon elastic scattering. We have calculated the polarized amplitudes, as well as unpolarized differential and total cross sections in the low energy region $\omega \ll m_e$, where ω is the energy of the photon and m_e is the mass of the electron. We have considered the electronic loop contribution to $\gamma\gamma \rightarrow \gamma\gamma$ and neglected all other heavy fermionic or bosonic loop contributions since at present available laser intensities, the electronic loop contribution to $\gamma\gamma \rightarrow \gamma\gamma$ is all that matters.

Photon-photon elastic scattering has never yet been observed experimentally because of smallness of cross section. We have outlined the main difficulties which the experimentalists are facing in trying to detect $\gamma\gamma \rightarrow \gamma\gamma$. We have discussed some of the important experiments which have set the most stringent upper bounds on the $\gamma\gamma \rightarrow \gamma\gamma$ cross section. The obtained upper bounds on the cross section in visible and X-ray regions were $1.5 \times 10^{-48}\text{cm}^2$ and $1.7 \times 10^{-20}\text{cm}^2$ respectively which correspond to QED cross sections of $1.8 \times 10^{-66}\text{cm}^2$ and $5.5 \times 10^{-43}\text{cm}^2$.

Acknowledgements

I would first of all like to thank Allah, Who bestowed on me His blessings and gave me the vision to choose a field of my interest and to accomplish my work successfully.

I invoke peace for the Holly prophet (PBUH), an eternal symbol of guidance for humanity and the source of knowledge, who declared it an obligatory duty of every muslim to seek knowlegde.

I would like to thank my supervisor, Dr. Rizwan khalid, for his sympathetic attitude and from whom I learent alot of things related to my field.

I am thankful to all of my teachers at School of Natural Sciences (SNS), especially, Prof. Asghar Qadir from whom I learent alot of things during my course work and Dr. Ali Paracha and Dr. Shahid Iqbal for their kind support. I am also thankful to Dr. Jamil Aslam (QAU), for guiding me when I stuck.

It will be injustice if I do not recognize the support and help of the friends arround me. I am so thankful to Mr. Mureed Hussain, Mr. Muhammad Usman and Mr. Mehar Ali Malik for their encouragement and useful discussions.

At last but not the least, I am honoured to acknowledge my family as it would have been impossible for me to complete this work succesfully without their support. I would like to thank my brothers and sisters as it was their love and encouragement that kept me going.

Ibrar Hussain

*Dedicated to my Family,
Especially my Father and Mother*

List of Figures

1.1	Lowest order Feynman diagram of photon-photon elastic scattering.	3
1.2	Feynman diagram for pair production	4
2.1	Head-on collision of two photons having frequencies ν_0 and $2\nu_0$. . .	11
2.2	Angular configuration of the experiment employing three photon beams	12
2.3	The experimental setup of the $\gamma\gamma$ elastic scattering in X-ray region at SACLA	15
2.4	A Comparison of the QED cross section and the upper bounds on QED cross section with (95% C.L) obtained in experiments	17
3.1	All six possible lowest order Feynman diagrams. The bottom graphs are distinct from the top ones only due to the directions of the loops	23
3.2	Possible lowest order labelled Feynman diagrams of photon-photon elastic scattering.	24
3.3	Photon-photon elastic scattering in center of mass frame	42
3.4	Angular dependence of the unpolarized differential scattering cross section	50
3.5	The $\gamma\gamma$ elastic scattering cross section as a function of center of mass photon energy.	51

Contents

1	Introduction	1
1.1	Notation and Conventions	5
1.2	Motivation and Outline of Thesis	5
2	Experimental Status of Photon-Photon Elastic Scattering	8
2.1	Historical Background	9
2.2	Photon-Photon Elastic Scattering in the Visible Domain	10
2.2.1	Experiment Employing Two Photon Beams	10
2.2.2	Experiment Employing Three Photon Beams	12
2.3	Photon-photon Elastic Scattering in X-ray region	14
2.4	Comparison of the Upper Limits in the Visible and X-ray Regions with the QED Cross Section	16
2.5	Main Difficulties Faced in Experiments	18
2.6	Current Laser and X-ray Technology	19
2.7	Summary of Experimental Challenges	20
3	QED Loop Calculations in the Low Energy Regime	22
3.1	Photon-Photon Elastic Scattering Amplitude	22
3.1.1	Computation of $\mathbf{M}_1^{\lambda\nu\mu\sigma}$	25
3.1.2	Amplitude \mathbf{M}_1	36

3.1.3	Amplitude \mathbf{M}_2	37
3.1.4	Amplitude \mathbf{M}_3	39
3.1.5	The Ward Identity	41
3.1.6	Photon Polarization Vectors	42
3.1.7	Polarized Amplitude of Photon-Photon Scattering	44
3.1.8	Polarized Amplitude M^{++++}	45
3.1.9	Kinematics For Polarized Amplitude M^{++++}	46
3.1.10	Results for the Polarized Photon-Photon Scattering Amplitude	47
3.1.11	Total Cross Section	48
3.2	Cross Section as a Function of Energy and Angular Distribution . .	49
3.3	Error From Neglecting The Regularization Scheme	51
3.4	Other Heavy Fermionic or Bosonic Loop Contributions to $\gamma\gamma \rightarrow \gamma\gamma$	54
4	Conclusions	56
	Appendices	58
A	Non-linear Classical Electrodynamics	58
B	QED Feynman Rules	63
C	Feynman Parameterization	66
D	Feyncalc Code	69

Chapter 1

Introduction

In classical electrodynamics, the superposition principle plays an important role as classical electrodynamics in source-free regions is a linear theory. This linearity disappears when we include quantum corrections, although this deviation from linearity is small. The reason for this non-linearity is the quantum fluctuations of the vacuum, as a result of which particle-antiparticle pairs pop out of nowhere, exist for a brief period of time allowed by the Heisenberg uncertainty principle, and annihilate once again. According to the Heisenberg uncertainty principle, we have

$$\Delta E \Delta t \geq \frac{1}{2}.$$

For a very brief period of time Δt , the energy ΔE for the production of virtual e^+e^- pairs can be borrowed from the vacuum and violation of the conservation of energy can take place for a brief period of time. These virtual particles can exist for a very short time and cannot be measured. So, technically, even in source-free regions, the vacuum itself may be polarized, giving rise to non-linearities in the theory.

QED is one of the two most successful and well tested theories, the other

one being General Relativity. QED is in excellent agreement with experiments and has been tested to order $O(\alpha^4)$ in perturbation theory [1, 2], where α is the fine structure constant and is equal to $1/137$. There are, of course, some QED processes which are not verified experimentally. Among them, one is photon-photon elastic scattering, which is difficult to see from an experimental point of view. The photon-photon elastic scattering is not allowed at the tree level in QED. While proper $\gamma\gamma \rightarrow \gamma\gamma$ has not yet been observed, a related process known as Delbruck elastic scattering of photons in the electrostatic field of a nucleus [3] has been seen.

Photon-photon scattering in vacuum is a pure quantum mechanical process. After the negative energy solutions of Dirac equation [4], it was proposed that photon-photon scattering can occur via polarizing the vacuum. The photon-photon elastic scattering was first considered by Halpern qualitatively [5] in the year 1933, and its low energy cross section was determined by Hans Heinrich Euler and B. Kockel [6, 7]. In 1937, high energy photon-photon scattering calculations [8] were performed by Akhiezer et. al. In 1950, by using the newly invented Feynman diagrammatic technique, a complete analysis of photon-photon scattering and partial cross sections for various polarization states was done [9, 10].

In this thesis, we have done the QED calculations for photon-photon elastic scattering in the low energy regime. As stated earlier, this process has never been seen in the lab. Part of the reason for this is the suppression of cross section due it being a loop process. The other reason, of course has to do with the difficulty of manipulating photons experimentally. In QED, photon-photon elastic scattering is represented by the Feynman diagram in Figure 1.1.

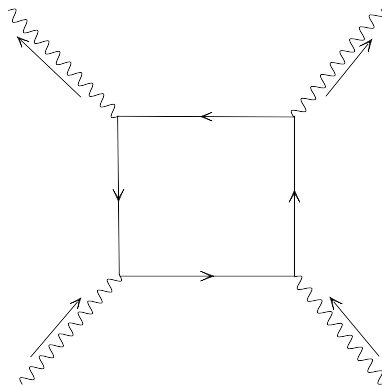


Figure 1.1: Lowest order Feynman diagram of photon-photon elastic scattering.

Loop diagrams are typically divergent. We can handle such divergent integrals with the help of regularization and renormalization schemes. These regularizations and renormalization tools ensure the amplitudes to be gauge invariant and to satisfy the Ward identity. There are many regularization schemes, for example, dimensional regularization and Pauli's Villars regularization. All regularization schemes produce identical results. In our calculations, we have adopted dimensional regularization. After regularization, counter terms are introduced in the lagrangian to absorb the divergences. However in our calculations all these infinities are canceled when we add contributions of all Feynman diagrams, and there is no need of adding counter terms. These regularizations and renormalization procedures can be applied to all orders in perturbation theory. There are some important QED predictions for inelastic photon-photon scattering *e.g* electron-positron pair production

$$\gamma + \gamma \longrightarrow e^+ + e^-,$$

which is an example of conversion of energy into matter. Pair production was for the first time considered by Breit and Wheeler [11]. The minimum energy in center of mass system required for electron-positron pair production is $2m_e c^2 \simeq 1\text{MeV}$. Pair production becomes abundant at the field strength known as the critical field

strength E_{cr} . The critical field strength, corresponds to that value of the field when the work done on an electron over a Compton wavelength is equal to the rest mass energy of the electron. i.e

$$\begin{aligned} eE_{cr}\lambda_c &= mc^2 \\ \text{or } E_{cr} &= \frac{mc^2}{e\lambda_c}, \end{aligned} \quad (1.1)$$

where λ_c is the wavelength of photon, whose energy is equal to rest mass energy of electron.

$$\frac{hc}{\lambda_c} = mc^2 \quad \text{or} \quad \lambda_c = \frac{h}{mc} = 2.42 \times 10^{-12}m. \quad (1.2)$$

The Equation (1.1) becomes

$$E_{cr} = \frac{m^2c^3}{eh} = 1.3 \times 10^{16} \text{ V/cm},$$

which corresponds to critical intensity $I_{cr} = \frac{c}{4\pi} E_{cr}^2 = 2.3 \times 10^{29} \text{ W/cm}^2$.

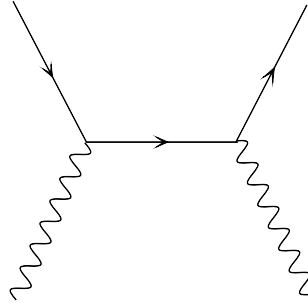


Figure 1.2: Feynman diagram for pair production

The available intensity at present time is about 10^{22} W/cm^2 , which is still much lower than I_{cr} . There are many laser projects in progress for the improvement of laser intensity and in near future we may reach very close to the required intensity for pair production. There is no direct experimental evidence for pair production (e^+e^-) but a somewhat indirect experimental evidence is available [12] which is based on a multi-photons scattering event.

1.1 Notation and Conventions

Here we list out some of the important notations and conventions which are used in this thesis.

- We use natural units $c = \hbar = 1$.
- We work in the usual Minkowski spacetime with the diagonal metric $(+, -, -, -)$.
- Four vectors are represented with roman letters. Components of four vectors are symbolized by greek letters. Three vectors are written in boldface. For instance \mathbf{k} is the spatial part of k_μ ($\mu = 0, 1, 2, 3$). In the case of the momentum 4-vector, ω is used for its energy.
- Repeated indices are summed over.
- The inner product is represented with a dot, $k_1 \cdot k_2 = k_{1\mu} k_2^\mu$.
- We use the Dirac slash shorthand, $\not{k} \equiv k \cdot \gamma = k_\mu \gamma^\mu$, where the γ^μ s are the usual Dirac γ matrices.
- Right and left handed photon polarization vectors are represented as ϵ^+ and ϵ^- , respectively.
- An asterick denotes the complex conjugate of a number.

1.2 Motivation and Outline of Thesis

The main motivation for writing this thesis is to investigate QED loop diagrams both qualitatively and quantitatively. The tree level processes are easy to handle but problems are created when we deal with Feynman loop diagrams, because loop diagrams involve divergent integrals which need to be regularized in order to make sense of the theory. Calculations of Feynman loop diagrams demand to have a command on mathematical tools such as Feynman parameterization, regularization and renormalization schemes. In this thesis, we have done QED calculations for photon-photon elastic scattering cross section for polarized and

unpolarized case in low energy regimes. Also we have discuss the experimental status, main difficulties and some suggestions to detect photon-photon scattering experimentally.

The main motivation to consider $\gamma\gamma \longrightarrow \gamma\gamma$ in low energy regimes is the unavailability of high energy and intensity laser technology. The minimum energy in center of mass system for real electron-positron pair production is $2mc^2 \simeq 1\text{MeV}$, which corresponds to a critical field strength $\mathbf{E}_{\text{cr}}=1.3 \times 10^{16}$ V/cm. The available intensity at present time is $10^{22}\text{W}/\text{cm}^2$ which is much smaller than critical intensity $I_{\text{cr}} = 2.3 \times 10^{29}\text{W}/\text{cm}^2$. So we consider $\gamma\gamma \longrightarrow \gamma\gamma$ in low energy regimes $\omega \ll m_e$, where ω is energy of photon and m_e is the mass of electron. The direct observation of the process will be a solid evidence for vacuum fluctuations which occur due to production of virtual electron-positron pairs. The outline of the thesis follows.

In chapter 02, we discuss the experimental status of $\gamma\gamma \longrightarrow \gamma\gamma$ process. In this chapter, we have given the historical background, important experiments performed in the visible and X-ray regions, and have outlined the difficulties faced in trying to detect $\gamma\gamma \longrightarrow \gamma\gamma$ scattering. The cross section of photon-photon scattering is very small and has never been observed experimentally, these experiments have set upper bounds on the total cross section.

Chapter 03 is dedicated to the QED calculations of low energy photon-photon elastic scattering. In this chapter, the mathematical tools of Feynman parameterization and dimensional regularization are discussed and are applied to low energy $\gamma\gamma \longrightarrow \gamma\gamma$ scattering. The polarized amplitudes, unpolarized differential cross section and the total scattering cross section are computed. All the necessary calculations are done using the extension Feyncalc [13] to mathematica.

We conclude our discussion in chapter 04 and we have also included appendices at the end. In appendix-A, we have given the one loop correction to classical electrodynamics lagrangian and also that how the non-linearities comes in

Maxwell's equations. The QED lagrangian and the QED Feynman rules are given in appendix-B. The photon polarization vectors and the numerator algebra are also given in appendix-B. In appendix-C, the mathematical tools of Feynman parameterization, standard results of dimensional regularization and the cross section formula for 2-2 process are discussed. We have done all the calculations of $\gamma\gamma \rightarrow \gamma\gamma$ helicity amplitudes by using extension Feyncalc to mathematica. The Feyncalc code written for all five independent helicity amplitudes have been given in appendix-D.

Chapter 2

Experimental Status of Photon-Photon Elastic Scattering

In this chapter, we will highlight the experimental status and explain the difficulties which the experimentalists are facing in trying to detect $\gamma\gamma \rightarrow \gamma\gamma$. We focus on energies for which laser technology is easily available (visible). At such energies inelastic scattering is forbidden from energy-momentum conservation. The cross section of elastic photon-photon scattering is extremely small as a result of which the experimental verification of the process involving photon-photon scattering is quite difficult to perform. Photon-photon collision has been conceived as a crossed beam experiment and requires the highest intensities and also most sensitive detecting equipments. With further developments of laser technology, we expect that photon-photon scattering would be possible to observe in the future. To date many attempts have been made to verify this process experimentally. The experiments have been able to set upper limits on photon-photon elastic scattering cross section. Current experimental endeavors to look for $\gamma\gamma$ scattering include CLF(Central Laser Facility) Vulcan 10 PW project at Rutherford Appleton Laboratory[14], HiPER (High Power laser Energy Research) project and European

Extreme Light Infrastructure(ELI) [15].

2.1 Historical Background

The original calculations of photon-photon scattering date back to 1936. The calculations of the process are not in question, however the experimental confirmation is a big challenge for the experimentalists. Many experiments have been performed to observe the process, but no confirmation has been made yet. Before original calculations of the photon-photon elastic scattering, an experiment was performed by colliding two sun light beams inside a dust free air box [16]. The interaction point was observed through green filter by a dark-adapted eye, but no scattering event was observed. Many experiments were made to detect directly the photon-photon scattering. In one experiment [17], a laser beam was split into two beams each of 4.66 eV. Then compton backscattered photons of 19.5 GeV were produced by colliding an electron beam against one of laser beams (4.66 eV). These compton backscattered photons (19.5 GeV) arrived against the other soft laser beam at the interaction point. Another experiment based on the idea of interaction of modes produced in the microwave waveguides [18] was proposed to detect photon-photon elastic scattering. In experiment [19], they proposed a concrete geometry of cavity and made a quantitative estimations for $\gamma\gamma \rightarrow \gamma\gamma$. Later in the visible range, two beams were collided head-on [20], which was then supplemented by a thir beam to improve the upper limit of cross section obtained [21]. In yet another experiment one was to collide three laser pulses and searched for scattered photons in a fourth direction with a new frequency [22, 23]. The search for photon-photon elastic scattering is also in progress at the Large Hadron Collider (LHC) located at Center European Research Nuclear(CERN). At LHC a high energy $\gamma\gamma$ scattering experiment was suggested by using large flux of quasi real photons produced in the

surroundings of proton (p) and lead (pb) ions when accelerated at high energies [24]. The quasi real photons are basically strong electromagnetic force carrier which surround (p) and (pb) ions accelerated at TeV. In the electromagnetic interaction of p-pb, p-p and pb-pb ions there is a great chance of $\gamma\gamma$ scattering. It has been shown by simulations that in pb-pb, there is a best probability of $\gamma\gamma$ scattering events and almost 20 $\gamma\gamma$ scattering events could be detected per year. This is a high energy experiment where our low energy approximations are not valid however, this experimental suggestion is a good way to look for photon-photon elastic scattering. Experiments have, thus far, failed to report any $\gamma\gamma$ scattering events. They have, therefore, set upper bounds on $\gamma\gamma$ cross section. Therefore, we need to improve the experimental geometry, sensitivity of the experiment and by producing more and more intense and energetic X-ray and laser beams. We now discuss in detail some important experiments which have given the best upper bounds on photon-photon scattering.

2.2 Photon-Photon Elastic Scattering in the Visible Domain

2.2.1 Experiment Employing Two Photon Beams

The first experimental exploration for photon-photon elastic scattering in the visible range was performed in 1995 at Laboratoire pour l'Utilisation des Lasers Intenses (LULI) in France. In this experiment two gaussian laser beams were brought to a head-on collision and a search for elastically scattered photons [20] was done. One of the beams was infrared (IR) with a wavelength of $\lambda_o=1.053 \mu m$ and the other a green laser with wavelength $\frac{\lambda_o}{2}=0.53 \mu m$ having energies 70 ± 5 J and 30 ± 5 J respectively. The spot size at $\frac{1}{e^2}$ scale was $w = 30 \mu m$ and

the pulse duration was 600 picosecond, with a repetition rate of one shot every 20 min. Where spot size $w = 30 \mu m$ at $\frac{1}{e^2}$ scale is basically a radial distance from axis of laser beam to points where intensity value is $\frac{1}{e^2}$ times of maximum value. The elastically scattered photons were searched at 45° with the green beam in the forward direction, which corresponded to yellow part of the spectrum with a wavelength of $0.6 \mu m$. The elastic head-on collision of two photons having frequencies ν_o and $2\nu_o$ are shown in Figure 2.1.

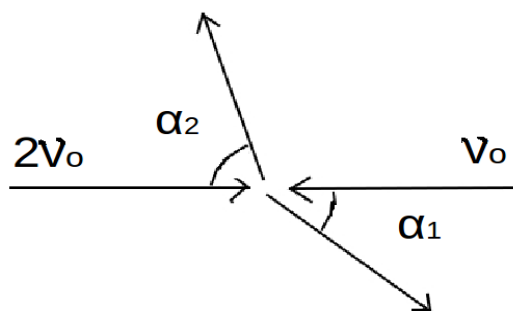


Figure 2.1: Head-on collision of two photons having frequencies ν_o and $2\nu_o$ are shown. The scattered photons were searched for angle $\alpha_1 = 45^\circ$.

The point of interaction was imaged at 45° with two $\frac{f}{5}$ lenses at the entrance of spectrometer-photomultiplier combination. The photomultiplier tube (PMT) was preceded by filters to minimize the background. No scattered photons were observed and an upper limit on the cross section obtained was

$$\sigma_{\gamma\gamma \rightarrow \gamma\gamma}(95\%CL) = 9.9 \times 10^{-40} \text{cm}^2$$

The details about this experiment are given in [20]. This was the first experiment in the low energy region since original calculations were done in 1936. The center of mass photon energy was 1.7 eV at which the QED cross section is $1.7 \times 10^{-64} \text{cm}^2$. The limit on cross section is twenty five orders of magnitude larger than the QED cross section.

2.2.2 Experiment Employing Three Photon Beams

This experiment was performed at Lab for Applied Optic Laboratory (LOA) at Ecole Polytechnique in Palaiseau France [21]. In this upgraded experiment not only was the process supplemented by a third beam, but beams of shorter pulse duration with a repetition rate of 10 Hz were focused to a spot of a smaller size. The energies ω_i and \mathbf{k}_i (wave vectors) where $i=1,\dots,4$ satisfy energy and momentum conservation conditions

$$\omega_1 + \omega_2 = \omega_3 + \omega_4$$

and $\mathbf{k}_1 + \mathbf{k}_2 = \mathbf{k}_3 + \mathbf{k}_4,$

where L.H.S and R.H.S represent the incoming and out going photons. All three beams used were infrared corresponding to wavelengths of $\lambda_1 = \lambda_2 = 800 \times 10^{-9}$ m and $\lambda_3 = 1300 \times 10^{-9}$ m. The signal to be detected was expected to be in the visible region with $\lambda_4 = (2/\lambda_1 - 1/\lambda_3)^{-1} = 577 \times 10^{-9}$ m and was searched for in the direction of $\mathbf{k}_4 = \mathbf{k}_1 + \mathbf{k}_2 - \mathbf{k}_3$.

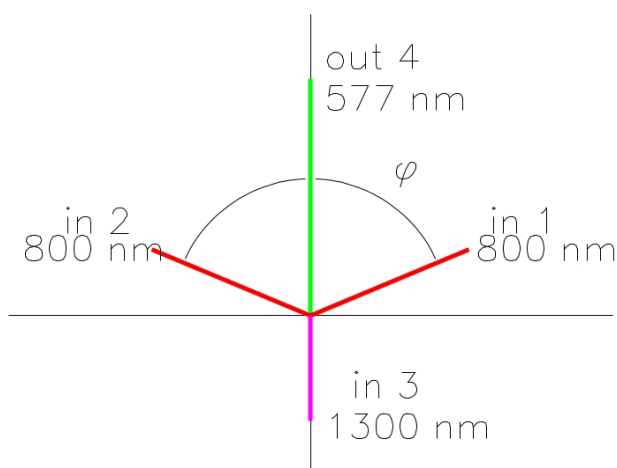


Figure 2.2: Angular configuration of the experiment employing three photon beams [21]. The wave vectors \mathbf{k}_i of the four beams on the plane are shown.

Bowen which is basically a single optics made of a pair of spherical mirrors is used to focus the three incoming beams having a focal length of 100 mm with a coronal pupil of width 30 mm. The half angle of cone formed by the paraxial surface of Bowen is 33.6° . A configuration with left-right symmetry was chosen (Fig.2.2), where the main beams are at an angle ϕ with respect to vertical direction, with $\cos\phi = 1 - \lambda_1/\lambda_3$ and $\phi = 67.4^\circ$. As three beams were injected on cone, the expected signal also lied on that cone. The detailed calculations of the experiment can be studied in [21]. The incoming beams were chosen in a way to have an excellent overlapping at interaction point. The spot sizes at $\frac{1}{e^2}$ in intensity were $4 \mu m$ and $6 \mu m$ for beams with wavelengths $800 nm$ and $1300 nm$ respectively. The beams first enter into the bowen and then overlape at interaction point. The alignment, synchronization and focussing of incoming beams at interaction point(IP) depends on each other due to experimental configuration used. All incident beams were aligned at IP by a camera located at the axis of the bowen. Beam spots lie on the plane perpendicular to axis of bowen and were brought to a common point to have a minimum aberration. Finally beams were synchronized to a precision of 100 fs.

Experimental Upper bound on the Elastic Cross Section

An upper bound of elastic cross section was derived by use of QED

$$\sigma_{upper} = \frac{N_{4,obs}}{N_{4,QED}} \times \sigma_{QED}.$$

They obtained a QED prediction of $N_{4,QED} \approx 7 \times 10^{-21}$ per shot while the observation was limited to $N_{4,obs} \approx 6 \times 10^{-3}$ per shot. The elastic QED cross-section at $\omega = 0.8eV$ is $\sigma_{QED} = 1.8 \times 10^{-66} cm^2$. The obtained upper bound was therefore $\sigma_{upper} = 1.5 \times 10^{-48}$, that is 18 orders of magnitude above QED cross section. So in this experiment, the result of the limit on cross section was further improved by

nine orders from $9.9 \times 10^{-40} \text{cm}^2$ to $1.5 \times 10^{-48} \text{cm}^2$ at the center of mass of photons energy 0.8 eV.

2.3 Photon-photon Elastic Scattering in X-ray region

The first experiment to detect $\gamma\gamma \rightarrow \gamma\gamma$ in the X-ray region was carried out at the SPring-8 Angstrom Compact Free-Electron Laser (SACLA) in Japan by using an X-ray free electron laser (XFEL) which provides the world best X-ray sources [25]. There are basically three X-ray laser facility available in different regions of the world. One is Linac Coherent Light Source (LCLS) in california (USA), the other is European X-ray Free-Electron Laser in Germany and third one is SACLA in japan. All these laser facilities have the same principle of operation i.e high intensity X-ray laser are produced by accelerarating the electrons at high energies and then electrons are made to oscillate and high intensity radiations are emitted. All these facilities produce good sources of X-ray beams, however experiment under discussion was performed at SACLA.

Procedure and Setup

The electron beam was accelarated in synchrotron to high energies and then they are made to undergo oscillations by tuning electron beam and vertical gaps in the magnetic dipoles of undulator. The undulators are basically periodic structure of magnetic dipoles which are designed to enhance the synchrotron radiations. Undulators are used in many devices like synchrotron etc. The experimental setup is shown in Figure 2.3.

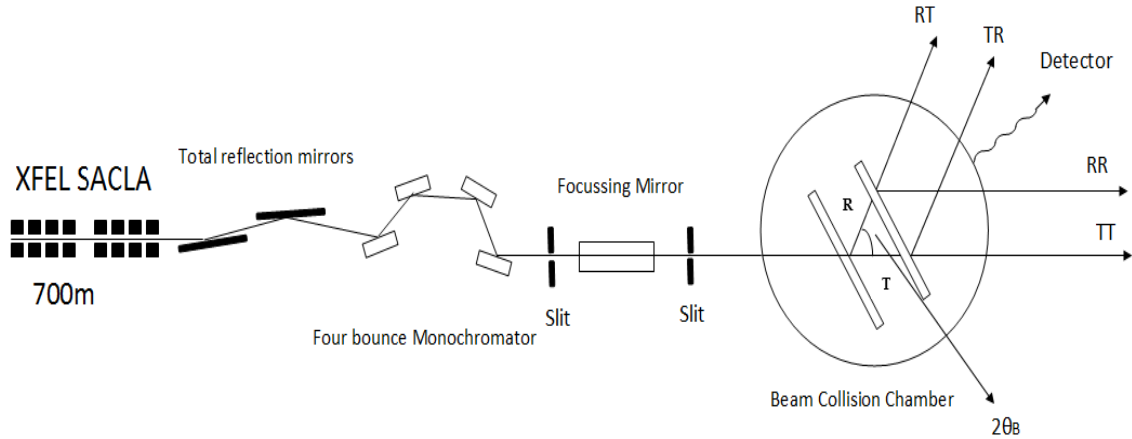


Figure 2.3: The experimental setup of the $\gamma\gamma$ elastic scattering in X-ray region at SACLA [25].

An X-ray beam with energy $\omega=10.985$ KeV was produced in undulator and each pulse containing about 10^{11} photons with a pulse length of less than 10 fs. The X-ray beam after undulator was linearly polarized in the horizontal direction with the horizontal and vertical directions lying in the plane normal to the X-ray beam axis. The undulated X-ray beam contained higher harmonic components which were removed by a pair of carbon coated mirrors. The monochromaticity of the beam was improved from ~ 50 eV to ~ 60 meV by a four-bounce monochromator after total reflection mirror. The horizontal beam size was focused from $\sim 200 \mu m$ to $\sim 1 \mu m$, while unaffected the vertical direction. To improve the quality, the beam was then passed through a pair of four slits on both sides of the focussing mirror. Finally in order to collide the X-ray beams, the original beam was split into two beams by two 0.6 mm thick blades of silicon crystal cut from a high quality single crystal in cylindrical vacuum chamber (beam collision chamber). An X-ray interferometer technique was applied to split the beam. The original beam was split into two coherent beams. One beam was a transmitted beam (T) and

the other was reflected (R) by the first blade. Then these two beams were again split into four more beams RT, RR, TR and TT. Two of the beams RR and TR were made to collide with a crossing angle of $2\theta_B$. The energy of each photon in center of mass system was $\omega_o \sin \theta_B$ and the two photon system was boosted with an energy of $2\omega_o \cos \theta_B$. The maximum and minimum energies for scattered photons were $\omega_o(1 \pm \cos \theta_B)$, for photons along the boosted axis. To detect the X-ray signals, a large Volume germanium detector was used.

Experimental Results

The experiment to search the elastic photon-photon scattering was performed in 2013 at SACLA. The data acquisition time was 9 hours in which a total of 6.5×10^5 pulses were injected into the system. Each pulse contained about 10^{11} no.of photons. No scattering event was observed in the signal region (18.1 KeV - 19.9 KeV). The upper limit on the signal (N_{UL}) obtained was 4.6×10^{-6} pulse⁻¹ at 95 % CL. The calculated luminosity was $(2.1 \pm 0.3) \times 10^{19} \text{m}^{-2} \text{pulse}^{-1}$. The obtained limit on the QED cross section was

$$\sigma_{\gamma\gamma \rightarrow \gamma\gamma} < 1.7 \times 10^{-20} \text{cm}^2,$$

at 95% CL. This result in the X-ray region was at $\omega_{\text{CMS}}=6.5$ KeV which is about 23 orders of magnitude above QED as shown in Figure 2.4.

2.4 Comparison of the Upper Limits in the Visible and X-ray Regions with the QED Cross Section

We have discussed the experiments performed for the search of $\gamma\gamma \rightarrow \gamma\gamma$ in visible and X-ray regions and the upper bounds on cross section obtained in each

experiment. The comparison of upper bounds on cross section and QED cross section at different energies are given in Figure 2.4.

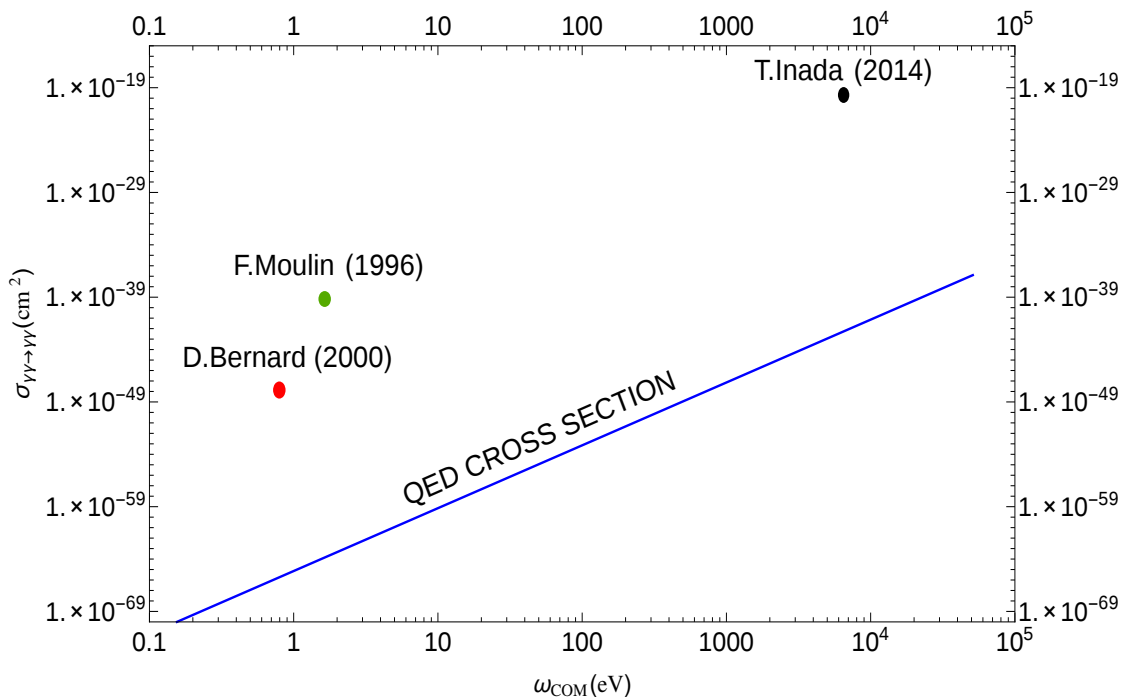


Figure 2.4: A Comparison of the QED cross section and the upper bounds on QED cross section with (95% C.L) obtained in experiments F.Moulin (1996) a head on collision of two laser beams [20], D.Bernard (2000) four wave induced by mixing three laser beams [21] and Inada.T (2014) a collision of X-ray beams [25].

The upper bound on cross section obtained in [21] was $1.5 \times 10^{-48} \text{cm}^2$ at the center of mass photon energy 0.8 eV at which QED cross section is $\sigma_{\text{QED}} = 1.8 \times 10^{-66} \text{cm}^2$. This upper bound was 18 order larger in magnitude than the QED value. In the X-ray region the upper limit obtained was $1.7 \times 10^{-20} \text{cm}^2$ which was 23 order above the QED. The upper bound on cross section in X-ray region is 28 order larger in magnitude than the upper bound in visible region. In visible region scattering events/background noise ratio is low, where as in X-ray region

background noise is low and photons are easy to count. The path of colliding photons and monochromaticity are easy to handle in X-ray region. So search for $\gamma\gamma \rightarrow \gamma\gamma$ in X-ray region is a better option.

2.5 Main Difficulties Faced in Experiments

The experiments to search for photon-photon elastic scattering in low energy regions have been performed i.e in KeV [25] and in eV [20, 21], many experimental proposals were also made, but no experimental confirmation has been made yet, however they were able to set upper bounds on cross section. The main difficulty to observe the process is basically the extremely small cross section specially in low energy region and large background noise. Because of the particle nature of photon, the $\gamma\gamma \rightarrow \gamma\gamma$ is a reaction process as compared to the diffraction and interference phenomenon which are the wave phenomena. The $\gamma\gamma \rightarrow \gamma\gamma$ is a crossed beam experiment which is quite difficult as compared to the conventional experiment in which the target is fixed, so there is a problem to control the initial conditions such as the photon-photon collision time and the focussing of the photon-photon beams. The improvements in search of the real photon-photon scattering may however be dominated by the experimental errors such as the difficulties to tune the laser pulses in exactly the same way as required by the process to be detected. There is a problem in creating a sufficiently good vacuum. There is no meaning to measure the cross section when the experimental uncertainties exceed the accuracy of the theory. The unavailability of the more energetic, intense, powerful and short pulse duration laser are among the main problems.

2.6 Current Laser and X-ray Technology

In the past many experiments have been performed to search for photon-photon scattering and also many experimental proposals were made, but due to laser (Intensity, energy) and experimental Limitations no observation has been made yet. In order to have the experimental confirmation of the process, we need more and more intense, energetic and focused laser beams. There are many laser projects which are under Progress and hopefully we shall have more intense, powerfull lasers in future. For instance CLF Vulcan 10 PW at Rutherford Appleton Laboratory[14], HiPER and European Extreme Light Infrastructure(ELI) [15].

The typical scale for vacuum polarization effect, where real electron-positron pairs creation can take place is given by critical field strength, which is $E_{cr} = \frac{m^2 c^3}{eh} = 1.3 \times 10^{16} \text{ Vcm}^{-1}$ and the equivalent Intensity is $I_{cr} = 2.3 \times 10^{29} \text{ Wcm}^{-2}$, where ‘m’ and ‘e’ are the mass and charge of electron. These intensities lies in magnitude about seven orders above the high produced record by laser [26]. The projects such as 10 PW to vulcan, HiPER and ELI will put the laser to three or four orders in magnitude below the critical value. An X-ray Free-Electron Laser (XFEL) facility, the SPring-8 Angstrom Compact free electron LAser (SACLA) in Japan started work around 2012, which provides the world brilliant X-ray sources [27, 28]. To perform experiments in X-ray region we must take a full advantage of such sources of X-rays.

Current Laser Magnitude

These are the laser magnitude which are available in the Laboratories

$$\begin{aligned}\text{Power } P &\rightarrow \gtrsim 10^{15} \text{ W} \\ \text{Intensity } I &\rightarrow \gtrsim 10^{22} \text{ Wcm}^{-2} \\ \text{MagneticField } B &\rightarrow \gtrsim 10^{10} \text{ G} \equiv 10^6 T \\ \text{ElectricField } E &\rightarrow \gtrsim 10^{14} \text{ Vm}^{-1}.\end{aligned}$$

Laser Projects in Progress

There are two main laser projects among many which are given below

I. CLF Vulcan 10 PW at Rutherford Appleton Laboratory

$$> 10^{23} \text{ Wcm}^{-2}.$$

II. European Extreme Light Infrastructure(ELI)

$$> 10^{25} \text{ Wcm}^{-2}$$

2.7 Summary of Experimental Challenges

The Equation (3.14) shows that the cross section of $\gamma\gamma \rightarrow \gamma\gamma$ is a fast growing function of energy. An improvement in laser technology in terms of both energy and intensity will be welcome. One of the main important step to detect the $\gamma\gamma \rightarrow \gamma\gamma$ is to control background noise because signal to be detected is very small and background signal is very large. There is a need to improve the sensitivity of the detectors because of small cross section specially in low energy region. Since the $\gamma\gamma \rightarrow \gamma\gamma$ is a crossed beam experiment because photons cannot be at rest, so one should need to control the initial conditions such as focussing of photon beams and

photon-photon collision time. In this way geometry of the experimental setup is important to have greater chances of photon-photon scattering. The experiments must be carried both in low and high energy regions. As far as the laser experiments are concerned, we need to improve the scattering events/background noise ratio, luminosity of the lasers and laser energy in the interaction spot. We should use laser beam of short pulse duration and high intensity. In the near coming years, we shall be able to produce the laser in schewinger intensity corresponding to 10^{30} Wcm^{-2} with the pulse duration in zeptosecond regimes which will enable us to detect the photon-photon scattering. On the other hand to search the photon-photon scattering in X-ray regime is also important because photons are easy to count and the path of colliding photons and monochromaticity can be handled easily.

Chapter 3

QED Loop Calculations in the Low Energy Regime

We consider a quantitative treatment of low energy photon-photon elastic scattering in this chapter. We will determine the differential cross section as well as the total scattering cross section for this case.

3.1 Photon-Photon Elastic Scattering Amplitude

The photon-photon elastic scattering process is not allowed at tree level in quantum electrodynamics but is allowed at the 1 loop level. Photon-photon elastic scattering occur due to production of virtual electron-positron pairs by two initial photons which then annihilate to produce two photons in the ‘out’ state. The amplitude of $\gamma\gamma \rightarrow \gamma\gamma$ is described to the lowest order by the Feynman box diagram. There are six possible topologically distinct Feynman diagrams for photon-photon elastic scattering which are given in Figure 3.1. Among these six diagrams, three diagrams differ only in the fermionic loop direction. These Feynman diagrams contribute equally to the scattering amplitude. This is characteristic of the n-point

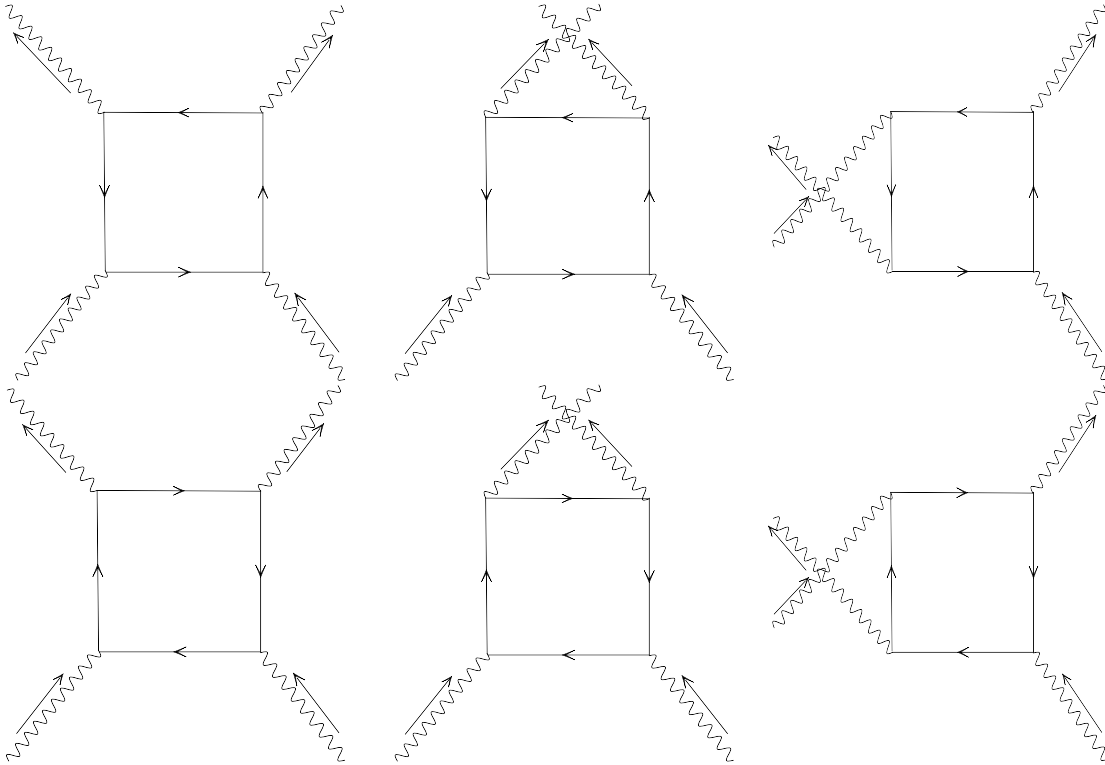


Figure 3.1: All six possible lowest order Feynman diagrams. The bottom graphs are distinct from the top ones only due to the directions of the loops

photon correlation amplitude for even n . Similar diagrams with odd n interfere destructively consistent with Furry's theorem [29]. Therefore, it is enough to consider only the first three Feynman diagrams in Figure 3.1 to calculate the total scattering amplitude. The fermionic loop in this Figure represents virtual particles, which may be thought of as being created and annihilated at intermediate stages. As stated earlier, in order to calculate the total scattering amplitude, it is enough to consider only the three diagrams given in Figure 3.2.

The external wavy lines represent photons with 4-momenta k_1, k_2, k_3 and k_4 , where k_1, k_2 are incoming and k_3, k_4 are outgoing photon 4-momenta and $k_1 + k_2 = k_3 + k_4$ from the law of conservation of energy-momentum. Here we represent the loop momentum by ' q '. The integral over the loop momentum q is divergent and

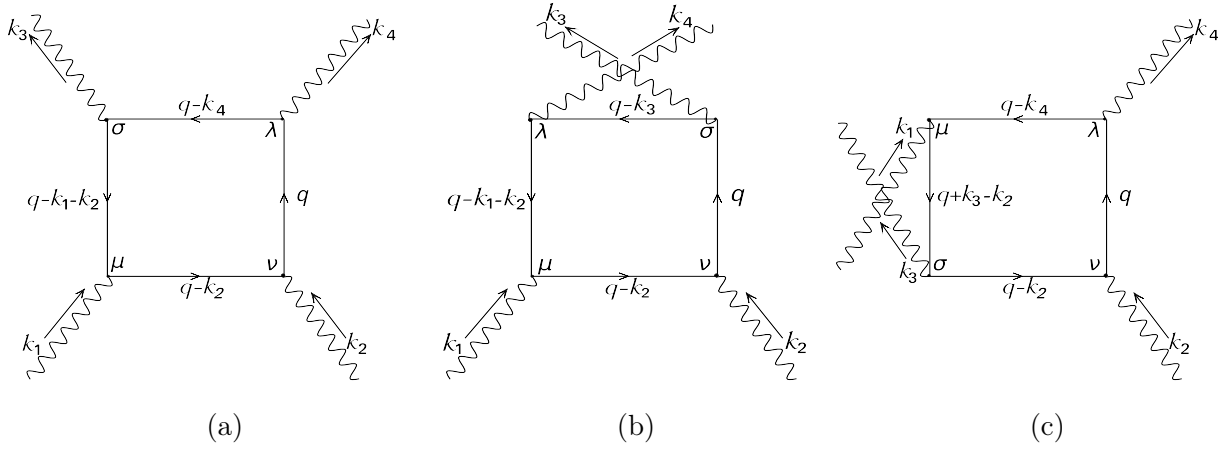


Figure 3.2: Possible lowest order labelled Feynman diagrams of photon-photon elastic scattering.

will be regularized by using dimensional regularization. It will be shown that the divergences cancel when we add the contributions of the three diagrams. The amplitude of $\gamma\gamma \rightarrow \gamma\gamma$ can be calculated by using Feynman rules of QED.

The total amplitude of photon-photon scattering can be written as

$$M = 2(M_1 + M_2 + M_3), \quad (3.1)$$

where M_1 , M_2 and M_3 are amplitudes of diagrams 3.2(a), (b) and (c) respectively. The factor 2 comes because of the equal contribution of the Feynman diagrams which differ only in the fermionic loop direction, as explained earlier. Now we write the total amplitude in terms of photon-photon scattering tensor and four polarization vectors separately.

$$M = 2(M_1^{\lambda\nu\mu\sigma} + M_2^{\sigma\nu\mu\lambda} + M_3^{\lambda\nu\sigma\mu})\epsilon_\lambda^*(k_4)\epsilon_\nu(k_2)\epsilon_\mu(k_1)\epsilon_\sigma^*(k_3),$$

where $\epsilon_\nu(k_2)$, $\epsilon_\mu(k_1)$ are incoming and $\epsilon_\lambda^*(k_4)$, $\epsilon_\sigma^*(k_3)$ are outgoing photon polarization vectors.

3.1.1 Computation of $M_1^{\lambda\nu\mu\sigma}$

Now by using Feynman rules of QED [30], the amplitude M_1 can be written as,

$$M_1 = -\frac{(ie)^4}{(2\pi)^4} \int d^4q \times \frac{\text{Tr}[\gamma^\lambda(\not{q} + m)\gamma^\nu(\not{q} - \not{k}_2 + m)\gamma^\mu(\not{q} - \not{k}_1 - \not{k}_2 + m)\gamma^\sigma(\not{q} - \not{k}_4 + m)]}{[q^2 - m^2 + i\epsilon][(q - k_2)^2 - m^2 + i\epsilon][(q - k_1 - k_2)^2 - m^2 + i\epsilon][(q - k_4)^2 - m^2 + i\epsilon]}, \quad (3.2)$$

where ‘e’ and ‘m’ are, respectively, the charge and mass of the electron. The integration is over loop 4-momentum ‘q’ and the slash is the usual Dirac slash which represents the scalar product, $e.g \not{q} \equiv \gamma \cdot q = \gamma^\mu q_\mu$.

Now we introduce the method of Feynman parameterization to combine the factors in the denominator.

Feynman Parameterization The aim of this technique is to reduce the factors in the denominator to a single factor in the loop momentum ‘q’. As a result of this technique, we have a spherically symmetric integral which can be easily solved. This technique is due to R.P.Feynman and is known as Feynman parameterization [31]. The denominator of Eq.(3.2) can be modified (See Appendix C for details) as follows,

$$\begin{aligned} \frac{1}{D} &= \frac{1}{[q^2 - m^2 + i\epsilon][(q - k_2)^2 - m^2 + i\epsilon][(q - k_1 - k_2)^2 - m^2 + i\epsilon][(q - k_4)^2 - m^2 + i\epsilon]} \\ &= \Gamma(3 + 1) \int_0^1 dx_1 \int_0^{x_1} dx_2 \int_0^{x_2} dx_3 \left[q^2 - m^2 + i\epsilon + \{(q - k_2)^2 - m^2 + i\epsilon - q^2 + m^2 - \right. \\ &\quad \left. i\epsilon\}x_1 + \{(q - k_1 - k_2)^2 - m^2 + i\epsilon - (q - k_2)^2 + m^2 - i\epsilon\}x_2 + \{(q - k_4)^2 - m^2 + i\epsilon - \right. \\ &\quad \left. (q - k_1 - k_2)^2 + m^2 - i\epsilon\}x_3 \right]^{-4}, \end{aligned}$$

where x_1, x_2 and x_3 are the usual ‘Feynman parameters’.

We now have a single factor instead of four in the denominator. We make some

simplifications as

$$\frac{1}{D} = 6 \int_0^1 dx_1 \int_0^{x_1} dx_2 \int_0^{x_2} dx_3 \times$$

$$\left[q^2 - m^2 + i\epsilon + \{(q - k_2)^2 - q^2\}x_1 + \{(q - k_1 - k_2)^2 - (q - k_2)^2\}x_2 + \{(q - k_4)^2 - (q - k_1 - k_2)^2\}x_3 \right]^{-4},$$

$$\frac{1}{D} = 6 \int_0^1 dx_1 \int_0^{x_1} dx_2 \int_0^{x_2} dx_3 \times$$

$$\left[q^2 - m^2 + i\epsilon + \{q^2 - 2q.k_2 + k_2^2 - q^2\}x_1 + \{q^2 - 2q.(k_1 + k_2) + (k_1 + k_2)^2 - q^2 + 2q.k_2 - k_2^2\}x_2 + \{(q^2 - 2q.k_4 + k_4^2 - q^2 + 2q.(k_1 + k_2) - (k_1 + k_2)^2\}x_3 \right]^{-4},$$

$$\frac{1}{D} = 6 \int_0^1 dx_1 \int_0^{x_1} dx_2 \int_0^{x_2} dx_3 \times$$

$$\left[q^2 - m^2 + i\epsilon + \{q^2 - 2q.k_2 + k_2^2 - q^2\}x_1 + \{q^2 - 2q.(k_1 + k_2) + k_1^2 + 2k_1.k_2 + k_2^2 - q^2 + 2q.k_2 - k_2^2\}x_2 + \{(q^2 - 2q.k_4 + k_4^2 - q^2 + 2q.(k_1 + k_2) - k_1^2 - 2k_1.k_2 - k_2^2\}x_3 \right]^{-4}.$$

Since the photon has a zero rest mass, we have $k_1^2 = k_2^2 = k_3^2 = k_4^2 = 0$.

With these substitutions, the above expression becomes

$$\frac{1}{D} = 6 \int_0^1 dx_1 \int_0^{x_1} dx_2 \int_0^{x_2} dx_3 \times \left[q^2 - m^2 + i\epsilon - 2q.k_2x_1 - 2q.(k_1 + k_2)x_2 + 2k_1.k_2x_2 + 2q.k_2x_2 - 2q.k_4x_3 + 2q.(k_1 + k_2)x_3 - 2k_1.k_2x_3 \right]^{-4},$$

$$\frac{1}{D} = 6 \int_0^1 dx_1 \int_0^{x_1} dx_2 \int_0^{x_2} dx_3 \left[q^2 - 2q.(k_2x_1 + k_1x_2 + k_2x_2 - k_2x_3 + k_4x_3 - k_1x_3 - k_2x_3) + 2k_1.k_2x_2 - 2k_1.k_2x_3 - m^2 + i\epsilon \right]^{-4},$$

$$\frac{1}{D} = 6 \int_0^1 dx_1 \int_0^{x_1} dx_2 \int_0^{x_2} dx_3 \times \left[q^2 - 2q.(k_2x_1 + k_1x_2 + (-k_2 + k_4 - k_1)x_3) + 2k_1.k_2x_2 - 2k_1.k_2x_3 - m^2 + i\epsilon \right]^{-4},$$

$$\frac{1}{D} = 6 \int_0^1 dx_1 \int_0^{x_1} dx_2 \int_0^{x_2} dx_3 \left[q^2 - 2q.(k_2x_1 + k_1x_2 - k_3x_3) + 2k_1.k_2(x_2 - x_3) - m^2 + i\epsilon \right]^{-4}.$$

Here we have a single factor with linear and quadratic powers of the loop momentum 'q'.

With this eq (3.2) becomes as

$$M_1^{\lambda\nu\mu\sigma} = -\frac{(ie)^4}{(2\pi)^4} 6 \int_0^1 dx_1 \int_0^{x_1} dx_2 \int_0^{x_2} dx_3 \int d^4q N_1^{\lambda\nu\mu\sigma} \times \left[q^2 - 2q.(k_2x_1 + k_1x_2 - k_3x_3) + 2k_1.k_2(x_2 - x_3) - m^2 + i\epsilon \right]^{-4},$$

there is a problem with the denominator as it has linear terms in 'q', whereas we want to have only those terms that are quadratic in 'q'. In order to get ride of this linear term we proceed as explained below.

$$\text{Let } A^\rho = k_2^\rho x_1 + k_1^\rho x_2 - k_3^\rho x_3$$

$$\text{where } N_1^{\lambda\nu\mu\sigma} = \text{Tr}[\gamma^\lambda(q+m)\gamma^\nu(q-\not{k}_2+m)\gamma^\mu(q-\not{k}_1-\not{k}_2+m)\gamma^\sigma(q-\not{k}_4+m)]$$

$$\text{and } B = 2k_1.k_2(x_2 - x_3) - m^2, \text{ so that}$$

$$M_1^{\lambda\nu\mu\sigma} = -\frac{(ie)^4}{(2\pi)^4} 6 \int_0^1 dx_1 \int_0^{x_1} dx_2 \int_0^{x_2} dx_3 \int d^4q \frac{N_1^{\lambda\nu\mu\sigma}}{\left[q^2 - 2q \cdot A + B + i\epsilon \right]^4}.$$

We substitute $q = l + A$, where 'l' is a new variable for the loop integration. The variable of loop integration 'l' and 'q' differ only by the constant A . This shifting of the variables of integration will help us to complete the square of loop momentum in the denominator. After shifting of variables of integration, the integral will only depends on ℓ^2 .

With this substitution, the above expression becomes,

$$M_1^{\lambda\nu\mu\sigma} = -\frac{(ie)^4}{(2\pi)^4} 6 \int_0^1 dx_1 \int_0^{x_1} dx_2 \int_0^{x_2} dx_3 \int d^4\ell \times$$

$$\frac{\text{Tr}[\gamma^\lambda(\ell + A + m)\gamma^\nu(\ell + A - k_2 + m)\gamma^\mu(\ell + A - k_1 - k_2 + m)\gamma^\sigma(\ell + A - k_4 + m)]}{\left[(\ell + A)^2 - 2(\ell + A) \cdot A + B + i\epsilon \right]^4}$$

or

$$M_1^{\lambda\nu\mu\sigma} = -\frac{(ie)^4}{(2\pi)^4} 6 \int_0^1 dx_1 \int_0^{x_1} dx_2 \int_0^{x_2} dx_3 \int d^4\ell \times$$

$$\frac{\text{Tr}[\gamma^\lambda(\ell + f + m)\gamma^\nu(\ell + g + m)\gamma^\mu(\ell + h + m)\gamma^\sigma(\ell + j + m)]}{\left[\ell^2 - A^2 + B + i\epsilon \right]^4},$$

where

$$f = A, \quad g = A - k_2, \quad h = A - k_1 - k_2, \quad \text{and } j = A - k_4.$$

Dimensional Regularization

Note that the above integral is divergent. Furthermore, it is easy to see from Naive power counting that the divergence is logarithmic due to terms of the type,

$$M_1^{\lambda\nu\mu\sigma} \propto \int_{-\infty}^{\infty} d^4\ell \frac{(\ell^2)^2}{[\ell^2 - \Delta + i\epsilon]^4}.$$

There is a need to regularize these integrals in order to make any sense of them. In $M_1^{\lambda\nu\mu\sigma}$, the loop momentum integral in 4-dimensional space-time is divergent and becomes convergent in dimension d less than 4. So we change the dimensionality from 4 to $D = 4 - \eta$, where $\eta \neq 0$. In this method, we may have fractional dimensions as D and η are not integers.

Also we substitute $\Delta = A^2 - B$, so in D-dimensional space-time, the expression for $M_1^{\lambda\nu\mu\sigma}$ becomes,

$$M_1^{\lambda\nu\mu\sigma} = -\frac{(ie)^4}{(2\pi)^d} 6 \int_0^1 dx_1 \int_0^{x_1} dx_2 \int_0^{x_2} dx_3 \int d^D \ell \times$$

$$\frac{\text{Tr}[\gamma^\lambda(\not{\ell} + \not{f} + m)\gamma^\nu(\not{\ell} + \not{g} + m)\gamma^\mu(\not{\ell} + \not{h} + m)\gamma^\sigma(\not{\ell} + \not{j} + m)]}{\left[\ell^2 - \Delta + i\epsilon\right]^4}, \quad (3.3)$$

Simplification of Numerator

Now we will use some techniques to simplify numerator of (3.3).

$$N_1^{\lambda\nu\mu\sigma} = \text{Tr} \left[\gamma^\lambda(\gamma \cdot f + \gamma \cdot \ell + m)\gamma^\nu(\gamma \cdot g + \gamma \cdot \ell + m)\gamma^\mu(\gamma \cdot h + \gamma \cdot \ell + m)\gamma^\sigma(\gamma \cdot j + \gamma \cdot \ell + m) \right]$$

Here l is the loop momentum, so terms having odd power of loop momenta vanish on integration due to symmetry. Also terms having odd number of gamma matrices vanish, as the trace of an odd number of γ matrices is zero.

$$\begin{aligned}
N_1^{\lambda\nu\mu\sigma} = & \text{Tr} \left[\gamma^\lambda(\gamma \cdot f) \cdot \gamma^\nu(\gamma \cdot g) \gamma^\mu(\gamma \cdot h) \gamma^\sigma(\gamma \cdot j) + m^2 [\gamma^\lambda(\gamma \cdot f) \gamma^\nu(\gamma \cdot g) \gamma^\mu \gamma^\sigma \right. \\
& + \gamma^\lambda(\gamma \cdot f) \gamma^\nu \gamma^\mu(\gamma \cdot h) \gamma^\sigma + \gamma^\lambda(\gamma \cdot f) \gamma^\nu \gamma^\mu \gamma^\sigma(\gamma \cdot j) + \gamma^\lambda \gamma^\nu(\gamma \cdot g) \gamma^\mu(\gamma \cdot h) \gamma^\sigma \\
& + \gamma^\lambda \gamma^\nu(\gamma \cdot g) \gamma^\mu \gamma^\sigma(\gamma \cdot j) + \gamma^\lambda \gamma^\nu \gamma^\mu(\gamma \cdot h) \gamma^\sigma(\gamma \cdot j) + \gamma^\lambda \gamma^\nu \gamma^\mu(\gamma \cdot \ell) \gamma^\sigma(\gamma \cdot \ell) \\
& + \gamma^\lambda \gamma^\nu(\gamma \cdot \ell) \gamma^\mu \gamma^\sigma(\gamma \cdot \ell) + \gamma^\lambda \gamma^\nu(\gamma \cdot \ell) \gamma^\mu(\gamma \cdot \ell) \gamma^\sigma + \gamma^\lambda(\gamma \cdot \ell) \gamma^\nu \gamma^\mu \gamma^\sigma(\gamma \cdot \ell) \\
& + \gamma^\lambda(\gamma \cdot \ell) \gamma^\nu \gamma^\mu(\gamma \cdot \ell) \gamma^\sigma + \gamma^\lambda(\gamma \cdot \ell) \gamma^\nu(\gamma \cdot \ell) \gamma^\mu \gamma^\sigma] \\
& + \gamma^\lambda(\gamma \cdot f) \gamma^\nu(\gamma \cdot g) \gamma^\mu(\gamma \cdot \ell) \gamma^\sigma(\gamma \cdot \ell) + \gamma^\lambda(\gamma \cdot f) \gamma^\nu(\gamma \cdot \ell) \gamma^\mu(\gamma \cdot h) \gamma^\sigma(\gamma \cdot \ell) \\
& + \gamma^\lambda(\gamma \cdot f) \gamma^\nu(\gamma \cdot \ell) \gamma^\mu(\gamma \cdot \ell) \gamma^\sigma(\gamma \cdot j) + \gamma^\lambda(\gamma \cdot \ell) \gamma^\nu(\gamma \cdot g) \gamma^\mu(\gamma \cdot h) \gamma^\sigma(\gamma \cdot \ell) \\
& + \gamma^\lambda(\gamma \cdot \ell) \gamma^\nu(\gamma \cdot g) \gamma^\mu(\gamma \cdot \ell) \gamma^\sigma(\gamma \cdot j) + \gamma^\lambda(\gamma \cdot \ell) \gamma^\nu(\gamma \cdot \ell) \gamma^\mu(\gamma \cdot h) \gamma^\sigma(\gamma \cdot j) \\
& \left. + \gamma^\lambda(\gamma \cdot \ell) \gamma^\nu(\gamma \cdot \ell) \gamma^\mu(\gamma \cdot \ell) \gamma^\sigma(\gamma \cdot \ell) + m^4 \gamma^\lambda \gamma^\nu \gamma^\mu \gamma^\sigma \right] \quad (3.4)
\end{aligned}$$

It is convenient to separately solve the different terms appearing in Eq.(3.4). To this end we define,

$$\begin{aligned}
T_1 &= m^4 \text{Tr}[\gamma^\lambda \gamma^\nu \gamma^\mu \gamma^\sigma] = 4m^4 (-g^{\lambda\mu} g^{\nu\sigma} + g^{\lambda\nu} g^{\mu\sigma} + g^{\lambda\sigma} g^{\mu\nu}) \\
T_2 &= \text{Tr}[m^2 \gamma^\lambda \gamma^\nu \gamma^\mu(\gamma \cdot \ell) \gamma^\sigma(\gamma \cdot \ell) + \gamma^\lambda \gamma^\nu(\gamma \cdot \ell) \gamma^\mu \gamma^\sigma(\gamma \cdot \ell) + \gamma^\lambda \gamma^\nu(\gamma \cdot \ell) \gamma^\mu(\gamma \cdot \ell) \gamma^\sigma \\
&+ \gamma^\lambda(\gamma \cdot \ell) \gamma^\nu \gamma^\mu \gamma^\sigma(\gamma \cdot \ell) + \gamma^\lambda(\gamma \cdot \ell) \gamma^\nu \gamma^\mu(\gamma \cdot \ell) \gamma^\sigma + \gamma^\lambda(\gamma \cdot \ell) \gamma^\nu(\gamma \cdot \ell) \gamma^\mu \gamma^\sigma] \\
T_3 &= \text{Tr}[\gamma^\lambda(\gamma \cdot \ell) \gamma^\nu(\gamma \cdot \ell) \gamma^\mu(\gamma \cdot \ell) \gamma^\sigma(\gamma \cdot \ell)] \\
T_4 &= \text{Tr}[\gamma^\lambda(\gamma \cdot f) \gamma^\nu(\gamma \cdot g) \gamma^\mu(\gamma \cdot \ell) \gamma^\sigma(\gamma \cdot \ell) + \gamma^\lambda(\gamma \cdot f) \gamma^\nu(\gamma \cdot \ell) \gamma^\mu(\gamma \cdot h) \gamma^\sigma(\gamma \cdot \ell) \\
&+ \gamma^\lambda(\gamma \cdot f) \gamma^\nu(\gamma \cdot \ell) \gamma^\mu(\gamma \cdot \ell) \gamma^\sigma(\gamma \cdot j) + \gamma^\lambda(\gamma \cdot \ell) \gamma^\nu(\gamma \cdot g) \gamma^\mu(\gamma \cdot h) \gamma^\sigma(\gamma \cdot \ell) + \\
&\gamma^\lambda(\gamma \cdot \ell) \gamma^\nu(\gamma \cdot g) \gamma^\mu(\gamma \cdot \ell) \gamma^\sigma(\gamma \cdot j) + \gamma^\lambda(\gamma \cdot \ell) \gamma^\nu(\gamma \cdot \ell) \gamma^\mu(\gamma \cdot h) \gamma^\sigma(\gamma \cdot j)] \\
T_5 &= \text{Tr}[\gamma^\lambda(\gamma \cdot f) \gamma^\nu(\gamma \cdot g) \gamma^\mu(\gamma \cdot h) \gamma^\sigma(\gamma \cdot j)]
\end{aligned}$$

$$\begin{aligned}
T_6 = & Tr[m^2(\gamma^\lambda(\gamma \cdot f)\gamma^\nu(\gamma \cdot g)\gamma^\mu\gamma^\sigma + \gamma^\lambda(\gamma \cdot f)\gamma^\nu\gamma^\mu(\gamma \cdot h)\gamma^\sigma + \\
& \gamma^\lambda(\gamma \cdot f)\gamma^\nu\gamma^\mu\gamma^\sigma(\gamma \cdot j) + \gamma^\lambda\gamma^\nu(\gamma \cdot g)\gamma^\mu(\gamma \cdot h)\gamma^\sigma + \gamma^\lambda\gamma^\nu(\gamma \cdot g)\gamma^\mu\gamma^\sigma(\gamma \cdot j) \\
& + \gamma^\lambda\gamma^\nu\gamma^\mu(\gamma \cdot h)\gamma^\sigma(\gamma \cdot j)]
\end{aligned}$$

It is important to first simplify those terms that involve the loop momentum, i.e T_2 , T_3 and T_4 . This can be done using the following relations

$$\begin{aligned}
\ell^\alpha \ell^\beta &= \frac{1}{D} \ell^2 g^{\alpha\beta} \\
\text{and } \ell^\alpha \ell^\beta \ell^\rho \ell^\delta &= \frac{1}{D(D+2)} (\ell^2)^2 (g^{\alpha\beta} g^{\rho\delta} + g^{\alpha\rho} g^{\beta\delta} + g^{\alpha\delta} g^{\beta\rho})
\end{aligned}$$

The simplified forms for T_2 , T_3 and T_4 are as follows;

$$\begin{aligned}
T_2 = & 8m^2(g^{\lambda\nu}g^{\mu\sigma} + g^{\lambda\sigma}g^{\mu\nu} + g^{\lambda\nu}g^{\mu\sigma} + g^{\lambda\sigma}g^{\mu\nu})\frac{1}{D}\ell^2 - \\
& 8m^2(-g^{\lambda\mu}g^{\nu\sigma} + g^{\lambda\nu}g^{\mu\sigma} + g^{\lambda\sigma}g^{\mu\nu})\ell^2
\end{aligned}$$

$$\begin{aligned}
T_3 = & 4(\ell^2)^2(-g^{\lambda\mu}g^{\nu\sigma} + g^{\lambda\nu}g^{\mu\sigma} + g^{\lambda\sigma}g^{\mu\nu}) - 16(g^{\lambda\nu}g^{\mu\sigma} + g^{\lambda\sigma}g^{\mu\nu})\frac{1}{D}(\ell^2)^2 + \\
& 32\ell^\lambda\ell^\mu\ell^\nu\ell^\sigma
\end{aligned}$$

$$\begin{aligned}
T_4 = & Tr[\gamma^\lambda(\gamma \cdot f)\gamma^\nu(\gamma \cdot g)\gamma^\mu\gamma^\alpha\gamma^\sigma\gamma^\beta + \gamma^\lambda(\gamma \cdot f)\gamma^\nu\gamma^\alpha\gamma^\mu(\gamma \cdot h)\gamma^\sigma\gamma^\beta + \\
& \gamma^\lambda(\gamma \cdot f)\gamma^\nu\gamma^\alpha\gamma^\mu\gamma^\beta\gamma^\sigma(\gamma \cdot j) + \gamma^\lambda\gamma^\alpha\gamma^\nu(\gamma \cdot g)\gamma^\mu(\gamma \cdot h)\gamma^\sigma\gamma^\beta + \\
& \gamma^\lambda\gamma^\alpha\gamma^\nu(\gamma \cdot g)\gamma^\mu\gamma^\beta\gamma^\sigma(\gamma \cdot j) + \gamma^\lambda\gamma^\alpha\gamma^\nu\gamma^\beta\gamma^\mu(\gamma \cdot h)\gamma^\sigma(\gamma \cdot j)]\frac{1}{D}g_{\alpha\beta}\ell^2 \\
= & T_7 \frac{1}{D} g_{\alpha\beta} \ell^2, \text{ where } T_7 \text{ is the trace of the terms in square bracket.}
\end{aligned}$$

By substituting T_1 , T_2 , T_3 , T_4 , T_5 and T_6 in (3.3), we get

$$M_1^{\lambda\nu\mu\sigma} = -\frac{(ie)^4}{(2\pi)^d} 6 \int_0^1 dx_1 \int_0^{x_1} dx_2 \int_0^{x_2} dx_3 \int d^D \ell \times \frac{T_1 + T_2 + T_3 + T_4 + T_5 + T_6}{\left[\ell^2 - \Delta + i\epsilon\right]^4},$$

$$\begin{aligned}
M_1^{\lambda\nu\mu\sigma} &= -\frac{(ie)^4}{(2\pi)^d} 6 \int_0^1 dx_1 \int_0^{x_1} dx_2 \int_0^{x_2} dx_3 \\
&\left\{ 4m^4 (-g^{\lambda\mu} g^{\nu\sigma} + g^{\lambda\nu} g^{\mu\sigma} + g^{\lambda\sigma} g^{\mu\nu}) \int d^D \ell \frac{1}{[\ell^2 - \Delta + i\epsilon]^4} + \right. \\
&16m^2 (g^{\lambda\nu} g^{\mu\sigma} + g^{\lambda\sigma} g^{\mu\nu}) \frac{1}{d} \int d^D \ell \frac{\ell^2}{[\ell^2 - \Delta + i\epsilon]^4} - \\
&8m^2 (-g^{\lambda\mu} g^{\nu\sigma} + g^{\lambda\nu} g^{\mu\sigma} + g^{\lambda\sigma} g^{\mu\nu}) \int d^D \ell \frac{\ell^2}{[\ell^2 - \Delta + i\epsilon]^4} + \\
&4 (-g^{\lambda\mu} g^{\nu\sigma} + g^{\lambda\nu} g^{\mu\sigma} + g^{\lambda\sigma} g^{\mu\nu}) \int d^D \ell \frac{(\ell^2)^2}{[\ell^2 - \Delta + i\epsilon]^4} - \\
&16 (g^{\lambda\nu} g^{\mu\sigma} + g^{\lambda\sigma} g^{\mu\nu}) \frac{1}{d} \int d^D \ell \frac{(\ell^2)^2}{[\ell^2 - \Delta + i\epsilon]^4} + \\
&32 \int d^D \ell \frac{\ell^\lambda \ell^\mu \ell^\nu \ell^\sigma}{[\ell^2 - \Delta + i\epsilon]^4} + T_7 \frac{g_{\alpha\beta}}{d} \int d^D \ell \frac{l^2}{[\ell^2 - \Delta + i\epsilon]^4} + \\
&\left. (T_5 + T_6) \int d^D \ell \frac{1}{[\ell^2 - \Delta + i\epsilon]^4} \right\}. \tag{3.5}
\end{aligned}$$

We use the dimensional regularization scheme to regularize the loop momentum integral [30]. Using the standard results (see Appendix C), we get

$$\begin{aligned}
M_1^{\lambda\nu\mu\sigma} &= -6(ie)^4 \int_0^1 dx_1 \int_0^{x_1} dx_2 \int_0^{x_2} dx_3 \\
&\left\{ 4m^4 (-g^{\lambda\mu}g^{\nu\sigma} + g^{\lambda\nu}g^{\mu\sigma} + g^{\lambda\sigma}g^{\mu\nu}) \frac{(-1)^4 i \Gamma(4 - D/2)}{(4\pi)^{D/2} \Gamma(4)} \left[\frac{1}{\Delta}\right]^{4-D/2} + \right. \\
&16m^2 (g^{\lambda\nu}g^{\mu\sigma} + g^{\lambda\sigma}g^{\mu\nu}) \frac{1}{d} \frac{i}{(4\pi)^{D/2}} \frac{D \Gamma(3 - D/2)}{2 \Gamma(4)} \left[\frac{1}{\Delta}\right]^{3-D/2} - \\
&8m^2 (-g^{\lambda\mu}g^{\nu\sigma} + g^{\lambda\nu}g^{\mu\sigma} + g^{\lambda\sigma}g^{\mu\nu}) \frac{i}{(4\pi)^{D/2}} \frac{D \Gamma(3 - D/2)}{2 \Gamma(4)} \left[\frac{1}{\Delta}\right]^{3-D/2} + \\
&4 (-g^{\lambda\mu}g^{\nu\sigma} + g^{\lambda\nu}g^{\mu\sigma} + g^{\lambda\sigma}g^{\mu\nu}) \frac{(-1)^4 i}{(4\pi)^{D/2}} \frac{d(D+2)}{4} \frac{\Gamma(2 - D/2)}{\Gamma(4)} \left[\frac{1}{\Delta}\right]^{2-D/2} - \\
&16 (g^{\lambda\nu}g^{\mu\sigma} + g^{\lambda\sigma}g^{\mu\nu}) \frac{1}{d} \frac{(-1)^4 i}{(4\pi)^{D/2}} \frac{d(D+2)}{4} \frac{\Gamma(2 - D/2)}{\Gamma(4)} \left[\frac{1}{\Delta}\right]^{2-D/2} + \\
&32 \frac{(-1)^4 i \Gamma(2 - D/2)}{(4\pi)^{D/2} \Gamma(4)} \left[\frac{1}{\Delta}\right]^{2-D/2} \frac{(g^{\lambda\mu}g^{\nu\sigma} + g^{\lambda\nu}g^{\mu\sigma} + g^{\lambda\sigma}g^{\mu\nu})}{4} + \\
&T_7 \frac{g_{\alpha\beta}}{d} \frac{i}{(4\pi)^{D/2}} \frac{D \Gamma(3 - D/2)}{2 \Gamma(4)} \left[\frac{1}{\Delta}\right]^{3-D/2} + \\
&(T_5 + T_6) \frac{(-1)^4 i \Gamma(4 - D/2)}{(4\pi)^{D/2} \Gamma(4)} \left[\frac{1}{\Delta}\right]^{4-D/2} \left. \right\}.
\end{aligned}$$

After a little algebra, we get

$$\begin{aligned}
M_1^{\lambda\nu\mu\sigma} = & -\frac{ie^4}{(4\pi)^{D/2}} \int_0^1 dx_1 \int_0^{x_1} dx_2 \int_0^{x_2} dx_3 \left\{ 4m^4 (-g^{\lambda\mu} g^{\nu\sigma} + g^{\lambda\nu} g^{\mu\sigma} + g^{\lambda\sigma} g^{\mu\nu}) \right. \\
& \Gamma(4 - D/2) \left[\frac{1}{\Delta} \right]^{4-D/2} + 8m^2 (g^{\lambda\nu} g^{\mu\sigma} + g^{\lambda\sigma} g^{\mu\nu}) \Gamma(3 - D/2) \left[\frac{1}{\Delta} \right]^{3-D/2} \\
& -4m^2 (-g^{\lambda\mu} g^{\nu\sigma} + g^{\lambda\nu} g^{\mu\sigma} + g^{\lambda\sigma} g^{\mu\nu}) d \Gamma(3 - D/2) \left[\frac{1}{\Delta} \right]^{3-D/2} \\
& + (-g^{\lambda\mu} g^{\nu\sigma} + g^{\lambda\nu} g^{\mu\sigma} + g^{\lambda\sigma} g^{\mu\nu}) D(D+2) \Gamma(2 - D/2) \left[\frac{1}{\Delta} \right]^{2-D/2} \\
& -4 (g^{\lambda\nu} g^{\mu\sigma} + g^{\lambda\sigma} g^{\mu\nu}) (D+2) \Gamma(2 - D/2) \left[\frac{1}{\Delta} \right]^{2-D/2} \\
& + 8 (g^{\lambda\mu} g^{\nu\sigma} + g^{\lambda\nu} g^{\mu\sigma} + g^{\lambda\sigma} g^{\mu\nu}) \Gamma(2 - D/2) \left[\frac{1}{\Delta} \right]^{2-D/2} \\
& \left. + T_7 \frac{g_{\alpha\beta}}{2} \Gamma(3 - D/2) \left[\frac{1}{\Delta} \right]^{3-D/2} + (T_5 + T_6) \Gamma(4 - D/2) \left[\frac{1}{\Delta} \right]^{4-D/2} \right\}.
\end{aligned}$$

As $D = 4 - \eta$ by letting η approaches to zero, D approaches to 4. When $\eta \rightarrow 0$, $\Gamma(2 - D/2)$ diverges i.e the loop integrals are still divergent . Since $D = 4 - \eta$ depends on η , so we expand divergent terms in a Laurent series in η ,

$$\Gamma(2 - D/2) \left[\frac{1}{\Delta} \right]^{2-D/2} = \Gamma\left(\frac{\eta}{2}\right) \left[\frac{1}{\Delta} \right]^{\frac{\eta}{2}} = \frac{2}{\eta} - \log \Delta - \eta + \log(4\pi) + O(\eta)$$

leting $\eta \rightarrow 0$ and $D \rightarrow 4$, $M_1^{\lambda\nu\mu\sigma}$ is still divergent. Substituting the above in $M_1^{\lambda\nu\mu\sigma}$, the scattering amplitude tensor becomes

$$\begin{aligned}
M_1^{\lambda\nu\mu\sigma} &= -\frac{ie^4}{(4\pi)^{D/2}} \int_0^1 dx_1 \int_0^{x_1} dx_2 \int_0^{x_2} dx_3 \left\{ 4m^4 (-g^{\lambda\mu} g^{\nu\sigma} + g^{\lambda\nu} g^{\mu\sigma} + g^{\lambda\sigma} g^{\mu\nu}) \frac{1}{\Delta^2} \right. \\
&+ 8m^2 (g^{\lambda\nu} g^{\mu\sigma} + g^{\lambda\sigma} g^{\mu\nu}) \frac{1}{\Delta} - 16m^2 (-g^{\lambda\mu} g^{\nu\sigma} + g^{\lambda\nu} g^{\mu\sigma} + g^{\lambda\sigma} g^{\mu\nu}) \frac{1}{\Delta} \\
&+ (-g^{\lambda\mu} g^{\nu\sigma} + g^{\lambda\nu} g^{\mu\sigma} + g^{\lambda\sigma} g^{\mu\nu}) \left(\frac{48}{\eta} - 24 \log \Delta - 24\eta + 24 \log(4\pi) - 20 \right. \\
&+ O(\eta) \left. \right) - 4 (g^{\lambda\nu} g^{\mu\sigma} + g^{\lambda\sigma} g^{\mu\nu}) \left(\frac{12}{\eta} - 6 \log \Delta - 6\eta + 6 \log(4\pi) - 2 + O(\eta) \right) \\
&+ 8 (g^{\lambda\mu} g^{\nu\sigma} + g^{\lambda\nu} g^{\mu\sigma} + g^{\lambda\sigma} g^{\mu\nu}) \left(\frac{2}{\eta} - \log \Delta - \eta + \log(4\pi) + O(\eta) \right) + \\
&\left. T_7 \frac{g_{\alpha\beta}}{2} \frac{1}{\Delta} + (T_5 + T_6) \frac{1}{\Delta^2} \right\}.
\end{aligned}$$

The above expression contains some terms like $\frac{1}{\Delta}$, $\frac{1}{\Delta^2}$ and $\log \Delta$, where $\Delta = A^2 - B = m^2(1 + \frac{U_1}{m^2})$ and U_1 is given as

$$U_1 = -2x_1x_3k_2 \cdot k_3 - 2x_3x_2k_2 \cdot k_4 - 2x_2k_3 \cdot k_4 + 2x_1x_2k_3 \cdot k_4 + 2x_3k_3 \cdot k_4.$$

We are considering the $\gamma\gamma \rightarrow \gamma\gamma$ in the low energy regimes, where we use the approximation $\frac{\omega}{m_e} \ll 1$. Since we are doing calculations of $\gamma\gamma \rightarrow \gamma\gamma$ by considering the electronic loop contribution, so the energy scale is the rest mass of electron m_e . We will expand the whole amplitude in terms of $\frac{\omega}{m_e}$ and will keep only the leading order terms in $\frac{\omega}{m_e}$ by neglecting the higher powers terms. The main reason for using this low energy approximation is the available laser and X-ray technology where the photon has energy ω very less than the rest mass of electron.

We use Binomial series to expand $\frac{1}{\Delta}$, $\frac{1}{\Delta^2}$ and logarithmic series to expand $\log \Delta$.

The binomial series is given as

$$(1+x)^n = 1 + nx + \frac{n(n-1)}{2!}x^2 + \dots \quad \text{where } |x| < 1$$

The logarithmic series expansion is

$$\ln(1+x) = x - \frac{1}{2}x^2 + \frac{1}{3}x^3 + \dots \quad \text{where } |x| < 1$$

So in our case, we have

$$\frac{1}{\Delta} = \frac{1}{m^2} - \frac{U_1}{m^4} + \frac{U_1 * U_1}{m^6} +,$$

$$\frac{1}{\Delta^2} = \frac{1}{m^4} - 2 \frac{U_1}{m^6} + 3 \frac{U_1 * U_1}{m^8}$$

$$\text{and } \ln \Delta = \frac{U_1}{m^2} - \frac{1}{2} \frac{U_1 * U_1}{m^4}$$

note that $U_1 \propto \omega^2$, where ω is the energy of photon.

3.1.2 Amplitude M_1

The amplitude M_1 is

$$M_1 = M_1^{\lambda\nu\mu\sigma} \epsilon_\lambda^*(k_4) \epsilon_\nu(k_2) \epsilon_\mu(k_1) \epsilon_\sigma^*(k_3).$$

Putting the values of all the above series expansions, the simplified form of the amplitude of diagram 3.2 (a) becomes

$$\begin{aligned}
M_1 = & -\frac{ie^4}{(4\pi)^{D/2}} \int_0^1 dx_1 \int_0^{x_1} dx_2 \int_0^{x_2} dx_3 \left\{ 4m^4 (-g^{\lambda\mu} g^{\nu\sigma} + g^{\lambda\nu} g^{\mu\sigma} + g^{\lambda\sigma} g^{\mu\nu}) \frac{1}{\Delta^2} \right. \\
& + 8m^2 (g^{\lambda\nu} g^{\mu\sigma} + g^{\lambda\sigma} g^{\mu\nu}) \frac{1}{\Delta} - 16m^2 (-g^{\lambda\mu} g^{\nu\sigma} + g^{\lambda\nu} g^{\mu\sigma} + g^{\lambda\sigma} g^{\mu\nu}) \frac{1}{\Delta} \\
& + (-g^{\lambda\mu} g^{\nu\sigma} + g^{\lambda\nu} g^{\mu\sigma} + g^{\lambda\sigma} g^{\mu\nu}) \left(\frac{48}{\eta} - 24 \log \Delta - 24\eta + 24 \log(4\pi) - 20 \right. \\
& \left. + O(\eta) \right) - 4 (g^{\lambda\nu} g^{\mu\sigma} + g^{\lambda\sigma} g^{\mu\nu}) \left(\frac{12}{\eta} - 6 \log \Delta - 6\eta + 6 \log(4\pi) - 2 + O(\eta) \right) \\
& + 8 (g^{\lambda\mu} g^{\nu\sigma} + g^{\lambda\nu} g^{\mu\sigma} + g^{\lambda\sigma} g^{\mu\nu}) \left(\frac{2}{\eta} - \log \Delta - \eta + \log(4\pi) + O(\eta) \right) + \\
& \left. T_7 \frac{g_{\alpha\beta}}{2} \frac{1}{\Delta} + (T_5 + T_6) \frac{1}{\Delta^2} \right\} \epsilon_\lambda^*(k_4) \epsilon_\nu(k_2) \epsilon_\mu(k_1) \epsilon_\sigma^*(k_3). \tag{3.6}
\end{aligned}$$

Here it can be seen that if we let η approaches to 0, Eq. 3.6 is still divergent and the divergences appear as $\frac{1}{\eta}$. However, we will not let η tends to 0 until we add the amplitudes of all the three Feynman diagrams to get total amplitude.

3.1.3 Amplitude M_2

The amplitude of Figure 3.2 (b) can be written directly from the amplitude of M_1 with a few changes. We interchange k_3 with k_4 and σ with λ .

$$\begin{aligned}
M_2 = & -\frac{ie^4}{(4\pi)^{D/2}} \int_0^1 dx_1 \int_0^{x_1} dx_2 \int_0^{x_2} dx_3 \left\{ 4m^4 (-g^{\sigma\mu} g^{\nu\lambda} + g^{\sigma\nu} g^{\mu\lambda} + g^{\sigma\lambda} g^{\mu\nu}) \frac{1}{\Delta'^2} \right. \\
& + 8m^2 (g^{\sigma\nu} g^{\mu\lambda} + g^{\sigma\lambda} g^{\mu\nu}) \frac{1}{\Delta'} - 16m^2 (-g^{\sigma\mu} g^{\nu\lambda} + g^{\sigma\nu} g^{\mu\lambda} + g^{\sigma\lambda} g^{\mu\nu}) \frac{1}{\Delta'} + \\
& (-g^{\sigma\mu} g^{\nu\lambda} + g^{\sigma\nu} g^{\mu\lambda} + g^{\sigma\lambda} g^{\mu\nu}) \left(\frac{48}{\eta} - 24 \log \Delta' - 24\eta + 24 \log(4\pi) - 20 + \right. \\
& \left. O(\eta) \right) - 4(g^{\sigma\nu} g^{\mu\lambda} + g^{\sigma\lambda} g^{\mu\nu}) \left(\frac{12}{\eta} - 6 \log \Delta' - 6\eta + 6 \log(4\pi) - 2 + O(\eta) \right) \\
& + 8 (g^{\sigma\mu} g^{\nu\lambda} + g^{\sigma\nu} g^{\mu\lambda} + g^{\sigma\lambda} g^{\mu\nu}) \left(\frac{2}{\eta} - \log \Delta' - \eta + \log(4\pi) + O(\eta) \right) + \\
& \left. T_{77} \frac{g_{\alpha\beta}}{2} \frac{1}{\Delta'} + (T_{55} + T_{66}) \frac{1}{\Delta'^2} \right\} \epsilon_\sigma^*(k_4) \epsilon_\nu(k_2) \epsilon_\mu(k_1) \epsilon_\lambda^*(k_3), \tag{3.7}
\end{aligned}$$

$$\begin{aligned}
\text{where } T_{77} = & Tr[\gamma^\sigma(\gamma.f')\gamma^\nu(\gamma.g')\gamma^\mu\gamma^\alpha\gamma^\lambda\gamma^\beta + \gamma^\sigma(\gamma.f')\gamma^\nu\gamma^\alpha\gamma^\mu(\gamma.h')\gamma^\lambda\gamma^\beta + \\
& \gamma^\sigma(\gamma.f')\gamma^\nu\gamma^\alpha\gamma^\mu\gamma^\beta\gamma^\lambda(\gamma.j') + \gamma^\sigma\gamma^\alpha\gamma^\nu(\gamma.g')\gamma^\mu(\gamma.h')\gamma^\lambda\gamma^\beta + \\
& \gamma^\sigma\gamma^\alpha\gamma^\nu(\gamma.g')\gamma^\mu\gamma^\beta\gamma^\lambda(\gamma.j') + \gamma^\sigma\gamma^\alpha\gamma^\nu\gamma^\beta\gamma^\mu(\gamma.h')\gamma^\lambda(\gamma.j')]
\end{aligned}$$

$$T_{55} = Tr[\gamma^\lambda(\gamma.f')\gamma^\nu(\gamma.g')\gamma^\mu(\gamma.h')\gamma^\sigma(\gamma.j')]$$

$$\begin{aligned}
T_{66} = & m^2 Tr[\gamma^\lambda(\gamma.f')\gamma^\nu(\gamma.g')\gamma^\mu\gamma^\sigma + \gamma^\lambda(\gamma.f')\gamma^\nu\gamma^\mu(\gamma.h')\gamma^\sigma + \\
& \gamma^\lambda(\gamma.f')\gamma^\nu\gamma^\mu\gamma^\sigma(\gamma.j') + \gamma^\lambda\gamma^\nu(\gamma.g')\gamma^\mu(\gamma.h')\gamma^\sigma + \\
& \gamma^\lambda\gamma^\nu(\gamma.g')\gamma^\mu\gamma^\sigma(\gamma.j') + \gamma^\lambda\gamma^\nu\gamma^\mu(\gamma.h')\gamma^\sigma(\gamma.j')]
\end{aligned}$$

$$A'^\rho = k_2^\rho x_1 + k_1^\rho x_2 - k_3^\rho x_4, \quad f' = \not{A}', \quad g' = \not{A}' - \not{k}_2, \quad h' = \not{A}' - \not{k}_1 - \not{k}_2, \quad j' = \not{A}' - \not{k}_3$$

$$\Delta' = A'^2 - B = m^2 \left(1 + \frac{U_2}{m^2}\right) = m^2 \left(1 + \frac{U_2}{m^2}\right)$$

$$\frac{1}{\Delta'} = \frac{1}{m^2} - \frac{U_2}{m^4} + \frac{U_2 * U_2}{m^6}$$

$$\frac{1}{\Delta'^2} = \frac{1}{m^4} - 2 \frac{U_2}{m^6} + 3 \frac{U_2 * U_2}{m^8}$$

$$\text{and } \ln \Delta' = \frac{U_2}{m^2} - \frac{1}{2} \frac{U_2 * U_2}{m^4}$$

where $U_2 = -2x_3x_2k_2 \cdot k_3 - 2x_1x_3k_2 \cdot k_4 - 2x_2k_3 \cdot k_4 + 2x_1x_2k_3 \cdot k_4 + 2x_3k_3 \cdot k_4$

3.1.4 Amplitude M_3

The amplitude of Figure 3.2 (c) can be written directly from the amplitude of M_1 with a few changes. We interchange $-k_1$ with k_3 and σ with μ .

$$\begin{aligned} M_3 = & -\frac{ie^4}{(4\pi)^{D/2}} \int_0^1 dx_1 \int_0^{x_1} dx_2 \int_0^{x_2} dx_3 \left\{ 4m^4 (-g^{\mu\sigma} g^{\nu\lambda} + g^{\mu\nu} g^{\sigma\lambda} + g^{\mu\lambda} g^{\sigma\nu}) \frac{1}{\Delta''^2} \right. \\ & + 8m^2 (g^{\mu\nu} g^{\sigma\lambda} + g^{\mu\lambda} g^{\sigma\nu}) \frac{1}{\Delta''} - 16m^2 (-g^{\mu\sigma} g^{\nu\lambda} + g^{\mu\nu} g^{\sigma\lambda} + g^{\mu\lambda} g^{\sigma\nu}) \frac{1}{\Delta''} \\ & + (-g^{\mu\sigma} g^{\nu\lambda} + g^{\mu\nu} g^{\sigma\lambda} + g^{\mu\lambda} g^{\sigma\nu}) \left(\frac{48}{\eta} - 24 \log \Delta'' - 24\eta + 24 \log(4\pi) - 20 \right. \\ & \left. + O(\eta) \right) - 4(g^{\mu\nu} g^{\sigma\lambda} + g^{\mu\lambda} g^{\sigma\nu}) \left(\frac{12}{\eta} - 6 \log \Delta'' - 6\eta + 6 \log(4\pi) - 2 + O(\eta) \right) \\ & \left. + 8 (g^{\mu\sigma} g^{\nu\lambda} + g^{\mu\nu} g^{\sigma\lambda} + g^{\mu\lambda} g^{\sigma\nu}) \left(\frac{2}{\eta} - \log \Delta'' - \eta + \log(4\pi) + O(\eta) \right) + \right. \\ & \left. T_{777} \frac{g_{\alpha\beta}}{2} \frac{1}{\Delta''} + (T_{555} + T_{666}) \frac{1}{\Delta''^2} \right\} \epsilon_\mu^*(k_4) \epsilon_\nu(k_2) \epsilon_\sigma(k_1) \epsilon_\lambda^*(k_3), \end{aligned} \quad (3.8)$$

$$\text{where } T_{777} = Tr[\gamma^\mu(\gamma.f'')\gamma^\nu(\gamma.g'')\gamma^\sigma\gamma^\alpha\gamma^\lambda\gamma^\beta + \gamma^\mu(\gamma.f'')\gamma^\nu\gamma^\alpha\gamma^\sigma(\gamma.h'')\gamma^\lambda\gamma^\beta + \\ \gamma^\mu(\gamma.f'')\gamma^\nu\gamma^\alpha\gamma^\sigma\gamma^\beta\gamma^\lambda(\gamma.j'') + \gamma^\mu\gamma^\alpha\gamma^\nu(\gamma.g'')\gamma^\sigma(\gamma.h'')\gamma^\lambda\gamma^\beta + \\ \gamma^\mu\gamma^\alpha\gamma^\nu(\gamma.g'')\gamma^\sigma\gamma^\beta\gamma^\lambda(\gamma.j'') + \gamma^\mu\gamma^\alpha\gamma^\nu\gamma^\beta\gamma^\sigma(\gamma.h'')\gamma^\lambda(\gamma.j'')]]$$

$$T_{555} = Tr[\gamma^\lambda(\gamma.f'')\gamma^\nu(\gamma.g'')\gamma^\sigma(\gamma.h'')\gamma^\mu(\gamma.j'')]]$$

$$T_{666} = m^2 Tr[\gamma^\lambda(\gamma.f'')\gamma^\nu(\gamma.g'')\gamma^\sigma\gamma^\mu + \gamma^\lambda(\gamma.f'')\gamma^\nu\gamma^\sigma(\gamma.h'')\gamma^\mu + \gamma^\lambda(\gamma.f'')\gamma^\nu\gamma^\sigma\gamma^\mu(\gamma.j'') \\ + \gamma^\lambda\gamma^\nu(\gamma.g'')\gamma^\sigma(\gamma.h'')\gamma^\mu + \gamma^\lambda\gamma^\nu(\gamma.g'')\gamma^\sigma\gamma^\mu(\gamma.j'') + \gamma^\lambda\gamma^\nu\gamma^\sigma(\gamma.h'')\gamma^\mu(\gamma.j'')]]$$

$$A''^\rho = k_2^\rho x_1 - k_3^\rho x_2 + k_1^\rho x_4, \quad f'' = \mathcal{A}'', \quad g'' = \mathcal{A}'' - k_2, \quad h'' = \mathcal{A}'' + k_3 - k_2, \quad j'' = \mathcal{A}'' + k_1$$

$$\Delta'' = A''^2 - B' = m^2(1 + \frac{U_3}{m^2}) = m^2(1 + \frac{U_3}{m^2})$$

$$\frac{1}{\Delta''} = \frac{1}{m^2} - \frac{U_3}{m^4} + \frac{U_3 * U_3}{m^6}$$

$$\frac{1}{\Delta''^2} = \frac{1}{m^4} - 2 \frac{U_3}{m^6} + 3 \frac{U_3 * U_3}{m^8}$$

$$\text{and } \ln \Delta'' = \frac{U_3}{m^2} - \frac{1}{2} \frac{U_3 * U_3}{m^4}$$

$$\text{where } U_3 = -2x_1x_2k_2 \cdot k_3 + 2x_2k_2 \cdot k_3 - 2x_3k_2 \cdot k_3 - 2x_3x_2k_2 \cdot k_4 + 2x_1x_3k_3 \cdot k_4$$

The total $\gamma\gamma \rightarrow \gamma\gamma$ amplitude is given by (3.1). Substituting (3.6), (3.7) and (3.8) in (3.1) we get the total amplitude. Now at this stage all the divergences cancel by adding amplitudes of all three diagrams. So we can let $\eta \rightarrow 0$ and the total amplitude is finite.

3.1.5 The Ward Identity

In QED lagrangian, the interaction term is $e j^\mu A_\mu$, where $j^\mu = \bar{\Psi} \gamma^\mu \Psi$ and Ψ , $\bar{\Psi}$ respectively correspond to fermionic and anti-fermionic fields. This current j^μ must be conserved, so we have

$$\partial_\mu j^\mu = 0,$$

this is basically a consequence of gauge symmetry

$$\Psi(x) \longrightarrow e^{i\alpha(x)} \Psi(x), \quad A_\mu \longrightarrow A_\mu - \frac{1}{e} \partial_\mu \alpha(x).$$

Now in our case, we have polarization vectors $\epsilon_\lambda^*(k_4)$, $\epsilon_\nu(k_2)$, $\epsilon_\mu(k_1)$, and $\epsilon_\sigma^*(k_3)$ for all external four photons in the amplitude. Now if we replace the external polarization vectors by their 4-momentum vectors, then the amplitude vanish i.e

$$k_{1\mu} k_{2\nu} k_{3\sigma} k_{4\lambda} (M_1^{\lambda\nu\mu\sigma} + M_2^{\sigma\nu\mu\lambda} + M_3^{\lambda\nu\sigma\mu}) = 0,$$

where $M_1^{\lambda\nu\mu\sigma}$, $M_2^{\sigma\nu\mu\lambda}$ and $M_3^{\lambda\nu\sigma\mu}$ are the amplitude tensors of the three Feynman diagrams 3.2 (a), (b) and (c). This famous relation is known as the Ward identity. The Ward identity is true for total amplitude but it may not be true for individual Feynman's diagram. This Ward identity holds if the amplitude is finite and it will make sure that the amplitude contains no divergence. Since the lagrangian is invariant under the gauge transformations and so will be its equations of motion. Therefore, QED amplitude must also be gauge invariant and this is ensure only if the Ward identity holds. Under the local gauge transformations the polarization vector transform as

$$\epsilon_\mu(k_1) M^{\lambda\nu\mu\sigma} \longrightarrow \epsilon'_\mu(k_1) M^{\lambda\nu\mu\sigma} \longrightarrow (\epsilon_\mu(k_1) - \frac{1}{e} k_{1\mu}) M^{\lambda\nu\mu\sigma} = 0.$$

The amplitude will be gauge invariant only if the $k_{1\mu} M^{\lambda\nu\mu\sigma} = 0$. So we can say that the gauge invariance, current conservation and Ward identity are basically different views of the same thing.

$$\text{Gauge Invariance} \longleftrightarrow \text{Current Conservation} \longleftrightarrow \text{Ward Identity}$$

3.1.6 Photon Polarization Vectors

The photon-photon elastic scattering involves four polarization vectors $\epsilon_\mu(k_1)$, $\epsilon_\nu(k_2)$, $\epsilon_\sigma^*(k_3)$ and $\epsilon_\lambda^*(k_4)$, where $\epsilon_\mu(k_1)$ and $\epsilon_\nu(k_2)$ are incoming and $\epsilon_\sigma^*(k_3)$ and $\epsilon_\lambda^*(k_4)$ are outgoing photon polarizations vectors. In our calculations, we consider circularly polarized vectors [32], which are mathematically given as

$$\epsilon^\pm = \frac{1}{\sqrt{2}}(\epsilon^1 \pm i\epsilon^2), \quad (3.9)$$

where ϵ^\pm represent right and left handed polarization vectors, with $+$ and $-$ sign respectively. The two orthogonal polarization vectors, which are perpendicular to the direction of propagation of photon are ϵ^1 , ϵ^2 . In order to derive the required form of polarization vectors, we use a frame of reference in which we express photons momenta k_1 , k_2 , k_3 and k_4 interms of basic kinematic variables, energies and angles. In our case, we chose a frame in center of mass system. For all external photons, the 4-momentum vectors are given below.

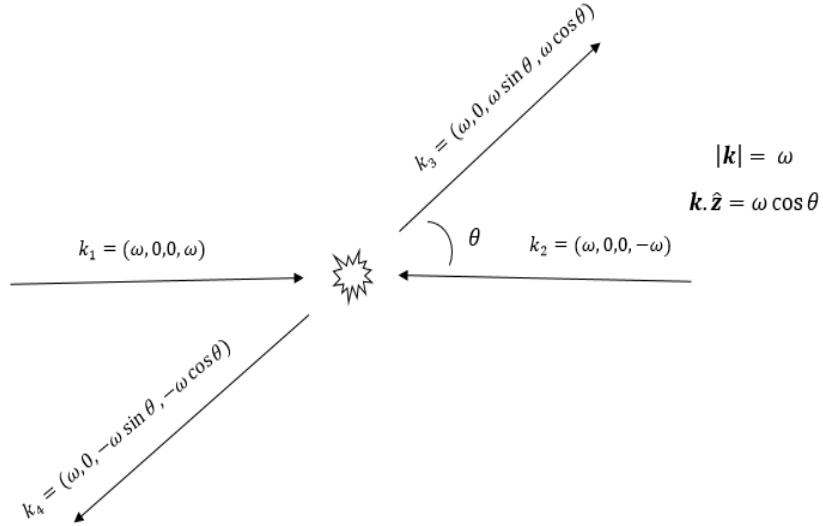


Figure 3.3: Photon-photon elastic scattering in center of mass frame, where momentum 4-vectors of the photons are shown.

Initially, incoming photons are set in the z-direction and their 4-momenta are $k_1=(\omega, 0, 0, \omega)$ and $k_2 = (\omega, 0, 0, -\omega)$. Then we have two orthogonal polarization vectors $\epsilon_\mu^1 = \frac{1}{\sqrt{2}}(0, 1, 0, 0)$ and $\epsilon_\mu^2 = \frac{1}{\sqrt{2}}(0, 0, 1, 0)$ for k_1 , which satisfy the conditions $k_1^\mu \epsilon_\mu = 0$ and $\epsilon_\mu \epsilon^\mu = -1$. We can write circularly polarized vectors for photon having 4-momentum k_1 as

$$\epsilon_\mu^{1\pm} = \frac{1}{\sqrt{2}}(0, 1, \pm i, 0).$$

For other incoming photon having 4-momentum $k_2 = (\omega, 0, 0, -\omega)$, we have two transverse polarization vectors $\epsilon_\nu^1 = \frac{1}{\sqrt{2}}(0, -1, 0, 0)$ and $\epsilon_\nu^2 = \frac{1}{\sqrt{2}}(0, 0, 1, 0)$. For this the circularly polarized vectors are

$$\epsilon_\nu^{2\pm} = \frac{1}{\sqrt{2}}(0, -1, \pm i, 0).$$

Now we write the circularly polarized vector for photon having 4-momentum $k_3=(\omega, 0, \omega \sin \theta, \omega \cos \theta)$ in spherical polar coordinates, where we have fixed $\phi=90^\circ$. We find two orthogonal polarization vectors for k_3 . For this we replace θ by $\theta + 90^\circ$, so we have one orthogonal vector as

$$\epsilon_\sigma^2 = \frac{1}{\sqrt{2}}(0, 0, \cos \theta, -\sin \theta),$$

for other orthogonal vector, we determine $\epsilon^2 \times k_3$ so that, we have a vector orthogonal to both ϵ^2 and k_3 as

$$\epsilon_\sigma^1 = \frac{1}{\sqrt{2}}(0, 1, 0, 0).$$

The circularly polarized vector for photon having 4-momentum k_3 is

$$\epsilon_\sigma^{3\pm} = \frac{1}{\sqrt{2}}(0, 1, \pm i \cos \theta, \mp i \sin \theta).$$

In the same way we proceed for the orthogonal polarization vector of photon having 4-momentum k_4 as

$$\epsilon_\lambda^1 = \frac{1}{\sqrt{2}}(0, 1, 0, 0)$$

$$\text{and } \epsilon_\lambda^2 = \frac{1}{\sqrt{2}}(0, 0, -\cos\theta, \sin\theta)$$

So the corresponding circularly polarized vector is

$$\epsilon_\lambda^{4\pm} = \frac{1}{\sqrt{2}}(0, 1, \mp i \cos\theta, \pm i \sin\theta).$$

3.1.7 Polarized Amplitude of Photon-Photon Scattering

Two independent polarization or helicity states can be assigned to each photon. So in terms of helicity states, the total amplitude can be written as

$$M^{r_1 r_2 r_3 r_4} = 2(M_1^{\lambda\nu\mu\sigma} + M_2^{\sigma\nu\mu\lambda} + M_3^{\lambda\nu\sigma\mu})\epsilon_\lambda^{r_4*}(k_4)\epsilon_\nu^{r_2}(k_2)\epsilon_\mu^{r_1}(k_1)\epsilon_\sigma^{r_3*}(k_3),$$

where $r_i = \pm 1$ are the helicity states of photons. The polarized amplitude $M^{\lambda_1 \lambda_2 \lambda_3 \lambda_4}$ is a fourth rank tensor, having two helicity states for each index. We, therefore, naively have 16 helicity amplitudes.

$$M^{++++}, M^{+++ -}, M^{++ - +}, M^{+ - ++}, M^{- +++}, M^{- + - +}, M^{+ - - +}, M^{- + - -}, \\ M^{----}, M^{--- +}, M^{- - + -}, M^{- - - +}, M^{+ - - -}, M^{- + - -}, M^{- - + +}, M^{- - - -}.$$

These polarized amplitudes are not all independent. In order to get independent polarized amplitudes, we use some symmetry operations.

One of these symmetries is the parity-invariance. This condition of parity-invariance can change only the helicity of the amplitudes leaving the Mandelstam variables s , t , and u unchanged, so we have

$$M^{r_1, r_2, r_3, r_4}(s, t, u) = M^{-r_1, -r_2, -r_3, -r_4}(s, t, u). \quad (3.10)$$

On the basis of this parity symmetry, all the sixteen polarized amplitudes reduce to eight polarized amplitudes as follows

$$M^{++++} = M^{----}, M^{+++ -} = M^{- + - -}, M^{++ - +} = M^{- - + -}, M^{+ - ++} = M^{- - - +}, \\ M^{- +++} = M^{+ - - -}, M^{- + - +} = M^{- - - +}, M^{- + - -} = M^{- - + -}, M^{- - + +} = M^{+ - - -}.$$

Finally, we have

$2M^{++++}, 2M^{+++}, 2M^{++-}, 2M^{+-+}, 2M^{-++}, 2M^{-+-}, 2M^{+--}, 2M^{+-}$.

Now we apply another symmetry, known as time-reversal symmetry. According to this symmetry

$$M^{r_1, r_2, r_3, r_4}(s, t, u) = M^{r_3, r_4, r_1, r_2}(s, t, u), \quad (3.11)$$

only initial and final states replace each other, while helicity and Mandelstam variables remain unaffected. In the same way, by using symmetry in which $k_1 \leftrightarrow k_2$ or $k_3 \leftrightarrow k_4$ we have

$$M^{r_1, r_2, r_3, r_4}(s, t, u) = M^{r_2, r_1, r_4, r_3}(s, t, u). \quad (3.12)$$

Having these symmetries in hand, we arrived at the following five independent invariant amplitudes as

$2M^{++++}, 2M^{+--}, 2M^{+-}, 2M^{--}, 8M^{++}$.

In all these symmetries the Mandelstam variables s, t and u remain unaltered.

Now we calculate these polarized amplitudes one by one. First we will do the calculations for M^{++++} .

3.1.8 Polarized Amplitude M^{++++}

We do the calculations of photon-photon elastic scattering helicity amplitude M^{++++} , in which all the incoming and outgoing photons have right handed circular polarization vectors. We do the algebraic calculations by using the extension FeynCalc to Mathematica. The 4-momentum vectors of photons are as follows

$k_1 = (\omega, 0, 0, \omega), \quad k_2 = (\omega, 0, 0, -\omega), \quad k_3 = (\omega, 0, \omega \sin \theta, \omega \cos \theta)$
and $k_4 = (\omega, 0, -\omega \sin \theta, -\omega \cos \theta)$.

Where, the four right handed polarization vectors are

$$\epsilon_\mu^{1+} = \frac{1}{\sqrt{2}}(0, 1, i, 0), \quad \epsilon_\nu^{2+} = \frac{1}{\sqrt{2}}(0, -1, +i, 0),$$

$$\epsilon_{\sigma}^{*3+} = \frac{1}{\sqrt{2}}(0, 1, -i \cos \theta, i \sin \theta), \quad \text{and} \quad \epsilon_{\lambda}^{*4+} = \frac{1}{\sqrt{2}}(0, 1, i \cos \theta, -i \sin \theta).$$

3.1.9 Kinematics For Polarized Amplitude M^{++++}

The photon-photon scattering amplitude M^{++++} contains scalar products of photon 4-momenta with itself and with their polarization vectors. Here we list out all the possible scalar products which are determined after long algebraic calculations. We are not going into the detail of these calculations, but we only list out their results.

$$k_1 \cdot k_1 = k_2 \cdot k_2 = k_3 \cdot k_3 = k_4 \cdot k_4 = 0 ;$$

$$k_1 \cdot k_2 = k_3 \cdot k_4 = \frac{s}{2} ;$$

$$k_1 \cdot k_3 = k_2 \cdot k_4 = -\frac{t}{2} ;$$

$$k_1 \cdot k_4 = k_2 \cdot k_3 = -\frac{u}{2} ;$$

$$\begin{aligned} k_4 \cdot \epsilon^{3+} &= k_4 \cdot \epsilon^{4+} = k_1 \cdot \epsilon^{1+} = k_1 \cdot \epsilon^{2+} = k_2 \cdot \epsilon^{1+} = k_2 \cdot \epsilon^{2+} \\ &= k_3 \cdot \epsilon^{3+} = k_3 \cdot \epsilon^{4+} = 0 ; \end{aligned}$$

$$\epsilon^{4+} \cdot k_1 = \frac{i}{\sqrt{2}} w \sin \theta ; \quad \epsilon^{4+} \cdot k_2 = -\frac{i}{\sqrt{2}} w \sin \theta ; \quad \epsilon^{1+} \cdot k_3 = -\frac{i}{\sqrt{2}} w \sin \theta ;$$

$$\epsilon^{1+} \cdot k_4 = \frac{i}{\sqrt{2}} w \sin \theta ; \quad \epsilon^{2+} \cdot k_3 = -\frac{i}{\sqrt{2}} w \sin \theta ; \quad \epsilon^{2+} \cdot k_4 = \frac{i}{\sqrt{2}} w \sin \theta ;$$

$$\epsilon^{3+} \cdot k_1 = -\frac{i}{\sqrt{2}} w \sin \theta ; \quad \epsilon^{3+} \cdot k_2 = \frac{i}{\sqrt{2}} w \sin \theta$$

$$\epsilon^{1+} \cdot \epsilon^{1+} = \epsilon^{2+} \cdot \epsilon^{2+} = \epsilon^{3+} \cdot \epsilon^{3+} = \epsilon^{4+} \cdot \epsilon^{4+} = 0 ;$$

$$\epsilon^{1+} \cdot \epsilon^{2+} = 1 \quad ; \quad \epsilon^{3+} \cdot \epsilon^{4+} = -1 \quad ;$$

$$\epsilon^{1+} \cdot \epsilon^{3+} = \frac{u}{s} \quad ; \quad \epsilon^{1+} \cdot \epsilon^{4+} = \frac{t}{s} \quad ; \quad \epsilon^{2+} \cdot \epsilon^{3+} = -\frac{t}{s} \quad ; \quad \epsilon^{2+} \cdot \epsilon^{4+} = -\frac{u}{s} \quad ;$$

The Mandelstam variables s , t and u can be written interms of energy and angle as

$$s = 4w^2, \quad t = -2w^2(1 - \cos \theta), \quad u = -2w^2(\cos \theta + 1) \quad \text{and} \quad s + t + u = 0.$$

3.1.10 Results for the Polarized Photon-Photon Scattering Amplitude

We have done the calculations for $\gamma\gamma \longrightarrow \gamma\gamma$ in the low energy regime $\omega \ll m_e$. We expand the amplitude interms of the powers of ratio of photon energy and electron mass. We retain, the leading order terms and omit all the higher power terms from the amplitudes. We have done our algebraic calculations by using extension Feyncalc to mathematica. Here we write the result for M^{++++} interms of $\frac{\omega}{m_e}$ as

$$M^{++++} = -\frac{11ie^4\omega^4}{45\pi^2m_e^4},$$

we have retained the leading order term $\frac{\omega^4}{m_e^4}$ and neglected all the higher powers. In the same way, we obtained the results for other polarized amplitude M^{++--} , M^{+-+-} , M^{+--+} and M^{+-+-} by using extension Feyncalc to mathematica and retained the leading order terms

$$M^{++--} = \frac{ie^4w^4(\cos^2\theta + 3)}{30\pi^2m^4},$$

$$M^{+-+-} = -\frac{11ie^4w^4(\cos \theta + 1)^2}{360\pi^2m^4},$$

$$M^{+--+} = \frac{11ie^4w^4(2 \cos \theta - \cos^2 \theta - 1)}{360\pi^2m^4},$$

$$\text{and } M^{++++} = \frac{ie^4\omega^6 \sin^2 \theta(11 \cos 2\theta + 49)}{7560\pi^2 m^6}.$$

Note that M^{++--} and seven related amplitudes vanish at the leading order $\frac{\omega^4}{m_e^4}$ at which other amplitudes have a finite value. Since M^{++++} has leading term of the order of $\frac{\omega^6}{m_e^6}$, so we have $M^{++--}=0$.

3.1.11 Total Cross Section

Now we determine the unpolarized differential scattering cross section and then total cross section. The formula for differential scattering cross section in the center of mass frame for $2 \rightarrow 2$ process is

$$\frac{d\sigma(\gamma\gamma \rightarrow \gamma\gamma)}{d\Omega} = \frac{1}{256\pi^2\omega^2}|M|^2, \quad (3.13)$$

where $|M|^2$ is the square of total amplitude. In order to calculate $|M|^2$, we average over initial and sum over final polarization

$$|M|^2 = \frac{1}{4}\{2|M^{++++}|^2 + 2|M^{++--}|^2 + 2|M^{+-+-}|^2 + 2|M^{+--+}|^2\}.$$

Substituting the values

$$|M|^2 = \frac{1}{2} \left\{ \frac{121e^8\omega^8}{2025\pi^4 m^8} + \frac{e^8\omega^8(\cos 2\theta + 7)^2}{3600\pi^4 m^8} + \frac{121(56e^8\omega^8 \cos \theta + 28e^8\omega^8 \cos 2\theta + 8e^8\omega^8 \cos 3\theta + e^8\omega^8 \cos 4\theta + 35e^8\omega^8)}{259200\pi^4 m^8} - \frac{121(56e^8\omega^8 \cos \theta - 28e^8\omega^8 \cos 2\theta + 8e^8\omega^8 \cos 3\theta - e^8\omega^8 \cos 4\theta - 35e^8\omega^8)}{259200\pi^4 m^8} \right\}$$

$$|M|^2 = \frac{1}{2} \frac{139e^8\omega^8(28 \cos 2\theta + \cos 4\theta + 99)}{129600\pi^4 m^8}$$

$$|M|^2 = \frac{139e^8\omega^8(\cos^2 \theta + 3)^2}{32400\pi^4 m^8}.$$

Substituting the value of $|M|^2$ in the relation for differential scattering cross section, we have

$$\frac{d\sigma(\gamma\gamma \longrightarrow \gamma\gamma)}{d\Omega} = \frac{1}{256\pi^2\omega^2} \frac{139e^8\omega^8(\cos^2\theta + 3)^2}{32400\pi^4m^8},$$

$$\frac{d\sigma(\gamma\gamma \longrightarrow \gamma\gamma)}{d\Omega} = \frac{e^8}{256\pi^6} \frac{\omega^6}{m^8} \frac{139(\cos^2\theta + 3)^2}{32400}.$$

The fine structure constant is $\alpha = \frac{e^2}{4\pi}$, so we write the differential scattering cross section in terms of fine structure constant α as

$$\frac{d\sigma(\gamma\gamma \longrightarrow \gamma\gamma)}{d\Omega} = \frac{\alpha^4}{\pi^2} \frac{\omega^6}{m^8} \frac{139(\cos^2\theta + 3)^2}{32400}. \quad (3.14)$$

This result of differential cross section agrees well with the result of H. Euler [6, 7], which was later confirmed by R. Karplus and M. Neuman [9, 10].

To determine the total scattering cross section, we integrate the differential scattering cross section over a solid angle $d\Omega = \sin\theta d\theta d\phi$ from $0 \longrightarrow \pi$, which is over one hemisphere because the photons in the final states are identical, we obtained total scattering cross section as follows

$$\sigma(\gamma\gamma \longrightarrow \gamma\gamma) = \frac{973\alpha^4\omega^6}{10125\pi m^8}, \quad (3.15)$$

which agrees with the result of total cross section of [33].

3.2 Cross Section as a Function of Energy and Angular Distribution

In this section, we discuss the dependence of cross section on the energy of photons ω and the scattering angle θ . Sometimes, we are interested to know the scattering angular distribution and for this we need the differential scattering cross section

$\frac{d\sigma}{d\Omega}$. Differential scattering cross section is very helpful in many cases as it gives information about the cross section of an event as a function of scattering angular distribution.

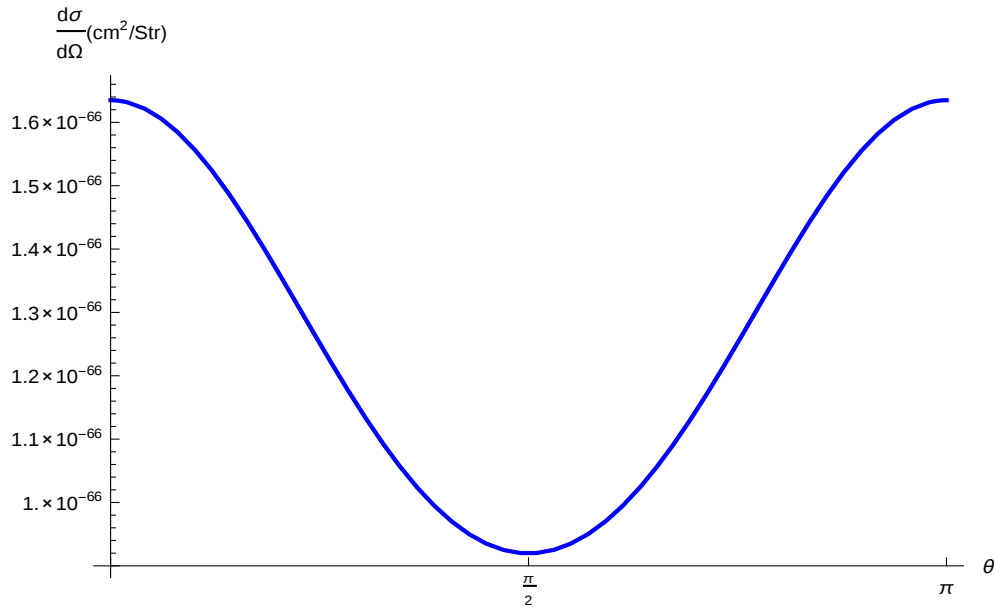


Figure 3.4: Angular dependence of the unpolarized differential scattering cross section at 1 eV, a typical energy of visible photon.

In our case, the low energy expression for unpolarized differential cross section $\frac{d\sigma}{d\Omega}$ of photon-photon elastic scattering is given by Eq. (3.14), where θ is the scattering angle in center of mass system. The dependence of differential scattering cross section on scattering angular distribution is shown in Figure. 3.4. The differential scattering cross section has maximum values at 0° and 180° and minimum at 90° . This means that the probability to detect $\gamma\gamma \rightarrow \gamma\gamma$ is maximum at 0° and 180° and minimum at 90° . We have done the calculations for scattering cross section of $\gamma\gamma \rightarrow \gamma\gamma$ in low energy regimes i.e $\omega \ll m_e$ or $\frac{\omega}{m_e} \ll 1$, where ω is the energy of photon and m_e is the rest mass of electron. The rest mass of

electron is $m_e = 0.511 \text{ MeV}$. For a particular process, we find the total scattering cross section by integrating the differential scattering cross section over θ and ϕ . The expression for total scattering cross section of $\gamma\gamma \rightarrow \gamma\gamma$ is given by Eq. 3.15, which is suppressed by $\frac{\omega^6}{m_e^8}$. The low energy total cross section at different energies is shown in Figure. 3.5. The cross section of photon is very small and at $\omega=1 \text{ eV}$, which is a typical visible energy, the cross section is $\sigma = 7.2 \times 10^{-66} \text{ cm}^2$, an extremely small value. However, the cross section is a fast growing function of photon energy as it can be seen in the Figure. 3.5.

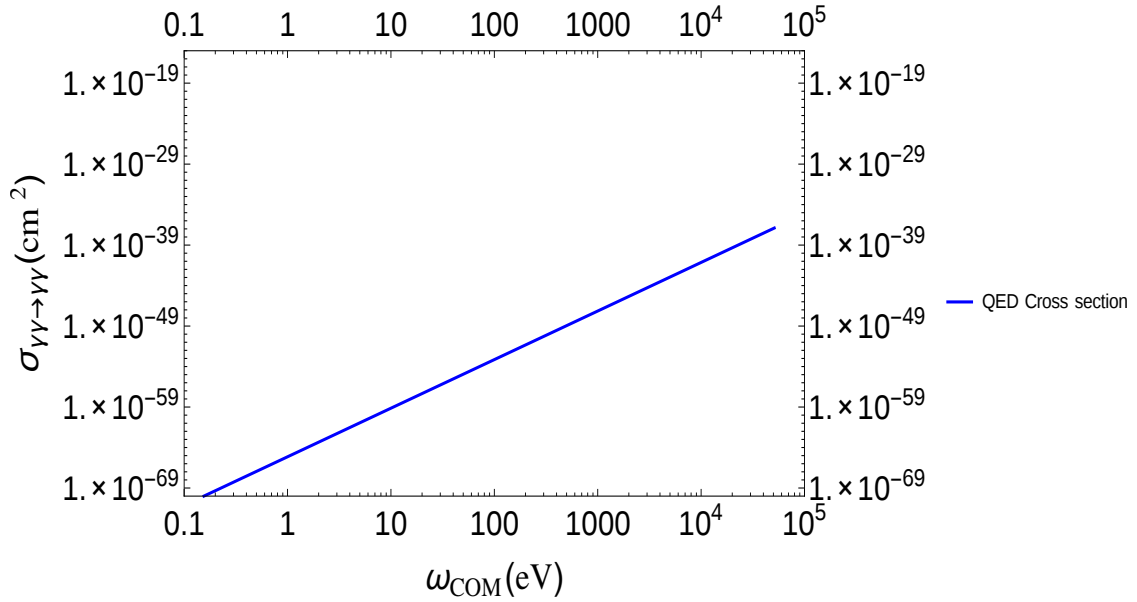


Figure 3.5: The $\gamma\gamma$ elastic scattering cross section as a function of center of mass photon energy.

3.3 Error From Neglecting The Regularization Scheme

In the calculation of photon-photon elastic scattering, regularization has a very important role. Although the total amplitude has no divergence, still it is necessary

to regularize each diagram separately. In (3.5) the integral having four powers of the loop momentum represents a divergent integral. Without regularization, these integrals have indeterminate forms. Now if we evaluate such amplitude without regularization in the low energy regime of $\frac{\omega}{m_e} \ll 1$, then we get an expression which depends only on external photon polarizations and not on their momenta.

To examine the error which arises due to neglecting regularization, we inspect that part of the total amplitude which is independent of the external photon momenta,

$$\begin{aligned}
M_l \sim & -2 \frac{(ie)^4}{(2\pi)^d} \int d^D \ell \frac{1}{\left[\ell^2 - \Delta + i\epsilon \right]^4} \times \\
& \left(\frac{2}{3} (l^2)^2 g^{\lambda\sigma} g^{\mu\nu} + \frac{2}{3} (l^2)^2 g^{\lambda\nu} g^{\mu\sigma} + \frac{2}{3} (l^2)^2 g^{\lambda\mu} g^{\nu\sigma} - \frac{4}{3} l^2 m^2 g^{\lambda\sigma} g^{\mu\nu} - \frac{4}{3} l^2 m^2 g^{\lambda\nu} g^{\mu\sigma} \right. \\
& - \frac{4}{3} l^2 m^2 g^{\lambda\mu} g^{\nu\sigma} + \frac{8}{3} m^2 l^\nu l^\sigma g^{\lambda\mu} + \frac{8}{3} m^2 l^\mu l^\sigma g^{\lambda\nu} + \frac{8}{3} m^2 l^\lambda l^\sigma g^{\mu\nu} + \frac{8}{3} m^2 l^\mu l^\nu g^{\lambda\sigma} + \frac{8}{3} m^2 l^\lambda l^\nu g^{\mu\sigma} \\
& + \frac{8}{3} m^2 l^\lambda l^\mu g^{\nu\sigma} - \frac{8}{3} l^2 l^\nu l^\sigma g^{\lambda\mu} - \frac{8}{3} l^2 l^\mu l^\sigma g^{\lambda\nu} - \frac{8}{3} l^2 l^\lambda l^\sigma g^{\mu\nu} - \frac{8}{3} l^2 l^\mu l^\nu g^{\lambda\sigma} - \frac{8}{3} l^2 l^\lambda l^\nu g^{\mu\sigma} - \frac{8}{3} l^2 l^\lambda l^\mu g^{\nu\sigma} \\
& \left. + \frac{2}{3} m^4 g^{\lambda\sigma} g^{\mu\nu} + \frac{2}{3} m^4 g^{\lambda\nu} g^{\mu\sigma} + \frac{2}{3} m^4 g^{\lambda\mu} g^{\nu\sigma} + 16 l^\lambda l^\mu l^\nu l^\sigma \right) \epsilon_\lambda^*(k_4) \epsilon_\nu(k_2) \epsilon_\mu(k_1) \epsilon_\sigma^*(k_3)
\end{aligned}$$

or more simply we can write it as

$$\begin{aligned}
M_l \sim & -\frac{(ie)^4}{(2\pi)^d} \frac{4}{3} \int d^D \ell \frac{1}{\left[\ell^2 - \Delta + i\epsilon \right]^4} \times \left[m^4 R_1^{\lambda\mu\nu\sigma} + 2m^2 \left(2R_2^{\lambda\mu\nu\sigma} - l^2 R_1^{\lambda\mu\nu\sigma} \right) \right. \\
& \left. - 4l^2 R_2^{\lambda\mu\nu\sigma} + (l^2)^2 R_1^{\lambda\mu\nu\sigma} + 24l^\lambda l^\mu l^\nu l^\sigma \right] \epsilon_\lambda^*(k_4) \epsilon_\nu(k_2) \epsilon_\mu(k_1) \epsilon_\sigma^*(k_3), \quad (3.16)
\end{aligned}$$

$$\text{where } R_1^{\lambda\mu\nu\sigma} = g^{\lambda\mu} g^{\nu\sigma} + g^{\lambda\nu} g^{\mu\sigma} + g^{\lambda\sigma} g^{\mu\nu}$$

$$\text{and } R_2^{\lambda\mu\nu\sigma} = l^\nu l^\sigma g^{\lambda\mu} + l^\mu l^\sigma g^{\lambda\nu} + l^\lambda l^\sigma g^{\mu\nu} + l^\mu l^\nu g^{\lambda\sigma} + l^\lambda l^\nu g^{\mu\sigma} + l^\lambda l^\mu g^{\nu\sigma}.$$

Both $R_1^{\lambda\mu\nu\sigma}$ and $R_2^{\lambda\mu\nu\sigma}$ are symmetric in λ, μ, ν and σ . The second line of (3.16) contains four powers of loop momentum l which shows that these are divergent

integrals. Now if we apply the averaging procedure Eq (C.1), then the second line as well as the m^2 term vanish and we left with $m^4 R_1^{\lambda\mu\nu\sigma}$, which after loop integration gives

$$M_l = -\frac{(ie)^4}{(2\pi)^4} \frac{4}{3} (\epsilon^1 \cdot \epsilon^4 \epsilon^2 \cdot \epsilon^3 + \epsilon^1 \cdot \epsilon^3 \epsilon^2 \cdot \epsilon^4 + \epsilon^1 \cdot \epsilon^2 \epsilon^3 \cdot \epsilon^4), \quad (3.17)$$

where ϵ^i are the photon polarization vectors. This means that the photon-photon scattering amplitude only depends on the vector potential A^μ and not on its derivative. This amplitude does not obey gauge invariance because

$$A_\alpha' A^{\alpha'} \longrightarrow \left(A_\alpha - \frac{1}{e} \partial_\alpha \alpha(x) \right) \left(A^\alpha - \frac{1}{e} \partial^\alpha \alpha(x) \right) \neq A_\alpha A^\alpha.$$

We cannot construct such induced coupling of polarization vectors in a gauge invariant way. Such a coupling leads to a mass term for the photon. So regularization of individual diagram is necessary. This error of neglecting regularization to the photon-photon elastic scattering has been done in [34, 35], in which they obtained an incorrect result for the cross section as follows

$$\frac{d\sigma(\gamma\gamma \longrightarrow \gamma\gamma)}{d\Omega} = \frac{\alpha^4}{(12\pi)^2} \frac{1}{\omega^2} (3 + 2 \cos^2 \theta + \cos^4 \theta). \quad (3.18)$$

This result is of many orders in magnitude larger than the result Eq.(3.14), which was obtained by H.Euler and B.Kockel in 1935 [4, 5] as this incorrect result is suppressed by $\frac{1}{\omega^2}$ and not $\frac{\omega^6}{m_e^8}$, where ω is the energy of photon and m_e is mass of electron. In all their calculations, they didn't employ the regularization scheme by saying that since total amplitude by adding contributions of all Feynman diagrams is finite, so there is no need of any regularization scheme. No doubt total amplitude is finite, still it is necessary to regularize each diagram separately. In these papers [34, 35], they have alleged the result of low energy cross section of photon-photon elastic scattering [6, 7] was incorrect. This claim does not hold It can also be easily shown that how their incorrect result of cross section Eq.(3.18) follows from Eq.(3.17).

3.4 Other Heavy Fermionic or Bosonic Loop Contributions to $\gamma\gamma \longrightarrow \gamma\gamma$

So far in this thesis, we have discussed electronic loop contribution to $\gamma\gamma \longrightarrow \gamma\gamma$ and derived explicit formulas for unpolarized differential and total scattering cross sections. In standard model, there are many other heavy fermionic or bosonic loops which can contribute to $\gamma\gamma \longrightarrow \gamma\gamma$ e.g $u\bar{u}$, $d\bar{d}$, muonic μ^\pm , tauonic τ^\pm and bosonic W^\pm loop contributions. All these fermions and bosons are much heavier than the electron as the electron has a rest mass of 0.511 MeV and that of muon is 105.7 MeV respectively. This is one of the reason that why such high energy loop contributions got not so much attention so far. However, the collider technique such as Large Hadron Collider (LHC) has opened many ways to detect high energy $\gamma\gamma \longrightarrow \gamma\gamma$ process. We will consider the effective muonic loop contribution to $\gamma\gamma \longrightarrow \gamma\gamma$ and compare it with the electronic loop contribution in the context of easily available laser technology in laboratories. In the low energy limit, the helicity amplitude for $\gamma\gamma \longrightarrow \gamma\gamma$ is suppressed by $\frac{1}{m^4}$ as

$$M^{++++} = -\frac{11ie^4\omega^4}{45\pi^2m_e^4}.$$

The minimum energy in C.O.M system to produce e^+e^- pairs is 1.022 MeV, which corresponds to intensity of the order $10^{29} W/cm^2$. The magnitude of available laser intensity in the laboratories are of the order of $10^{22} W/cm^2$ much lower than $10^{29} W/cm^2$. In order to have $\mu^+\mu^-$ pair production, we need minimum energy of 111.4 MeV in C.O.M system. The muon is much heavier than electron and the ratio of muon and electron masses is

$$\frac{m_\mu^4}{m_e^4} \simeq (200)^4.$$

So the effective contribution of muonic loop to $\gamma\gamma \longrightarrow \gamma\gamma$ is $(206.8)^4$ times less than that of electronic loop contribution. Therefore, the probability to have electronic

loop contribution is greater than the muonic loop contribution in the context of available laser technology. This is one of the reason that why such high energy loop contributions have been neglected so far. However, at high energies and intensity due to collider techniques such as Large Hadron Collider (LHC), the heavy charged loop contributions dominate over the electronic loop contribution. In high energy regimes, many experimental proposals has been made to detect $\gamma\gamma \longrightarrow \gamma\gamma$. For instance, in 1993, $\gamma\gamma \longrightarrow \gamma\gamma$ at Photon Linear Collider was considered [36]. In this experimental proposal, they considered the W boson loop contribution and obtained explicit formulas for helicity amplitudes of photon-photon elastic scattering and showed that how W loop contribution to $\gamma\gamma \longrightarrow \gamma\gamma$ will dominate at high energies. Recently, another experimental was made at Large Hadron Collider (LHC) as discussed earlier [24]. So at high energies in collider, such heavy charged loop contributions cannot be ignore. However, in the context of easily available laser technology, we can ignore all such loop contributions to $\gamma\gamma \longrightarrow \gamma\gamma$.

Chapter 4

Conclusions

In this thesis, we have demonstrated how Feynman loop diagrams can be evaluated theoretically by using mathematical tools such as Feynman parameterization, regularization and renormalization schemes used in particle physics. We have shown both qualitative and quantitative treatment of the QED process of photon-photon elastic scattering in the low energy region. Also the gauge invariance and Ward identity which are basic requirements of the theory have been discussed.

We have discussed the experimental status of $\gamma\gamma$ elastic scattering and report the upper bounds on the cross section 10^{-48}cm^2 in visible and 10^{-20}cm^2 in the X-ray region. We have shown QED low energy calculations of photon-photon elastic scattering for all polarized amplitudes and the scattering total cross section. To evaluate the divergent loop integrals, Feynman parameterization and dimensional regularization has been used. We have discussed how dimensional regularization preserves the gauge invariance of the amplitude.

We have also discussed the errors resulting from neglecting the regularization scheme. Although the total amplitude does not contain any divergence, still regularization of each individual diagram is necessary. Without regularization, amplitude is not gauge invariant and this violation of the gauge invariance leads to

a mass term for the photon. It has been discussed that how claim of [34, 35] was incorrect. In these papers, they have rejected the result for the low energy cross section of photon-photon elastic scattering [6, 7]. We have also shown that how they obtained an incorrect result for the low energy cross section of $\gamma\gamma \rightarrow \gamma\gamma$ by treating the divergent loop integrals without regularization and how gauge invariance has been violated.

In chapter 02, $\gamma\gamma \rightarrow \gamma\gamma$ experimental status has been discussed in detail. The $\gamma\gamma$ elastic scattering still awaits experimental confirmation. The main reason for this is the suppression of cross section due it being a loop process. Since the $\gamma\gamma \rightarrow \gamma\gamma$ is a crossed beam experiment because photons cannot be at rest, so one should need to have photon beams of high intensity and also to control the initial conditions such as focussing of photon beams and photon-photon collision time. One of the main important step to detect the process is to control background noise because signal noise ratio is very low. There is a need to improve the sensitivity of the detectors due to small cross section specially in the low energy regions.

Appendix A

Non-linear Classical Electrodynamics

In classical electrodynamics, the self interaction of electromagnetic fields in vacuum does not occur, because Maxwell's equations are linear in electric and magnetic fields. However, an effective theory can be formulated which contains only electromagnetic fields in terms of lagrangian of W. Heisenberg and his student H. Euler [1], which is valid for the fields below the critical field strength 1.3×10^{16} V/cm at which real electron-positron pair production becomes dominated and wavelengths above the Compton wavelength 2.42×10^{-12} cm. Under these conditions the electromagnetic interaction shows up as non-linear corrections to Maxwell's equations. So the electromagnetic fields self interaction can be treated in classical non-linear electrodynamics. Here we will show how the effective lagrangian can be constructed, which causes non-linearities in the Maxwell's equations. The classical electromagnetic lagrangian density in source-free regions is given as

$$\mathcal{L}_f = -\frac{1}{16\pi} F_{\alpha\beta} F^{\alpha\beta} = \frac{1}{8\pi} (E^2 - B^2), \quad (\text{A.1})$$

where $F^{\alpha\beta} = \partial^\alpha A^\beta - \partial^\beta A^\alpha$ is electromagnetic field tensor and $A^\alpha = (\phi, \mathbf{A})$ is 4-vector potential. Electric and magnetic fields are related to potentials via

$$\mathbf{E} = -\frac{1}{c} \frac{\partial \mathbf{A}}{\partial t} - \nabla \phi \quad \text{and} \quad \mathbf{B} = \nabla \times \mathbf{A}, \quad (\text{A.2})$$

The Euler lagrangian equation, of course, is

$$\partial^\nu \frac{\partial \mathcal{L}_f}{\partial (\partial^\nu A_\mu)} - \frac{\partial \mathcal{L}_f}{\partial A_\mu} = 0. \quad (\text{A.3})$$

The Maxwell's equations in vacuum derived from the Euler lagrangian equation in covariant form are

$$\partial_\alpha F^{\alpha\beta} = 0, \quad (\text{A.4})$$

$$\text{or} \quad \partial_\alpha \partial^\alpha A^\beta - \partial_\alpha \partial^\beta A^\alpha = 0. \quad (\text{A.5})$$

The electromagnetic field tensor $F^{\alpha\beta}$ obeys the Bianchi identity, which is given below

$$\partial^\lambda F^{\alpha\beta} + \partial^\alpha F^{\beta\lambda} + \partial^\beta F^{\lambda\alpha} = 0. \quad (\text{A.6})$$

The electromagnetic field tensor is given by

$$F^{\alpha\beta} = \begin{pmatrix} 0 & -E_x & -E_y & -E_z \\ E_x & 0 & -B_z & B_y \\ E_y & B_z & 0 & -B_x \\ E_z & -B_y & B_x & 0 \end{pmatrix}$$

the Maxwell's equations in terms of \mathbf{E} and \mathbf{B} can be derived from (A.4) and Bianchi identity (A.6)

$$\nabla \cdot \mathbf{E} = 0 \quad (\text{A.7})$$

$$\nabla \cdot \mathbf{B} = 0 \quad (\text{A.8})$$

$$\nabla \times \mathbf{E} = -\frac{\partial \mathbf{B}}{\partial t} \quad (\text{A.9})$$

$$\nabla \times \mathbf{B} = \frac{\partial \mathbf{E}}{\partial t} \quad (\text{A.10})$$

If we include possible magnetization \mathbf{M} and polarization \mathbf{P} , then above Maxwell's equation becomes as

$$\nabla \cdot \mathbf{E} = -\nabla \cdot \mathbf{P} \quad (\text{A.11})$$

$$\nabla \cdot \mathbf{B} = 0 \quad (\text{A.12})$$

$$\nabla \times \mathbf{E} = -\frac{\partial \mathbf{B}}{\partial t} \quad (\text{A.13})$$

$$\nabla \times \mathbf{B} = \frac{\partial \mathbf{E}}{\partial t} + \frac{\partial \mathbf{P}}{\partial t} + \nabla \times \mathbf{M} \quad (\text{A.14})$$

Quantum Corrections

In order to construct the effective lagrangian \mathcal{L}_{ef} which describe the self interaction of electromagnetic fields, we write E.H lagrangian as an expansion of powers of $F_{\alpha\beta}$. In order to do lowest order corrections to classical electromagnetic lagrangian, we retain only those terms which respect symmetries like parity, gauge invariance and lorentz invariance.

The first contribution occur at order $O\left(\frac{1}{m_e^4}\right)$, where m_e is the mass of electron since we are considering QED having energies and momenta smaller as compared to electron mass. We have only two terms which satisfy all symmetries to this order.

$$\mathcal{L}_{ef} = \frac{\alpha^2}{m_e^4} \left\{ a_1 F_{\mu\nu} F^{\mu\nu} F_{\alpha\beta} F^{\alpha\beta} + a_2 F_{\mu\nu} \mathcal{F}^{\mu\nu} F_{\alpha\beta} \mathcal{F}^{\alpha\beta} \right\} + O\left(\frac{1}{m_e^6}\right), \quad (\text{A.15})$$

where $\alpha = \frac{e^2}{4\pi}$ is the fine structure constant. This represents the quantum corrections to classical electromagnetic lagrangian. So finally after finding a_1 and a_2 the one loop QED correction to classical electromagnetic lagrangian corresponds to the effective lagrangian

$$\mathcal{L}_{ef} = \frac{\eta}{8\pi} \left(\frac{1}{4} F_{\mu\nu} F^{\mu\nu} F_{\alpha\beta} F^{\alpha\beta} + \frac{7}{16} F_{\mu\nu} \mathcal{F}^{\mu\nu} F_{\alpha\beta} \mathcal{F}^{\alpha\beta} \right), \quad (\text{A.16})$$

where $\mathcal{F}^{\alpha\beta}$ is the dual electromagnetic field tensor and $\eta = \frac{e^4}{45\pi m^4}$, which is very small and can be neglected for weak fields. This effective lagrangian is valid for wavelength above $10^{-12}m$ and fields below $10^{16}V/cm$.

The dual electromagnetic field tensor is given by

$$\mathcal{F}^{\alpha\beta} \equiv \frac{1}{2}\epsilon^{\alpha\beta\mu\nu}F_{\mu\nu} = \begin{pmatrix} 0 & -B_x & -B_y & -B_z \\ B_x & 0 & E_z & -E_y \\ B_y & -E_z & 0 & E_x \\ B_z & E_y & -E_x & 0 \end{pmatrix}$$

$$E^2 - B^2 = -\frac{1}{2}F_{\alpha\beta}F^{\alpha\beta} \quad (\text{A.17})$$

$$\text{and } \mathbf{E} \cdot \mathbf{B} = -\frac{1}{4}F_{\alpha\beta}\mathcal{F}^{\alpha\beta} \quad (\text{A.18})$$

So in terms of \mathbf{E} and \mathbf{B} effective lagrangian is

$$\mathcal{L}_{ef} = \frac{\eta}{8\pi} \left[(E^2 - B^2)^2 + 7(\mathbf{E} \cdot \mathbf{B})^2 \right] \quad (\text{A.19})$$

The total lagrangian can be written as

$$\begin{aligned} \mathcal{L} &= \mathcal{L}_f + \mathcal{L}_{ef} \\ &= -\frac{1}{16\pi}F_{\mu\nu}F^{\mu\nu} + \frac{\eta}{8\pi} \left(\frac{1}{4}F_{\mu\nu}F^{\mu\nu}F_{\alpha\beta}F^{\alpha\beta} + \frac{7}{16}F_{\mu\nu}\mathcal{F}^{\mu\nu}F_{\alpha\beta}\mathcal{F}^{\alpha\beta} \right). \end{aligned} \quad (\text{A.20})$$

In terms of \mathbf{E} and \mathbf{B} total lagrangian is

$$\mathcal{L} = \mathcal{L}_f + \mathcal{L}_{ef} = \frac{1}{8\pi} (E^2 - B^2) + \frac{\eta}{8\pi} \left[(E^2 - B^2)^2 + 7(\mathbf{E} \cdot \mathbf{B})^2 \right]. \quad (\text{A.21})$$

When we put this total lagrangian in Euler lagrangian equation we get non linear Maxwell's equations as

$$\partial_\nu F^{\mu\nu} = \eta \partial_\nu \left[-2(E^2 - B^2) F^{\mu\nu} - 7(\mathbf{E} \cdot \mathbf{B}) \mathcal{F}^{\mu\nu} \right] \quad (\text{A.22})$$

The Maxwell's equations in \mathbf{E} and \mathbf{B} are

$$\nabla \cdot \mathbf{E} = -\eta \nabla \cdot [\mathbf{2} (E^2 - B^2) \mathbf{E} + \mathbf{7} (\mathbf{E} \cdot \mathbf{B}) \mathbf{B}] \quad (\text{A.23})$$

and

$$\begin{aligned} \nabla \times \mathbf{B} = & \frac{\partial \mathbf{E}}{\partial t} + \eta \frac{\partial}{\partial t} [2 (E^2 - B^2) \mathbf{E} + 7 (\mathbf{E} \cdot \mathbf{B}) \mathbf{B}] + \\ & \eta \nabla \times [-2 (E^2 - B^2) \mathbf{B} + 7 (\mathbf{E} \cdot \mathbf{B}) \mathbf{E}]. \end{aligned} \quad (\text{A.24})$$

The other two equations remain unchanged.

Comparing eqs (A.14) and (A.24), we have

$$\mathbf{P} = 2 (E^2 - B^2) \mathbf{E} + 7 (\mathbf{E} \cdot \mathbf{B}) \mathbf{B} \quad (\text{A.25})$$

$$\mathbf{M} = -2 (E^2 - B^2) \mathbf{B} + 7 (\mathbf{E} \cdot \mathbf{B}) \mathbf{E} \quad (\text{A.26})$$

These polarization and magnetization express the non linear corrections to classical Maxwell's equations as a result of photon-photon scattering. The first ever calculations of photon-photon scattering by Euler, Heisenberg and Kockel were based on effective theory and these results were reproduced by Numan and Karplus by doing QED calculations of $\gamma\gamma \rightarrow \gamma\gamma$ in low energy limit.

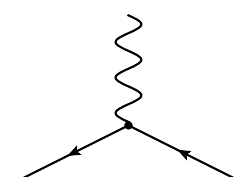
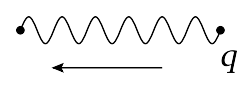
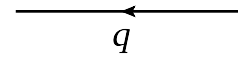
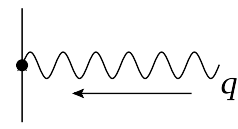
Appendix B

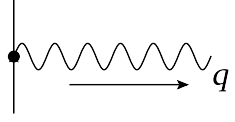
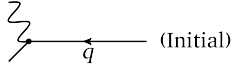
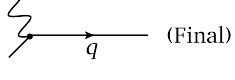
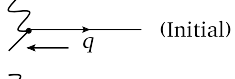
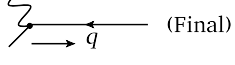
QED Feynman Rules

As we know that in quantum field theory, the evaluation of Feynman diagrams demand the conservation of momentum and charge at each vertex. The fermionic loop has an additional factor of (-1) in scattering amplitude. The QED lagrangian is

$$\mathcal{L}_{QED} = \bar{\psi} (i\gamma^\alpha \partial_\alpha - m) \psi - \frac{1}{4} F_{\alpha\beta} F^{\alpha\beta} - e\bar{\psi}\gamma^\alpha\psi A_\alpha, \quad (\text{B.1})$$

where the first term is the Dirac lagrangian, second is classical electromagnetic lagrangian and third one is the interaction term. QED Feynman rules are given by

QED Vertex	:	$-ie\gamma^\alpha$	=	
Photon Propagator	:	$-\frac{ig^{\alpha\beta}}{q^2 + i\epsilon}$	=	
Dirac Propagator	:	$-\frac{i(q+m)}{q^2 - m^2 + i\epsilon}$	=	
Initial Photon	:	$\epsilon_\alpha(q)$	=	

Final Photon	:	$\varepsilon_{\alpha}^*(q)$	=	
External Fermion	:	$u^s(q)$	=	
External Fermion	:	$\bar{u}^s(q)$	=	
External Anti Fermion	:	$\bar{v}^s(q)$	=	
External Anti Fermion	:	$v^s(q)$	=	

Polarization of External Photons

In our case all external particles are photons having polarization vectors $\epsilon_{\mu}(k_1)$, $\epsilon_{\nu}(k_2)$, $\epsilon_{\sigma}^*(k_3)$ and $\epsilon_{\lambda}^*(k_4)$, where $\epsilon_{\mu}(k_1)$, $\epsilon_{\nu}(k_2)$ are incoming and $\epsilon_{\sigma}^*(k_3)$, $\epsilon_{\lambda}^*(k_4)$ are outgoing photon polarization vectors. The massless bosons i.e photons must obey transversality condition given as

$$\epsilon_{\mu} = (0, \epsilon) \quad \text{and} \quad \mathbf{p} \cdot \epsilon = \mathbf{0} . \quad (\text{B.2})$$

In center of mass frame, where initial photons have momentum in the Z-direction, the circular polarization vectors for initial photons are

$$\epsilon^{1\pm} = \frac{1}{\sqrt{2}} (0, 1, \pm i, 0) , \quad (\text{B.3})$$

$$\text{and} \quad \epsilon^{2\pm} = \frac{1}{\sqrt{2}} (0, -1, \pm i, 0) \quad (\text{B.4})$$

For external outgoing photons polarization vectors are

$$\epsilon^{3\pm} = \frac{1}{\sqrt{2}} (0, 1, \pm i \cos \theta, \mp i \sin \theta) , \quad (\text{B.5})$$

$$\text{and} \quad \epsilon^{4\pm} = \frac{1}{\sqrt{2}} (0, 1, \mp i \cos \theta, \pm i \sin \theta) \quad (\text{B.6})$$

with + and - for left handed and right handed circular polarizations respectively. If there involve massless photons in calculations of scattering cross section then following replacement can be made

$$\sum_{\alpha\beta} \epsilon_{\alpha}\epsilon_{\beta} = -g_{\alpha\beta} . \quad (\text{B.7})$$

Numerator Algebra

The anticommutation relation for Dirac matrices is

$$\{\gamma^{\alpha}, \gamma^{\beta}\} = 2g^{\alpha\beta} .$$

Trace of Dirac gamma matrices are

$$Tr(\mathbf{1}) = 4 ,$$

$$Tr(\gamma^{\lambda}\gamma^{\nu}) = 4g^{\lambda\nu} ,$$

$$Tr(\text{Odd no. of matrices}) = 0 ,$$

$$Tr(\gamma^{\lambda}\gamma^{\nu}\gamma^{\mu}\gamma^{\sigma}) = 4(-g^{\lambda\mu}g^{\nu\sigma} + g^{\lambda\nu}g^{\mu\sigma} + g^{\lambda\sigma}g^{\mu\nu}) ,$$

$$Tr(\gamma^{\lambda}\gamma^{\nu}\gamma^{\mu}\gamma^{\sigma} \dots) = Tr(\dots\gamma^{\sigma}\gamma^{\mu}\gamma^{\nu}\gamma^{\lambda}) .$$

A complete set of trace identities and contractions of gamma matrices see [30].

Appendix C

Feynman Parameterization

The aim of this technique is to reduce the multiple factors in denominator into a single factor, in the loop momentum 'q'. As a result of this technique, we have a spherically symmetric integral which can be easily solved. This technique is due to R.P.Feynman and is known as Feynman parameterization [31]. In this method, we introduce some parameters over which we have to integrate. In general loop integral has many factors in the denominator, but usually one deals with standard integrals having a single factor raised to a power 'n'

$$\frac{1}{d_0 d_1 d_2 d_3 \dots d_n} = \Gamma(n+1) \int_0^1 dx_1 \int_0^{x_1} dx_2 \dots \int_0^{x_{n-1}} dx_n$$

$$\times \frac{1}{\left[d_0 + (d_1 - d_0)x_1 + (d_2 - d_1)x_2 + \dots + (d_n - d_{n-1})x_n \right]^{n+1}}.$$

For n=1, the above expression reduces to

$$\frac{1}{d_0 d_1} = \int_0^1 dx_1 \frac{1}{\left[d_0 + (d_1 - d_0)x_1 \right]^2}.$$

In our case, we have n=3

$$\frac{1}{d_0 d_1 d_2 d_3} = 3! \int_0^1 dx_1 \int_0^{x_1} dx_2 \int_0^{x_2} dx_3 \frac{1}{\left[d_0 + (d_1 - d_0)x_1 + (d_2 - d_1)x_2 + (d_3 - d_2)x_3 \right]^4}.$$

Loop Integrals and Dimensional Regularization

The Feynman loop diagrams involve loop momentum integrals which are divergent in 4-dimensional space-time. In dimension $D = 4 - \eta$, these divergent loop momentum integrals become convergent. There is a need to regularize these integrals in order to make any sense of them. So we change the dimensionality from $D = 4$ to $D = 4 - \eta$, where $\eta \neq 0$. In this method, we may have fractional dimensions as D and η are not integers. At the end, physical predictions of the original theory can be restored by letting $\eta \rightarrow 0$. This method of regularization is known as dimensional regularization. The main advantage of dimensional regularization is that it preserve the gauge invariance and hence the Ward identity. The terms having odd no. of loop momentum vanish because of integration due to symmetry.

$$\ell^\alpha \ell^\beta = \frac{1}{D} \ell^2 g^{\alpha\beta} \text{ and } \ell^\alpha \ell^\beta \ell^\rho \ell^\delta = \frac{1}{D(D+2)} (\ell^2)^2 (g^{\alpha\beta} g^{\rho\delta} + g^{\alpha\rho} g^{\beta\delta} + g^{\alpha\delta} g^{\beta\rho}) \quad (\text{C.1})$$

Here we give a list of standard D-dimensional space-time integrals in minkoski space which can be used directly for dimensional regularization

$$\int \frac{d^D \ell}{(2\pi)^D} \frac{1}{(\ell^2 - \Delta)^n} = i \frac{(-1)^n \Gamma(n - D/2)}{(4\pi)^{D/2} \Gamma(n)} \left(\frac{1}{\Delta}\right)^{n-D/2}, \quad (\text{C.2})$$

$$\int \frac{d^D \ell}{(2\pi)^D} \frac{\ell^2}{(\ell^2 - \Delta)^n} = i \frac{(-1)^{n-1} D \Gamma(n - 1 - D/2)}{(4\pi)^{D/2} 2 \Gamma(n)} \left(\frac{1}{\Delta}\right)^{n-1-D/2}, \quad (\text{C.3})$$

$$\int \frac{d^D \ell}{(2\pi)^D} \frac{\ell^\lambda \ell^\nu}{(\ell^2 - \Delta)^n} = i \frac{(-1)^{n-1} g^{\lambda\nu} \Gamma(n - 1 - D/2)}{(4\pi)^{D/2} 2 \Gamma(n)} \left(\frac{1}{\Delta}\right)^{n-1-D/2}, \quad (\text{C.4})$$

$$\int \frac{d^D \ell}{(2\pi)^D} \frac{(\ell^2)^2}{(\ell^2 - \Delta)^n} = i \frac{(-1)^n D(D+2) \Gamma(n - 2 - D/2)}{(4\pi)^{D/2} 4 \Gamma(n)} \left(\frac{1}{\Delta}\right)^{n-2-D/2}, \quad (\text{C.5})$$

$$\begin{aligned} \int \frac{d^D \ell}{(2\pi)^D} \frac{\ell^\lambda \ell^\mu \ell^\nu \ell^\sigma}{(\ell^2 - \Delta)^n} &= i \frac{(-1)^n \Gamma(n - 2 - D/2)}{(4\pi)^{D/2} \Gamma(n)} \left(\frac{1}{\Delta}\right)^{n-2-D/2} \\ &\times \frac{(g^{\lambda\mu} g^{\nu\sigma} + g^{\lambda\nu} g^{\mu\sigma} + g^{\lambda\sigma} g^{\mu\nu})}{4}. \end{aligned} \quad (\text{C.6})$$

The gamma function is given as

$$\Gamma(n) = (n-1)! \quad (\text{C.7})$$

Generally binomial series is given as

$$(1+x)^n = 1 + nx + \frac{n(n-1)}{2!}x^2 + \dots$$

Also we use logarithmic expansion as

$$\ln(1+x) = x - \frac{1}{2}x^2 + \frac{1}{3}x^3 + \dots$$

The following replacement in $D = 4 - \eta$ can be used in dimensional regularization scheme

$$\Gamma(2 - D/2) \left(\frac{1}{\Delta}\right)^{2-D/2} = \Gamma\left(\frac{\eta}{2}\right) \left(\frac{1}{\Delta}\right)^{\frac{\eta}{2}} = \frac{2}{\eta} - \log \Delta - \eta + \log(4\pi) + O(\eta)$$

Cross Section

After finding the scattering matrix, following relation can be used to find differential cross section

$$d\sigma = \frac{1}{2E_a 2E_b |V_a - V_b|} \left(\prod_f \frac{d^3k_f}{(2\pi)^3} \frac{1}{2E_f} \right) \times |M(k_a, k_b \rightarrow k_f)|^2 (2\pi)^4 \delta^4(k_a + k_b - \sum k_f), \quad (\text{C.8})$$

where k_a, k_b are initial and k_f are final 4-momentum.

In center of mass frame having two particles in final state, the above relation reduces to

$$\left(\frac{d\sigma}{d\Omega}\right)_{CM} = \frac{1}{2E_a 2E_b |V_a - V_b|} \frac{|k_1|}{(2\pi)^2 4E_{CM}} |M(k_a, k_b \rightarrow k_1, k_2)|^2. \quad (\text{C.9})$$

For 2-2 process all having identical masses, we have

$$\left(\frac{d\sigma}{d\Omega}\right)_{CM} = \frac{|M|^2}{64\pi^2 E_{CM}^2}. \quad (\text{C.10})$$

Appendix D

Feyncalc Code

All the necessary calculations of photon-photon elastic scattering are done by using Feyncalc a Mathematica package. The Feyncalc package is basically a tool used to handle algebraic calculations of scattering amplitude both at tree and loop level on Mathematica. Here in this appendix, we present Feyncalc code written for polarized photon-photon elastic scattering amplitudes. We provide the Feyncalc code separately for all five independent invariant polarized amplitudes. Note that e_1 , e_2 , e_3 and e_4 represent the polarization 4-vectors for the external photons. Here the Feyncalc code for all five helicity scattering amplitudes M^{++++} , M^{++--} , M^{+--+} , M^{--++} and M^{+-+-} are given.

Photon-photon Elastic Scattering Amplitude M^{++++} Kinematics

$$\text{ScalarProduct}[k_3, k_3] = \text{ScalarProduct}[k_4, k_4] = 0;$$

$$\text{ScalarProduct}[k_1, k_1] = \text{ScalarProduct}[k_2, k_2] = 0;$$

$$\text{ScalarProduct}[k_1, k_2] = \text{ScalarProduct}[k_3, k_4] = \frac{s}{2};$$

$$\text{ScalarProduct}[k_1, k_3] = \text{ScalarProduct}[k_2, k_4] = -\frac{t}{2};$$

$$\text{ScalarProduct}[k_1, k_4] = \text{ScalarProduct}[k_2, k_3] = -\frac{u}{2};$$

$$\text{ScalarProduct}[k_1, e_1] = \text{ScalarProduct}[k_1, e_2] = 0;$$

$$\text{ScalarProduct}[k_2, e_1] = \text{ScalarProduct}[k_2, e_2] = 0;$$

$$\text{ScalarProduct}[k_3, e_3] = \text{ScalarProduct}[k_3, e_4] = 0;$$

$$\text{ScalarProduct}[k_4, e_3] = \text{ScalarProduct}[k_4, e_4] = 0;$$

$$\text{ScalarProduct}[e_1, k_3] = \text{ScalarProduct}[e_2, k_3] = \frac{-\text{Sqrt}[-1]}{\text{Sqrt}[2]} * \omega * \text{Sin}[\theta];$$

$$\text{ScalarProduct}[e_1, k_4] = \text{ScalarProduct}[e_2, k_4] = \frac{\text{Sqrt}[-1]}{\text{Sqrt}[2]} * \omega * \text{Sin}[\theta];$$

$$\text{ScalarProduct}[e_3, k_1] = \text{ScalarProduct}[e_4, k_2] = \frac{-\text{Sqrt}[-1]}{\text{Sqrt}[2]} * \omega * \text{Sin}[\theta];$$

$$\text{ScalarProduct}[e_3, k_2] = \text{ScalarProduct}[e_4, k_1] = \frac{\text{Sqrt}[-1]}{\text{Sqrt}[2]} * \omega * \text{Sin}[\theta];$$

$$\text{ScalarProduct}[e_1, e_2] = 1;$$

$$\text{ScalarProduct}[e_3, e_4] = -1;$$

$$\text{ScalarProduct}[e_1, e_3] = \frac{u}{s};$$

$$\text{ScalarProduct}[e_2, e_4] = -\frac{u}{s};$$

$$\text{ScalarProduct}[e_1, e_4] = \frac{t}{s};$$

$$\text{ScalarProduct}[e_2, e_3] = -\frac{t}{s};$$

$$\text{ScalarProduct}[e_1, e_1] = \text{ScalarProduct}[e_2, e_2] = 0;$$

$$\text{ScalarProduct}[e_3, e_3] = \text{ScalarProduct}[e_4, e_4] = 0;$$

Photon-photon Elastic Scattering Amplitude M^{++--} Kinematics

$$\text{ScalarProduct}[k_3, k_3] = \text{ScalarProduct}[k_4, k_4] = 0;$$

$$\text{ScalarProduct}[k_1, k_1] = \text{ScalarProduct}[k_2, k_2] = 0;$$

$$\text{ScalarProduct}[k_1, k_2] = \text{ScalarProduct}[k_3, k_4] = \frac{s}{2};$$

$$\text{ScalarProduct}[k_1, k_3] = \text{ScalarProduct}[k_2, k_4] = -\frac{t}{2};$$

$$\text{ScalarProduct}[k_1, k_4] = \text{ScalarProduct}[k_2, k_3] = -\frac{t}{2};$$

$$\text{ScalarProduct}[k_1, e_1] = \text{ScalarProduct}[k_1, e_2] = 0;$$

$$\text{ScalarProduct}[k_2, e_1] = \text{ScalarProduct}[k_2, e_2] = 0;$$

$$\text{ScalarProduct}[k_3, e_3] = \text{ScalarProduct}[k_3, e_4] = 0;$$

$$\text{ScalarProduct}[k_4, e_3] = \text{ScalarProduct}[k_4, e_4] = 0;$$

$$\begin{aligned} \text{ScalarProduct}[e1, k3] &= \text{ScalarProduct}[e2, k3] = \frac{-\text{Sqrt}[-1]}{\text{Sqrt}[2]} * \omega * \text{Sin}[\theta]; \\ \text{ScalarProduct}[e1, k4] &= \text{ScalarProduct}[e2, k4] = \frac{\text{Sqrt}[-1]}{\text{Sqrt}[2]} * \omega * \text{Sin}[\theta]; \\ \text{ScalarProduct}[e3, k1] &= \text{ScalarProduct}[e4, k2] = \frac{\text{Sqrt}[-1]}{\text{Sqrt}[2]} * \omega * \text{Sin}[\theta]; \\ \text{ScalarProduct}[e3, k2] &= \text{ScalarProduct}[e4, k1] = \frac{-\text{Sqrt}[-1]}{\text{Sqrt}[2]} * \omega * \text{Sin}[\theta]; \end{aligned}$$

$$\begin{aligned} \text{ScalarProduct}[e1, e2] &= 1; \\ \text{ScalarProduct}[e3, e4] &= -1; \\ \text{ScalarProduct}[e1, e3] &= \frac{t}{s}; \\ \text{ScalarProduct}[e2, e4] &= -\frac{t}{s}; \\ \text{ScalarProduct}[e1, e4] &= \frac{u}{s}; \\ \text{ScalarProduct}[e2, e3] &= -\frac{u}{s}; \\ \text{ScalarProduct}[e1, e1] &= \text{ScalarProduct}[e2, e2] = 0; \\ \text{ScalarProduct}[e3, e3] &= \text{ScalarProduct}[e4, e4] = 0; \end{aligned}$$

Photon-photon Elastic Scattering Amplitude M^{+-+-} Kinematics

$$\begin{aligned} \text{ScalarProduct}[k3, k3] &= \text{ScalarProduct}[k4, k4] = 0; \\ \text{ScalarProduct}[k1, k1] &= \text{ScalarProduct}[k2, k2] = 0; \\ \text{ScalarProduct}[k1, k2] &= \text{ScalarProduct}[k3, k4] = \frac{s}{2}; \\ \text{ScalarProduct}[k1, k3] &= \text{ScalarProduct}[k2, k4] = \frac{-t}{2}; \\ \text{ScalarProduct}[k1, k4] &= \text{ScalarProduct}[k2, k3] = \frac{-u}{2}; \end{aligned}$$

$$\begin{aligned} \text{ScalarProduct}[k1, e1] &= \text{ScalarProduct}[k1, e2] = 0; \\ \text{ScalarProduct}[k2, e1] &= \text{ScalarProduct}[k2, e2] = 0; \\ \text{ScalarProduct}[k3, e3] &= \text{ScalarProduct}[k3, e4] = 0; \\ \text{ScalarProduct}[k4, e3] &= \text{ScalarProduct}[k4, e4] = 0; \end{aligned}$$

$$\begin{aligned} \text{ScalarProduct}[e1, k3] &= \text{ScalarProduct}[e2, k4] = \frac{-\text{Sqrt}[-1]}{\text{Sqrt}[2]} * \omega * \text{Sin}[\theta]; \\ \text{ScalarProduct}[e1, k4] &= \text{ScalarProduct}[e2, k3] = \frac{\text{Sqrt}[-1]}{\text{Sqrt}[2]} * \omega * \text{Sin}[\theta]; \\ \text{ScalarProduct}[e3, k1] &= \text{ScalarProduct}[e4, k1] = \frac{-\text{Sqrt}[-1]}{\text{Sqrt}[2]} * \omega * \text{Sin}[\theta]; \end{aligned}$$

$$\text{ScalarProduct}[e3, k2] = \text{ScalarProduct}[e4, k2] = \frac{\text{Sqrt}[-1]}{\text{Sqrt}[2]} * \omega * \text{Sin}[\theta];$$

$$\text{ScalarProduct}[e1, e2] = \text{ScalarProduct}[e3, e4] = 0;$$

$$\text{ScalarProduct}[e1, e3] = \frac{u}{s};$$

$$\text{ScalarProduct}[e2, e4] = -\frac{u}{s};$$

$$\text{ScalarProduct}[e1, e4] = \frac{u}{s};$$

$$\text{ScalarProduct}[e2, e3] = -\frac{u}{s};$$

$$\text{ScalarProduct}[e1, e1] = \text{ScalarProduct}[e2, e2] = 0;$$

$$\text{ScalarProduct}[e3, e3] = \text{ScalarProduct}[e4, e4] = 0;$$

Photon-photon Elastic Scattering Amplitude M^{+--+} Kinematics

$$\text{ScalarProduct}[k3, k3] = \text{ScalarProduct}[k4, k4] = 0;$$

$$\text{ScalarProduct}[k1, k1] = \text{ScalarProduct}[k2, k2] = 0;$$

$$\text{ScalarProduct}[k1, k2] = \text{ScalarProduct}[k3, k4] = \frac{s}{2};$$

$$\text{ScalarProduct}[k1, k3] = \text{ScalarProduct}[k2, k4] = \frac{-t}{2};$$

$$\text{ScalarProduct}[k1, k4] = \text{ScalarProduct}[k2, k3] = \frac{-u}{2};$$

$$\text{ScalarProduct}[k1, e1] = \text{ScalarProduct}[k1, e2] = 0;$$

$$\text{ScalarProduct}[k2, e1] = \text{ScalarProduct}[k2, e2] = 0;$$

$$\text{ScalarProduct}[k3, e3] = \text{ScalarProduct}[k3, e4] = 0;$$

$$\text{ScalarProduct}[k4, e3] = \text{ScalarProduct}[k4, e4] = 0;$$

$$\text{ScalarProduct}[e1, k3] = \text{ScalarProduct}[e2, k4] = \frac{-\text{Sqrt}[-1]}{\text{Sqrt}[2]} * \omega * \text{Sin}[\theta];$$

$$\text{ScalarProduct}[e1, k4] = \text{ScalarProduct}[e2, k3] = \frac{\text{Sqrt}[-1]}{\text{Sqrt}[2]} * \omega * \text{Sin}[\theta];$$

$$\text{ScalarProduct}[e3, k1] = \text{ScalarProduct}[e4, k1] = \frac{\text{Sqrt}[-1]}{\text{Sqrt}[2]} * \omega * \text{Sin}[\theta];$$

$$\text{ScalarProduct}[e3, k2] = \text{ScalarProduct}[e4, k2] = \frac{-\text{Sqrt}[-1]}{\text{Sqrt}[2]} * \omega * \text{Sin}[\theta];$$

$$\text{ScalarProduct}[e1, e2] = 0;$$

$$\text{ScalarProduct}[e3, e4] = 0;$$

$$\text{ScalarProduct}[e1, e3] = \frac{t}{s};$$

$$\begin{aligned}
\text{ScalarProduct}[e2, e4] &= -\frac{t}{s}; \\
\text{ScalarProduct}[e1, e4] &= \frac{t}{s}; \\
\text{ScalarProduct}[e2, e3] &= -\frac{t}{s}; \\
\text{ScalarProduct}[e1, e1] &= \text{ScalarProduct}[e2, e2] = 0;
\end{aligned}$$

Photon-photon Elastic Scattering Amplitude M^{++--} Kinematics

$$\begin{aligned}
\text{ScalarProduct}[k3, k3] &= \text{ScalarProduct}[k4, k4] = 0; \\
\text{ScalarProduct}[k1, k1] &= \text{ScalarProduct}[k2, k2] = 0; \\
\text{ScalarProduct}[k1, k2] &= \text{ScalarProduct}[k3, k4] = \frac{s}{2}; \\
\text{ScalarProduct}[k1, k3] &= \text{ScalarProduct}[k2, k4] = \frac{-t}{2}; \\
\text{ScalarProduct}[k1, k4] &= \text{ScalarProduct}[k2, k3] = \frac{-u}{2};
\end{aligned}$$

$$\begin{aligned}
\text{ScalarProduct}[k1, e1] &= \text{ScalarProduct}[k1, e2] = 0; \\
\text{ScalarProduct}[k2, e1] &= \text{ScalarProduct}[k2, e2] = 0; \\
\text{ScalarProduct}[k3, e3] &= \text{ScalarProduct}[k3, e4] = 0; \\
\text{ScalarProduct}[k4, e3] &= \text{ScalarProduct}[k4, e4] = 0;
\end{aligned}$$

$$\begin{aligned}
\text{ScalarProduct}[e1, k3] &= \text{ScalarProduct}[e2, k3] = \frac{-\text{Sqrt}[-1]}{\text{Sqrt}[2]} * \omega * \text{Sin}[\theta]; \\
\text{ScalarProduct}[e1, k4] &= \text{ScalarProduct}[e2, k4] = \frac{\text{Sqrt}[-1]}{\text{Sqrt}[2]} * \omega * \text{Sin}[\theta]; \\
\text{ScalarProduct}[e3, k1] &= \text{ScalarProduct}[e4, k1] = \frac{\text{Sqrt}[-1]}{\text{Sqrt}[2]} * \omega * \text{Sin}[\theta]; \\
\text{ScalarProduct}[e3, k2] &= \text{ScalarProduct}[e4, k2] = \frac{-\text{Sqrt}[-1]}{\text{Sqrt}[2]} * \omega * \text{Sin}[\theta];
\end{aligned}$$

$$\begin{aligned}
\text{ScalarProduct}[e1, e2] &= 1; \\
\text{ScalarProduct}[e3, e4] &= 0; \\
\text{ScalarProduct}[e1, e3] &= \frac{t}{s}; \\
\text{ScalarProduct}[e2, e4] &= -\frac{u}{s}; \\
\text{ScalarProduct}[e1, e4] &= \frac{t}{s}; \\
\text{ScalarProduct}[e2, e3] &= -\frac{u}{s}; \\
\text{ScalarProduct}[e1, e1] &= \text{ScalarProduct}[e2, e2] = 0; \\
\text{ScalarProduct}[e3, e3] &= \text{ScalarProduct}[e4, e4] = 0;
\end{aligned}$$

For Diagram 3.2 (a)

$$\begin{aligned}
A &= \text{FV}[k_2, \tau] * x_1 + \text{FV}[k_1, \tau] * x_2 - \text{FV}[k_3, \tau] * x_3; \\
\text{Asquare} &= \text{Contract}[A * A]; \\
B &= 2\text{ScalarProduct}[k_1, k_2] * x_2 - 2\text{ScalarProduct}[k_1, k_2] * x_3 - m^2; \\
f &= \text{GS}[k_2] * x_1 + \text{GS}[k_1] * x_2 - \text{GS}[k_3] * x_3; \\
g &= \text{GS}[k_2] * x_1 + \text{GS}[k_1] * x_2 - \text{GS}[k_3] * x_3 - \text{GS}[k_2]; \\
h &= \text{GS}[k_2] * x_1 + \text{GS}[k_1] * x_2 - \text{GS}[k_3] * x_3 - \text{GS}[k_1] - \text{GS}[k_2]; \\
j &= \text{GS}[k_2] * x_1 + \text{GS}[k_1] * x_2 - \text{GS}[k_3] * x_3 - \text{GS}[k_4]; \\
U_1 &= \text{Asquare} - B - m^2; \\
\text{DM1} &= \text{Expand}\left[\frac{U_1}{m^2} - \frac{1}{2}\frac{(U_1 * U_1)}{m^4}\right]; \\
\text{DM2} &= \text{Expand}\left[\frac{1}{m^2} - \frac{U_1}{m^4} + \frac{(U_1 * U_1)}{m^6}\right]; \\
\text{DM3} &= \text{Expand}\left[\frac{1}{m^4} - 2\frac{U_1}{m^6} + 3\frac{(U_1 * U_1)}{m^8}\right];
\end{aligned}$$

For Diagram 3.2 (b)

$$\begin{aligned}
\text{Aprime} &= \text{FV}[k_2, \tau] * x_1 + \text{FV}[k_1, \tau] * x_2 - \text{FV}[k_4, \tau] * x_3; \\
\text{Apsquare} &= \text{Contract}[\text{Aprime} * \text{Aprime}]; \\
\text{fprime} &= \text{GS}[k_2] * x_1 + \text{GS}[k_1] * x_2 - \text{GS}[k_4] * x_3; \\
\text{gprime} &= \text{GS}[k_2] * x_1 + \text{GS}[k_1] * x_2 - \text{GS}[k_4] * x_3 - \text{GS}[k_2]; \\
\text{hprime} &= \text{GS}[k_2] * x_1 + \text{GS}[k_1] * x_2 - \text{GS}[k_4] * x_3 - \text{GS}[k_1] - \text{GS}[k_2]; \\
\text{jprime} &= \text{GS}[k_2] * x_1 + \text{GS}[k_1] * x_2 - \text{GS}[k_4] * x_3 - \text{GS}[k_3]; \\
U_2 &= \text{Apsquare} - B - m^2; \\
\text{DM11} &= \text{Expand}\left[\frac{U_2}{m^2} - \frac{1}{2}\frac{(U_2 * U_2)}{m^4}\right]; \\
\text{DM22} &= \text{Expand}\left[\frac{1}{m^2} - \frac{U_2}{m^4} + \frac{(U_2 * U_2)}{m^6}\right]; \\
\text{DM33} &= \text{Expand}\left[\frac{1}{m^4} - 2\frac{U_2}{m^6} + 3\frac{(U_2 * U_2)}{m^8}\right];
\end{aligned}$$

For Diagram 3.2 (c)

$$\begin{aligned}
\text{Adprime} &= \text{FV}[k_2, \tau] * x_1 - \text{FV}[k_3, \tau] * x_2 + \text{FV}[k_1, \tau] * x_3; \\
\text{Adpsquare} &= \text{Contract}[\text{Adprime} * \text{Adprime}];
\end{aligned}$$

$$\begin{aligned}
\text{Bprime} &= 2\text{ScalarProduct}[k_3, k_2] * x_3 - 2\text{ScalarProduct}[k_3, k_2] * x_2 - m^2; \\
\text{fdprime} &= \text{GS}[k_2] * x_1 - \text{GS}[k_3] * x_2 + \text{GS}[k_1] * x_3; \\
\text{gdprime} &= \text{GS}[k_2] * x_1 - \text{GS}[k_3] * x_2 + \text{GS}[k_1] * x_3 - \text{GS}[k_2]; \\
\text{hdprime} &= \text{GS}[k_2] * x_1 - \text{GS}[k_3] * x_2 + \text{GS}[k_1] * x_3 + \text{GS}[k_3] - \text{GS}[k_2]; \\
\text{jdprime} &= \text{GS}[k_2] * x_1 - \text{GS}[k_3] * x_2 + \text{GS}[k_1] * x_3 - \text{GS}[k_4]; \\
\text{U}_3 &= \text{Adpsquare} - \text{Bprime} - m^2; \\
\text{DM111} &= \text{Expand}\left[\frac{\text{U}_3}{m^2} - \frac{1}{2} \frac{(\text{U}_3 * \text{U}_3)}{m^4}\right]; \\
\text{DM222} &= \text{Expand}\left[\frac{1}{m^2} - \frac{\text{U}_3}{m^4} + \frac{(\text{U}_3 * \text{U}_3)}{m^6}\right]; \\
\text{DM333} &= \text{Expand}\left[\frac{1}{m^4} - 2 \frac{\text{U}_3}{m^6} + 3 \frac{(\text{U}_3 * \text{U}_3)}{m^8}\right];
\end{aligned}$$

Amplitude of Diagram 3.2 (a)

$$\begin{aligned}
T_4 &= \text{Contract}[\text{Tr}[\text{DiracGamma}[\text{LorentzIndex}[\lambda]].f.\text{DiracGamma}[\text{LorentzIndex}[\nu]].g. \\
&\text{DiracGamma}[\text{LorentzIndex}[\mu]].\text{DiracGamma}[\text{LorentzIndex}[\alpha]].\text{DiracGamma}[\text{LorentzIndex}[\sigma]]. \\
&\text{DiracGamma}[\text{LorentzIndex}[\beta]] + \text{DiracGamma}[\text{LorentzIndex}[\lambda]].f.\text{DiracGamma}[\text{LorentzIndex}[\nu]]. \\
&\text{DiracGamma}[\text{LorentzIndex}[\alpha]].\text{DiracGamma}[\text{LorentzIndex}[\mu]].h.\text{DiracGamma}[\text{LorentzIndex}[\sigma]]. \\
&\text{DiracGamma}[\text{LorentzIndex}[\beta]] + \text{DiracGamma}[\text{LorentzIndex}[\lambda]].f.\text{DiracGamma}[\text{LorentzIndex}[\nu]]. \\
&\text{DiracGamma}[\text{LorentzIndex}[\alpha]].\text{DiracGamma}[\text{LorentzIndex}[\mu]].\text{DiracGamma}[\text{LorentzIndex}[\beta]]. \\
&\text{DiracGamma}[\text{LorentzIndex}[\sigma]].j + \text{DiracGamma}[\text{LorentzIndex}[\lambda]].\text{DiracGamma}[\text{LorentzIndex}[\alpha]]. \\
&\text{DiracGamma}[\text{LorentzIndex}[\nu]].g.\text{DiracGamma}[\text{LorentzIndex}[\mu]].h.\text{DiracGamma}[\text{LorentzIndex}[\sigma]]. \\
&\text{DiracGamma}[\text{LorentzIndex}[\beta]] + \text{DiracGamma}[\text{LorentzIndex}[\lambda]].\text{DiracGamma}[\text{LorentzIndex}[\alpha]]. \\
&\text{DiracGamma}[\text{LorentzIndex}[\nu]].g.\text{DiracGamma}[\text{LorentzIndex}[\mu]].\text{DiracGamma}[\text{LorentzIndex}[\beta]]. \\
&\text{DiracGamma}[\text{LorentzIndex}[\sigma]].j + \text{DiracGamma}[\text{LorentzIndex}[\lambda]].\text{DiracGamma}[\text{LorentzIndex}[\alpha]]. \\
&\text{DiracGamma}[\text{LorentzIndex}[\nu]].\text{DiracGamma}[\text{LorentzIndex}[\beta]].\text{DiracGamma}[\text{LorentzIndex}[\mu]].h. \\
&\text{DiracGamma}[\text{LorentzIndex}[\sigma]].j] * \text{Pair}[\text{LorentzIndex}[\alpha], \text{LorentzIndex}[\beta]];
\end{aligned}$$

$$\begin{aligned}
T_5 &= \text{Tr}[\text{DiracGamma}[\text{LorentzIndex}[\lambda]].f.\text{DiracGamma}[\text{LorentzIndex}[\nu]].g. \\
&\text{DiracGamma}[\text{LorentzIndex}[\mu]].h.\text{DiracGamma}[\text{LorentzIndex}[\sigma]].j];
\end{aligned}$$

$$\begin{aligned}
T_6 &= m^2 \text{Tr}[\text{DiracGamma}[\text{LorentzIndex}[\lambda]].\text{DiracGamma}[\text{LorentzIndex}[\nu]]. \\
&\text{DiracGamma}[\text{LorentzIndex}[\mu]].h.\text{DiracGamma}[\text{LorentzIndex}[\sigma]].j + \text{DiracGamma}[\text{LorentzIndex}[\lambda]]. \\
&\text{DiracGamma}[\text{LorentzIndex}[\nu]].g.\text{DiracGamma}[\text{LorentzIndex}[\mu]].\text{DiracGamma}[\text{LorentzIndex}[\sigma]].j \\
&+ \text{DiracGamma}[\text{LorentzIndex}[\lambda]].\text{DiracGamma}[\text{LorentzIndex}[\nu]].g.\text{DiracGamma}[\text{LorentzIndex}[\mu]].h.
\end{aligned}$$

$\text{DiracGamma}[\text{LorentzIndex}[\sigma]] + \text{DiracGamma}[\text{LorentzIndex}[\lambda]].f.\text{DiracGamma}[\text{LorentzIndex}[\nu]].$
 $\text{DiracGamma}[\text{LorentzIndex}[\mu]].\text{DiracGamma}[\text{LorentzIndex}[\sigma]].j + \text{DiracGamma}[\text{LorentzIndex}[\lambda]].$
 $f.\text{DiracGamma}[\text{LorentzIndex}[\nu]].\text{DiracGamma}[\text{LorentzIndex}[\mu]].h.\text{DiracGamma}[\text{LorentzIndex}[\sigma]]$
 $+ \text{DiracGamma}[\text{LorentzIndex}[\lambda]].f.\text{DiracGamma}[\text{LorentzIndex}[\nu]].g.\text{DiracGamma}[\text{LorentzIndex}[\mu]].$
 $\text{DiracGamma}[\text{LorentzIndex}[\sigma]]];$

$$\begin{aligned}
\text{POLARIZEDAMP1} = & -\text{Sqrt}[-1] * e^4 * \frac{1}{(4\text{Pi})^2} \\
& (4m^4(\text{Pair}[\text{LorentzIndex}[\lambda], \text{LorentzIndex}[\sigma]]\text{Pair}[\text{LorentzIndex}[\mu], \text{LorentzIndex}[\nu]] + \\
& \text{Pair}[\text{LorentzIndex}[\lambda], \text{LorentzIndex}[\nu]]\text{Pair}[\text{LorentzIndex}[\mu], \text{LorentzIndex}[\sigma]] \\
& - \text{Pair}[\text{LorentzIndex}[\lambda], \text{LorentzIndex}[\mu]]\text{Pair}[\text{LorentzIndex}[\nu], \text{LorentzIndex}[\sigma]]).DM3 \\
& - 8m^2(\text{Pair}[\text{LorentzIndex}[\lambda], \text{LorentzIndex}[\nu]]\text{Pair}[\text{LorentzIndex}[\mu], \text{LorentzIndex}[\sigma]] \\
& + \text{Pair}[\text{LorentzIndex}[\lambda], \text{LorentzIndex}[\sigma]]\text{Pair}[\text{LorentzIndex}[\mu], \text{LorentzIndex}[\nu]]).DM2 \\
& + 16m^2(\text{Pair}[\text{LorentzIndex}[\lambda], \text{LorentzIndex}[\sigma]]\text{Pair}[\text{LorentzIndex}[\mu], \text{LorentzIndex}[\nu]] \\
& + \text{Pair}[\text{LorentzIndex}[\lambda], \text{LorentzIndex}[\nu]]\text{Pair}[\text{LorentzIndex}[\mu], \text{LorentzIndex}[\sigma]] \\
& - \text{Pair}[\text{LorentzIndex}[\lambda], \text{LorentzIndex}[\mu]]\text{Pair}[\text{LorentzIndex}[\nu], \text{LorentzIndex}[\sigma]]).DM2 \\
& + (\text{Pair}[\text{LorentzIndex}[\lambda], \text{LorentzIndex}[\sigma]]\text{Pair}[\text{LorentzIndex}[\mu], \text{LorentzIndex}[\nu]] \\
& + \text{Pair}[\text{LorentzIndex}[\lambda], \text{LorentzIndex}[\nu]]\text{Pair}[\text{LorentzIndex}[\mu], \text{LorentzIndex}[\sigma]] \\
& - \text{Pair}[\text{LorentzIndex}[\lambda], \text{LorentzIndex}[\mu]]\text{Pair}[\text{LorentzIndex}[\nu], \text{LorentzIndex}[\sigma]]) \\
& \left(\frac{48}{v} - 24 * \text{Log}[m^2] - 24 * \frac{U_1}{m^2} + 12 * \frac{(U_1 * U_1)}{m^4} - 24 * c + 24\text{Log}[4 * \text{Pi}] - 20 \right) \\
& - 4(\text{Pair}[\text{LorentzIndex}[\lambda], \text{LorentzIndex}[\nu]]\text{Pair}[\text{LorentzIndex}[\mu], \text{LorentzIndex}[\sigma]] \\
& + \text{Pair}[\text{LorentzIndex}[\lambda], \text{LorentzIndex}[\sigma]]\text{Pair}[\text{LorentzIndex}[\mu], \text{LorentzIndex}[\nu]]) \\
& \left(\frac{12}{v} - 6 * \text{Log}[m^2] - 6 * \frac{U_1}{m^2} + 3 * \frac{(U_1 * U_1)}{m^4} - 6 * c + 6\text{Log}[4 * \text{Pi}] - 2 \right) \\
& + 8(\text{Pair}[\text{LorentzIndex}[\lambda], \text{LorentzIndex}[\sigma]]\text{Pair}[\text{LorentzIndex}[\mu], \text{LorentzIndex}[\nu]] \\
& + \text{Pair}[\text{LorentzIndex}[\lambda], \text{LorentzIndex}[\nu]]\text{Pair}[\text{LorentzIndex}[\mu], \text{LorentzIndex}[\sigma]] \\
& + \text{Pair}[\text{LorentzIndex}[\lambda], \text{LorentzIndex}[\mu]]\text{Pair}[\text{LorentzIndex}[\nu], \text{LorentzIndex}[\sigma]]) \\
& \left(\frac{2}{v} - \text{Log}[m^2] - \frac{U_1}{m^2} + \frac{1}{2} * \frac{(U_1 * U_1)}{m^4} - c + \text{Log}[4 * \text{Pi}] \right) - T_4 * \frac{1}{2} * DM2 + (T_5 + T_6) * DM3);
\end{aligned}$$

$$M_1 = \text{Contract}[\text{POLARIZEDAMP1} * \text{FV}[e1, \mu]\text{FV}[e2, \nu]\text{FV}[e3, \sigma]\text{FV}[e4, \lambda]];$$

Amplitude of Diagram 3.2 (b)

$T_{44} = \text{Contract}[\text{Tr}[\text{DiracGamma}[\text{LorentzIndex}[\sigma]].\text{fprime}.\text{DiracGamma}[\text{LorentzIndex}[\nu]].\text{gprime}.$
 $\text{DiracGamma}[\text{LorentzIndex}[\mu]].\text{DiracGamma}[\text{LorentzIndex}[\alpha]].\text{DiracGamma}[\text{LorentzIndex}[\lambda]].$
 $\text{DiracGamma}[\text{LorentzIndex}[\beta]] + \text{DiracGamma}[\text{LorentzIndex}[\sigma]].\text{fprime}.\text{DiracGamma}[\text{LorentzIndex}[\nu]].$

DiracGamma[LorentzIndex[α]].DiracGamma[LorentzIndex[μ]].hprime.DiracGamma[LorentzIndex[λ]].
 DiracGamma[LorentzIndex[β]]+DiracGamma[LorentzIndex[σ]].fprime.DiracGamma[LorentzIndex[ν]].
 DiracGamma[LorentzIndex[α]].DiracGamma[LorentzIndex[μ]].DiracGamma[LorentzIndex[β]].
 DiracGamma[LorentzIndex[λ]].jprime+DiracGamma[LorentzIndex[σ]].DiracGamma[LorentzIndex[α]].
 DiracGamma[LorentzIndex[ν]].gprime.DiracGamma[LorentzIndex[μ]].hprime.
 DiracGamma[LorentzIndex[λ]].DiracGamma[LorentzIndex[β]] + DiracGamma[LorentzIndex[σ]].
 DiracGamma[LorentzIndex[α]].DiracGamma[LorentzIndex[ν]].gprime.DiracGamma[LorentzIndex[μ]].
 DiracGamma[LorentzIndex[β]].DiracGamma[LorentzIndex[λ]].jprime+DiracGamma[LorentzIndex[σ]].
 DiracGamma[LorentzIndex[α]].DiracGamma[LorentzIndex[ν]].DiracGamma[LorentzIndex[β]].
 DiracGamma[LorentzIndex[μ]].hprime.DiracGamma[LorentzIndex[λ]].jprime *
 Pair[LorentzIndex[α], LorentzIndex[β]];

$T_{55} = \text{Tr}[\text{DiracGamma}[\text{LorentzIndex}[\sigma]].\text{fprime}.\text{DiracGamma}[\text{LorentzIndex}[\nu]].$
 $\text{gprime}.\text{DiracGamma}[\text{LorentzIndex}[\mu]].\text{hprime}.\text{DiracGamma}[\text{LorentzIndex}[\lambda]].\text{jprime}];$

$T_{66} = m^2 \text{Tr}[\text{DiracGamma}[\text{LorentzIndex}[\sigma]].\text{DiracGamma}[\text{LorentzIndex}[\nu]].$
 $\text{DiracGamma}[\text{LorentzIndex}[\mu]].\text{hprime}.\text{DiracGamma}[\text{LorentzIndex}[\lambda]].\text{jprime}$
 $+ \text{DiracGamma}[\text{LorentzIndex}[\sigma]].\text{DiracGamma}[\text{LorentzIndex}[\nu]].\text{gprime}.\text{DiracGamma}[\text{LorentzIndex}[\mu]].$
 $\text{DiracGamma}[\text{LorentzIndex}[\lambda]].\text{jprime} + \text{DiracGamma}[\text{LorentzIndex}[\sigma]].\text{DiracGamma}[\text{LorentzIndex}[\nu]].$
 $\text{gprime}.\text{DiracGamma}[\text{LorentzIndex}[\mu]].\text{hprime}.\text{DiracGamma}[\text{LorentzIndex}[\lambda]]$
 $+ \text{DiracGamma}[\text{LorentzIndex}[\sigma]].\text{fprime}.\text{DiracGamma}[\text{LorentzIndex}[\nu]].\text{DiracGamma}[\text{LorentzIndex}[\mu]].$
 $\text{DiracGamma}[\text{LorentzIndex}[\lambda]].\text{jprime} + \text{DiracGamma}[\text{LorentzIndex}[\sigma]].\text{fprime}.$
 $\text{DiracGamma}[\text{LorentzIndex}[\nu]].\text{DiracGamma}[\text{LorentzIndex}[\mu]].\text{hprime}.\text{DiracGamma}[\text{LorentzIndex}[\lambda]]$
 $+ \text{DiracGamma}[\text{LorentzIndex}[\sigma]].\text{fprime}.\text{DiracGamma}[\text{LorentzIndex}[\nu]].\text{gprime}.$
 $\text{DiracGamma}[\text{LorentzIndex}[\mu]].\text{DiracGamma}[\text{LorentzIndex}[\lambda]]];$

$\text{POLARIZEDAMP2} = -\text{Sqrt}[-1] * e^4 * \frac{1}{(4\text{Pi})^2}$
 $(4m^4(\text{Pair}[\text{LorentzIndex}[\sigma], \text{LorentzIndex}[\lambda]]\text{Pair}[\text{LorentzIndex}[\mu], \text{LorentzIndex}[\nu]] +$
 $\text{Pair}[\text{LorentzIndex}[\sigma], \text{LorentzIndex}[\nu]]\text{Pair}[\text{LorentzIndex}[\mu], \text{LorentzIndex}[\lambda]]$
 $- \text{Pair}[\text{LorentzIndex}[\sigma], \text{LorentzIndex}[\mu]]\text{Pair}[\text{LorentzIndex}[\nu], \text{LorentzIndex}[\lambda]]) *$
 $\text{DM33} - 8m^2(\text{Pair}[\text{LorentzIndex}[\sigma], \text{LorentzIndex}[\nu]]\text{Pair}[\text{LorentzIndex}[\mu], \text{LorentzIndex}[\lambda]]$
 $+ \text{Pair}[\text{LorentzIndex}[\sigma], \text{LorentzIndex}[\lambda]]\text{Pair}[\text{LorentzIndex}[\mu], \text{LorentzIndex}[\nu]]) *$
 $\text{DM22} + 16m^2(\text{Pair}[\text{LorentzIndex}[\sigma], \text{LorentzIndex}[\lambda]]\text{Pair}[\text{LorentzIndex}[\mu], \text{LorentzIndex}[\nu]]$

$$\begin{aligned}
& + \text{Pair}[\text{LorentzIndex}[\sigma], \text{LorentzIndex}[\nu]] \text{Pair}[\text{LorentzIndex}[\mu], \text{LorentzIndex}[\lambda]] \\
& - \text{Pair}[\text{LorentzIndex}[\sigma], \text{LorentzIndex}[\mu]] \text{Pair}[\text{LorentzIndex}[\nu], \text{LorentzIndex}[\lambda]] \\
& * \text{DM22} + (\text{Pair}[\text{LorentzIndex}[\sigma], \text{LorentzIndex}[\lambda]] \text{Pair}[\text{LorentzIndex}[\mu], \text{LorentzIndex}[\nu]] \\
& + \text{Pair}[\text{LorentzIndex}[\sigma], \text{LorentzIndex}[\nu]] \text{Pair}[\text{LorentzIndex}[\mu], \text{LorentzIndex}[\lambda]] \\
& - \text{Pair}[\text{LorentzIndex}[\sigma], \text{LorentzIndex}[\mu]] \text{Pair}[\text{LorentzIndex}[\nu], \text{LorentzIndex}[\lambda]]) \\
& \left(\frac{48}{v} - 24 * \text{Log}[m^2] - 24 * \frac{U_2}{m^2} + 12 * \frac{(U_2 * U_2)}{m^4} - 24 * c + 24 \text{Log}[4 * \text{Pi}] - 20 \right) \\
& - 4(\text{Pair}[\text{LorentzIndex}[\sigma], \text{LorentzIndex}[\nu]] \text{Pair}[\text{LorentzIndex}[\mu], \text{LorentzIndex}[\lambda]] \\
& + \text{Pair}[\text{LorentzIndex}[\sigma], \text{LorentzIndex}[\lambda]] \text{Pair}[\text{LorentzIndex}[\mu], \text{LorentzIndex}[\nu]]) \\
& \left(\frac{12}{v} - 6 * \text{Log}[m^2] - 6 * \frac{U_2}{m^2} + 3 * \frac{(U_2 * U_2)}{m^4} - 6 * c + 6 \text{Log}[4 * \text{Pi}] - 2 \right) \\
& + 8(\text{Pair}[\text{LorentzIndex}[\sigma], \text{LorentzIndex}[\lambda]] \text{Pair}[\text{LorentzIndex}[\mu], \text{LorentzIndex}[\nu]] \\
& + \text{Pair}[\text{LorentzIndex}[\sigma], \text{LorentzIndex}[\nu]] \text{Pair}[\text{LorentzIndex}[\mu], \text{LorentzIndex}[\lambda]] \\
& + \text{Pair}[\text{LorentzIndex}[\sigma], \text{LorentzIndex}[\mu]] \text{Pair}[\text{LorentzIndex}[\nu], \text{LorentzIndex}[\lambda]]) \\
& \left(\frac{2}{v} - \text{Log}[m^2] - \frac{U_2}{m^2} + \frac{1}{2} * \frac{(U_2 * U_2)}{m^4} - c + \text{Log}[4 * \text{Pi}] \right) - T_{44} * \frac{1}{2} * \text{DM22} + (T_{55} + T_{66}) * \text{DM33} \Big);
\end{aligned}$$

$$M_2 = \text{Contract}[\text{POLARIZEDAMP2} * \text{FV}[e1, \mu] \text{FV}[e2, \nu] \text{FV}[e3, \sigma] \text{FV}[e4, \lambda]];$$

Amplitude of Diagram 3.2 (c)

$$\begin{aligned}
T_{444} = & \text{Contract}[\text{Tr}[\text{DiracGamma}[\text{LorentzIndex}[\lambda]].\text{fdprime}.\text{DiracGamma}[\text{LorentzIndex}[\nu]].\text{gdprime} \\
& \text{DiracGamma}[\text{LorentzIndex}[\sigma]].\text{DiracGamma}[\text{LorentzIndex}[\alpha]].\text{DiracGamma}[\text{LorentzIndex}[\mu]]. \\
& \text{DiracGamma}[\text{LorentzIndex}[\beta]] + \text{DiracGamma}[\text{LorentzIndex}[\lambda]].\text{fdprime}.\text{DiracGamma}[\text{LorentzIndex}[\nu]]. \\
& \text{DiracGamma}[\text{LorentzIndex}[\alpha]].\text{DiracGamma}[\text{LorentzIndex}[\sigma]].\text{hdprime}.\text{DiracGamma}[\text{LorentzIndex}[\mu]]. \\
& \text{DiracGamma}[\text{LorentzIndex}[\beta]] + \text{DiracGamma}[\text{LorentzIndex}[\lambda]].\text{fdprime}.\text{DiracGamma}[\text{LorentzIndex}[\nu]]. \\
& \text{DiracGamma}[\text{LorentzIndex}[\alpha]].\text{DiracGamma}[\text{LorentzIndex}[\sigma]].\text{DiracGamma}[\text{LorentzIndex}[\beta]]. \\
& \text{DiracGamma}[\text{LorentzIndex}[\mu]].\text{jdprime} + \text{DiracGamma}[\text{LorentzIndex}[\lambda]].\text{DiracGamma}[\text{LorentzIndex}[\alpha]]. \\
& \text{DiracGamma}[\text{LorentzIndex}[\nu]].\text{gdprime}.\text{DiracGamma}[\text{LorentzIndex}[\sigma]].\text{hdprime} \\
& \text{DiracGamma}[\text{LorentzIndex}[\mu]].\text{DiracGamma}[\text{LorentzIndex}[\beta]] + \text{DiracGamma}[\text{LorentzIndex}[\lambda]]. \\
& \text{DiracGamma}[\text{LorentzIndex}[\alpha]].\text{DiracGamma}[\text{LorentzIndex}[\nu]].\text{gdprime}.\text{DiracGamma}[\text{LorentzIndex}[\sigma]]. \\
& \text{DiracGamma}[\text{LorentzIndex}[\beta]].\text{DiracGamma}[\text{LorentzIndex}[\mu]].\text{jdprime} + \text{DiracGamma}[\text{LorentzIndex}[\lambda]]. \\
& \text{DiracGamma}[\text{LorentzIndex}[\alpha]].\text{DiracGamma}[\text{LorentzIndex}[\nu]].\text{DiracGamma}[\text{LorentzIndex}[\beta]]. \\
& \text{DiracGamma}[\text{LorentzIndex}[\sigma]].\text{hdprime}.\text{DiracGamma}[\text{LorentzIndex}[\mu]].\text{jdprime}] \\
& \text{Pair}[\text{LorentzIndex}[\alpha], \text{LorentzIndex}[\beta]]];
\end{aligned}$$

$$\begin{aligned}
T_{555} = & \text{Tr}[\text{DiracGamma}[\text{LorentzIndex}[\lambda]].\text{fdprime}.\text{DiracGamma}[\text{LorentzIndex}[\nu]]. \\
& \text{gdprime}.\text{DiracGamma}[\text{LorentzIndex}[\sigma]].\text{hdprime}.\text{DiracGamma}[\text{LorentzIndex}[\mu]].\text{jdprime}];
\end{aligned}$$

$$\begin{aligned}
T_{666} = & m^2 \text{Tr}[\text{DiracGamma}[\text{LorentzIndex}[\lambda]].\text{DiracGamma}[\text{LorentzIndex}[\nu]]. \\
& \text{DiracGamma}[\text{LorentzIndex}[\sigma]].\text{hdprime}.\text{DiracGamma}[\text{LorentzIndex}[\mu]].\text{jdprime} \\
& + \text{DiracGamma}[\text{LorentzIndex}[\lambda]].\text{DiracGamma}[\text{LorentzIndex}[\nu]].\text{gdprime}.\text{DiracGamma}[\text{LorentzIndex}[\sigma]]. \\
& \text{DiracGamma}[\text{LorentzIndex}[\mu]].\text{jdprime} + \text{DiracGamma}[\text{LorentzIndex}[\lambda]].\text{DiracGamma}[\text{LorentzIndex}[\nu]]. \\
& \text{gdprime}.\text{DiracGamma}[\text{LorentzIndex}[\sigma]].\text{hdprime}.\text{DiracGamma}[\text{LorentzIndex}[\mu]] \\
& + \text{DiracGamma}[\text{LorentzIndex}[\lambda]].\text{fdprime}.\text{DiracGamma}[\text{LorentzIndex}[\nu]].\text{DiracGamma}[\text{LorentzIndex}[\sigma]]. \\
& \text{DiracGamma}[\text{LorentzIndex}[\mu]].\text{jdprime} + \text{DiracGamma}[\text{LorentzIndex}[\lambda]].\text{fdprime}.\text{DiracGamma}[\text{LorentzIndex}[\nu]]. \\
& \text{DiracGamma}[\text{LorentzIndex}[\sigma]].\text{hdprime}.\text{DiracGamma}[\text{LorentzIndex}[\mu]] + \\
& \text{DiracGamma}[\text{LorentzIndex}[\lambda]].\text{fdprime}.\text{DiracGamma}[\text{LorentzIndex}[\nu]].\text{gdprime}.\text{DiracGamma}[\text{LorentzIndex}[\sigma]]. \\
& \text{DiracGamma}[\text{LorentzIndex}[\mu]]];
\end{aligned}$$

$$\begin{aligned}
\text{POLARIZEDAMP3} = & -\text{Sqrt}[-1] * e^4 * \frac{1}{(4\text{Pi})^2} \\
& (4m^4(\text{Pair}[\text{LorentzIndex}[\lambda], \text{LorentzIndex}[\mu]]\text{Pair}[\text{LorentzIndex}[\sigma], \text{LorentzIndex}[\nu]] + \\
& \text{Pair}[\text{LorentzIndex}[\lambda], \text{LorentzIndex}[\nu]]\text{Pair}[\text{LorentzIndex}[\sigma], \text{LorentzIndex}[\mu]] \\
& - \text{Pair}[\text{LorentzIndex}[\lambda], \text{LorentzIndex}[\sigma]]\text{Pair}[\text{LorentzIndex}[\nu], \text{LorentzIndex}[\mu]])\text{DM333} \\
& - 8m^2(\text{Pair}[\text{LorentzIndex}[\lambda], \text{LorentzIndex}[\nu]]\text{Pair}[\text{LorentzIndex}[\sigma], \text{LorentzIndex}[\mu]] \\
& + \text{Pair}[\text{LorentzIndex}[\lambda], \text{LorentzIndex}[\mu]]\text{Pair}[\text{LorentzIndex}[\sigma], \text{LorentzIndex}[\nu]])\text{DM222} \\
& + 16m^2(\text{Pair}[\text{LorentzIndex}[\lambda], \text{LorentzIndex}[\mu]]\text{Pair}[\text{LorentzIndex}[\sigma], \text{LorentzIndex}[\nu]] \\
& + \text{Pair}[\text{LorentzIndex}[\lambda], \text{LorentzIndex}[\nu]]\text{Pair}[\text{LorentzIndex}[\sigma], \text{LorentzIndex}[\mu]] \\
& - \text{Pair}[\text{LorentzIndex}[\lambda], \text{LorentzIndex}[\sigma]]\text{Pair}[\text{LorentzIndex}[\nu], \text{LorentzIndex}[\mu]])\text{DM222} \\
& + (\text{Pair}[\text{LorentzIndex}[\lambda], \text{LorentzIndex}[\mu]]\text{Pair}[\text{LorentzIndex}[\sigma], \text{LorentzIndex}[\nu]] \\
& + \text{Pair}[\text{LorentzIndex}[\lambda], \text{LorentzIndex}[\nu]]\text{Pair}[\text{LorentzIndex}[\sigma], \text{LorentzIndex}[\mu]] \\
& - \text{Pair}[\text{LorentzIndex}[\lambda], \text{LorentzIndex}[\sigma]]\text{Pair}[\text{LorentzIndex}[\nu], \text{LorentzIndex}[\mu]]) \\
& \left(\frac{48}{v} - 24 * \text{Log}[m^2] - 24 * \frac{U_3}{m^2} + 12 * \frac{(U_3 * U_3)}{m^4} - 24 * c + 24\text{Log}[4 * \text{Pi}] - 20 \right) \\
& - 4(\text{Pair}[\text{LorentzIndex}[\lambda], \text{LorentzIndex}[\nu]]\text{Pair}[\text{LorentzIndex}[\sigma], \text{LorentzIndex}[\mu]] \\
& + \text{Pair}[\text{LorentzIndex}[\lambda], \text{LorentzIndex}[\mu]]\text{Pair}[\text{LorentzIndex}[\sigma], \text{LorentzIndex}[\nu]] \\
& \left(\frac{12}{v} - 6 * \text{Log}[m^2] - 6 * \frac{U_3}{m^2} + 3 * \frac{(U_3 * U_3)}{m^4} - 6 * c + 6\text{Log}[4 * \text{Pi}] - 2 \right) \\
& + 8(\text{Pair}[\text{LorentzIndex}[\lambda], \text{LorentzIndex}[\mu]]\text{Pair}[\text{LorentzIndex}[\sigma], \text{LorentzIndex}[\nu]] \\
& + \text{Pair}[\text{LorentzIndex}[\lambda], \text{LorentzIndex}[\nu]]\text{Pair}[\text{LorentzIndex}[\sigma], \text{LorentzIndex}[\mu]] \\
& + \text{Pair}[\text{LorentzIndex}[\lambda], \text{LorentzIndex}[\sigma]]\text{Pair}[\text{LorentzIndex}[\nu], \text{LorentzIndex}[\mu]]) \\
& \left(\frac{2}{v} - \text{Log}[m^2] - \frac{U_3}{m^2} + \frac{1}{2} * \frac{(U_3 * U_3)}{m^4} - c + \text{Log}[4 * \text{Pi}] \right) - T_{444} * \frac{1}{2} * \text{DM222} + (T_{555} + T_{666}) * \text{DM333} \Big);
\end{aligned}$$

$$M_3 = \text{Contract}[\text{POLARIZEDAMP3} * \text{FV}[e1, \mu]\text{FV}[e2, \nu]\text{FV}[e3, \sigma]\text{FV}[e4, \lambda];$$

Total Amplitude

$$M = M_1 + M_2 + M_3;$$

$$MEXP = \text{Expand}[M];$$

$$MSIMPLIFIED = MEXP / \frac{1}{m^8} \rightarrow 0;$$

$$MMORSIMPLIFIED = MSIMPLIFIED / \frac{1}{m^6} \rightarrow 0;$$

$$\text{MINTEGRATED} = \text{Integrate}[\text{MMORSIMPLIFIED}, \{x_1, 0, 1\}, \{x_2, 0, x_1\}, \{x_3, 0, x_2\}];$$

$$s = 4w^2;$$

$$t = -2w^2(1 - \text{Cos}[\theta]);$$

$$u = -2w^2(1 + \text{Cos}[\theta]);$$

$$Mf = \text{Simplify}[\text{MINTEGRATED}]$$

Bibliography

- [1] B. Odom, D. Hanneke, B. D’Urso, and G. Gabrielse, “New Measurement of the Electron Magnetic Moment Using a One-Electron Quantum Cyclotron”, *Phys. Rev. Lett.* **97** (2006) 030801+4.
- [2] G. Gabrielse, D. Hanneke, T. Kinoshita, M. Nio, and B. Odom, “ New Determination of the Fine Structure Constant from the Electron g Value and QED”, *Phys. Rev. Lett.* **97** (2006) 030802+4; Erratum, *Phys. Rev. Lett.* **99** (2007) 039902+2.
- [3] G. Jarlskog et. al., “Measurement of Delbruck Scattering and Observation of Photon Splitting at High Energies”, *Phys. Rev. D* **8** (1973) 3813-3823.
- [4] P. A. M. Dirac, “A Theory of Electrons and Protons”, *Proc. Roy. Soc. Lond.* **A126** (1930) 360-365.
- [5] O. Halpern, “Scattering Processes Produced by Electrons in Negative Energy States”, *Phys. Rev.* **44** (1933) 855-856.
- [6] H. Euler and B. Kockel, “The Scattering of Light by Light in Dirac’s Theory”, *Naturwissenschaften* **23** (1935) 246-247.
- [7] H. Euler, “On the Scattering of Light by Light in Dirac’s Theory”, *Ann. Physik.* **26** (1936) 398-448.

- [8] A. Akhieser, L. Landau, and I. Pomeranchuk, “Scattering of Light by Light”, *Nature* **138** (1936) 206-206;
- [9] R. Karplus and M. Neuman, “Non-Linear Interactions between Electromagnetic Fields”, *Phys. Rev.* **80** (1950) 380-385.
- [10] R. Karplus and M. Neuman, “The Scattering of Light by Light”, *Phys. Rev.* **83** (1951) 776-784.
- [11] G. Breit and J. A. Wheeler, “Collision of Two Light Quanta”, *Phys. Rev.* **46** (1934) 1087-1091.
- [12] D.L. Burke et al., “Positron Production in Multiphoton Light-by-Light Scattering”, *Phys. Rev. Lett.* **79** (1997) 1626-1629.
- [13] R. Mertig, M. Bohm and A. Denner, “FEYN CALC: Computer Algebraic Calculation of Feynman Amplitudes,” *Comput. Phys. Commun.* **64** (1991) 345-359.
- [14] CLF Facilities Vulcan Glass Laser <http://www.clf.rl.ac.uk/Facilities/Vulcan/12248.aspx>.
- [15] Information about the ELI project is available at the official web site <http://www.extreme-light-infrastructure.eu>.
- [16] A.L. Hughes, G.E.M. Jauncey, “An Attempt to Detect Collision of Photons”, *Phys. Rev.* **36** (1930) 773-777.
- [17] K. O. Mikaelian, “Detection of Elastic Light-By-Light Scattering at SLAC”, *Phys. Lett. B* **115** (1982) 267-269.
- [18] G. Brodin, M. Marklund, and L. Stenflo, “Proposal for Detection of QED Vacuum Nonlinearities in Maxwell’s Equations by the Use of Waveguides”, *Phys. Rev. Lett.* **87** (2001) 171801+3.

- [19] D. Eriksson, G. Brodin, M. Marklund, and L. Stenflo, “Possibility to Measure Elastic Photon-photon Scattering in Vacuum”, *Phys. Rev. A* **70** (2004) 013808+6.
- [20] F. Moulin, D. Bernard and F. Amiranoff, “Photon-photon Elastic Scattering in the Visible Domain,” *Z. Phys. C* **72** (1996) 607-611.
- [21] D. Bernard et al., “Search for Stimulated Photon-Photon Scattering in Vacuum,” *Eur. Phys. J. D* **10** (2000) 141-145 [arXiv:1007.0104 [physics.optics]].
- [22] E. Lundstrom et al., “Using High-power Lasers for Detection of Elastic Photon-photon Scattering,” *Phys. Rev. Lett.* **96** (2006) 083602+4 [arXiv:hep-ph/0510076].
- [23] J. Lundin et al., “Analysis of Four-wave Mixing of High-power Lasers for the Detection of Elastic Photon-photon Scattering,” *Phys. Rev. A* **74** (2006) 043821+10 [arXiv:hep-ph/0606136].
- [24] D. Enterria and G.G. da Silveira, “Observing Light-by-Light Scattering at the Large Hadron Collider”, *Phys. Rev. Lett.* **111** (2013) 080405+5.
- [25] T. Inada “Search for Photon–Photon Elastic Scattering in the X-ray Region” *Physics Letters B* **732** (2014) 356–359 [arXiv:1403.2547v2 [hep-ex]].
- [26] V. Yanovsky et al., Ultra-high Intensity-300-TW Laser at 0.1 Hz Repetition Rate. *Opt. Express* **16** (2008) 2109-2114.
- [27] T. Ishikawa, et al., “A compact X-ray Free-electron Laser Emitting in the Sub-ångström Region”, *Nat. Photonics* **6** (2012) 540-544.
- [28] K. Tono, et al., “Beamline, Experimental Stations and Photon Beam Diagnostics for the Hard X-ray Free Electron Laser of SACLA”, *New J. Phys.* **15** (2013) 083035+21.

- [29] W. H. Furry, “A Symmetry Theorem in the Positron Theory”, *Phys. Rev.* **51** (1937) 125-129.
- [30] M.E. Peskin, and D.V. Schroeder, “An Introduction to Quantum Field Theory”, Frontiers in physics, Westview Press, 1995.
- [31] F. Mandl and G. Shaw, “Quantum Field Theory”, Second Edition, Wiley, 2010.
- [32] Y. Liang and A. Czarnecki, “Photon-photon Scattering: A Tutorial,” *Can. J. Phys.* **90** (2012) 11-16 [arXiv:1111.6126 [hep-ph]].
- [33] V.B. Berestetskii, E.M. Lifshitz and L.P. Pitaevskii, “Quantum Electrodynamics” Course of Theoretical Physics, Second Edition, Volume **4**, Butterworth-Heinemann, 1982.
- [34] N. Kanda, “Light-Light Scattering,” arXiv:1106.0592 [hep-ph].
- [35] T. Fujita and N. Kanda, “A Proposal to Measure Photon-photon Scattering”, arXiv:1106.0465, 2011.
- [36] G. Jikia and A. Tkabladze, “Photon-Photon Scattering at the Photon Linear Collider,” *Phys. Lett. B* **323** (1994) 453-458.